Stony Brook University

Probing *O*-GlcNAc Modifications Via Metabolic Labeling Using Unnatural Sugars

A Dissertation Presented

by

Lakshmi Rajaram

to

The Graduate School

in Partial Fulfillment of the

Requirements

for the Degree of

Doctor of Philosophy

in

Chemistry

Stony Brook University

August 2013

Stony Brook University

The Graduate School

Lakshmi Rajaram

We, the dissertation committee for the above candidate for the

Doctor of Philosophy degree, hereby recommend

acceptance of this dissertation.

Isaac S. Carrico, Ph.D. – Dissertation Advisor
Associate Professor, Department of Chemistry

Dale Drueckhammer, Ph.D. - Chairperson of Defense
Professor, Department of Chemistry

Stephen Koch, Ph.D. – Third Member
Professor, Department of Chemistry

Antonius Koller, Ph.D. – Outside Member
Research Assistant Professor, Department of Pathology
Stony Brook University School of Medicine

This dissertation is accepted by the Graduate School

Charles Taber
Interim Dean of the Graduate School

Abstract of the Dissertation

Probing *O*-GlcNAc Modifications Via Metabolic Labeling Using Unnatural Sugars

by

Lakshmi Rajaram

Doctor of Philosophy

in

Chemistry

Stony Brook University

2013

Understanding the impact of post-translational modifications in the context of the complexity of the human proteome is extremely challenging. Part of the challenge lies in cataloging the proteins that are modified with any given post-translational modification, and how this list changes in response to changes in cellular/tissue physiology. The *O*-GlcNAc modification is one such modification that involves an addition of a single *N*-acetylglucosamine moiety onto serines and threonines of eukaryotic proteins. This dynamic modification is mediated via two enzymes: *O*-GlcNAc transferase (OGT) for installing the sugar and *O*-GlcNAcase (OGA) for cleaving the sugar off modified proteins. *O*-GlcNAcylation occurs mainly in nuclear and cytosolic proteins ranging from structural proteins and enzymes to transcription factors and tumor suppressors. The dynamic nature of the modification, which can be compared to phosphorylation, has emerged as an important player in signaling, regulation of metabolism, nutrient response and disease onset.

Despite being implicated as a key regulator of cellular physiology, *O*-GlcNAc remains ill-defined due to a lack of effective analytical tools. In this context, the chemical reporter strategy, which installs a chemical handle that can be later modified and monitored, provides a potential solution. Here we detail efforts towards installing chemical reporter mimics of *O*-GlcNAc and using them to profile the repertoire of proteins modified with this post-translational modification. In particular, we chose to scrutinize the involvement of *O*-GlcNAc in the activation of T lymphocytes, which was prompted by the discovery that OGT is essential for T and B lymphocyte activation.

Table of Contents

List of Figures/Schemes/Tables

List of figures: Page

List of figures Page

Schemes:

Tables:

List of Abbreviations

GlcNAc: N-acetylglucosamine

GalNAc: N- acetylgalactosamine

OGT: *O*-GlcNAc transferase

OGA: *O*-GlcNAcase

HBP: Hexosamine biosynthetic pathway

UDP: Uridine diphosphate

GalT: galactosyl transferase

DTT: dithiothrietol

CuAAC: Copper accelerated Azide Alkyne Cycloaddition

SDS: Sodium dodecyl sulfate

SPAAC: Strain promoted alkyne azide cycloaddition

TCR: T cell receptor

BCR: B cell receptor

PMA: phorbol 12-myristate 13-acetate

Az-Rho: azido rhodamine

PNGase F: peptide: *N*-glyocosidase F

Aha: azidohomoalanine

Ad/Ad5: adenovirus type 5

Acknowledgements

My years spent in graduate school have truly been the defining years of my life. I have many people to thank for making this journey possible and enjoyable. Firstly, my advisor Isaac, I have learnt so much from him. Besides his scientific guidance he has given me so much clarity and objectivity in my thinking, lessons I will always value. I have to thank my labmates Lisa, Partha, Yanjie and Yoon for being the perfect sounding board over the years. The graduate school experience can be challenging and I certainly could not have done it without my friends, Cindy, Dhruv, Juhi and Tarun, many thanks to them for keeping me going. I also have to thank Vikram, for being my best friend, for growing up together and for being there. My parents, Amma and Appa, I have so much to thank them for, words cannot describe my gratitude for their unconditional love and support.

Chapter 1

Study of *O*-GlcNAc modifications via metabolic labeling with unnatural sugars

Abstract:

The *O*-GlcNAc modification is a post-translational modification that involves an addition of a single *N*-acetylglucosamine moiety onto serines and threonines of eukaryotic proteins. This dynamic modification is mediated via two enzymes: *O*-GlcNAc transferase (OGT) for installing the sugar and *O*-GlcNAcase (OGA) for cleaving the sugar off the protein. *O*-GlcNAcylation occurs mainly in nuclear and cytosolic proteins ranging from structural proteins and enzymes to transcription factors and tumor suppressors. The dynamic nature of the modification, which can be compared to phosphorylation, has emerged as an important player in signaling, regulation of metabolism, nutrient response and disease onset. In this chapter, efforts to probe *O*-GlcNAc dynamics via metabolic incorporation of unnatural sugars containing azido and alkynyl functional groups are presented.

Introduction:

Glycosylation as a post-translational modification:

Amongst the numerous post-translational modifications that eukaryotic proteins are subjected to, glycosylation remains one of the most widespread and complex. Essentially eukaryotic post-translational glycosylation can be categorized into three types: *N*-linked glycosylation that involves modification of asparagine residues of proteins, *O*-linked mucin type glycosylation of serine and threonine residues on extracellular proteins and the nucleo-cytosplasmic *O*-GlcNAc modifications of serines and threonines.

N-linked glycosylation occurs in the endoplasmic reticulum and demonstrates a consensus sequence of Asn-Xaa-Ser/Thr where the amino acid Xaa cannot be proline.[1] *N*-linked glycans have a complex structure that begins co-translationally in the endoplasmic reticulum with the addition of a 14 sugar glycan, thereafter, this core structure undergoes trimming in the Golgi apparatus to yield the final *N*-linked glycan.

O-linked mucin type glycosylation[2] involves the addition of complex oligosaccharides onto serine and threonine residues and is found on extracellular proteins. Unlike *N*-linked glycans, there is no consensus sequence for this modification adding to challenges in its study. This post-translational modification occurs in the Golgi apparatus and is most common on secreted and membrane bound proteins, giving rise to the name “mucins”. There are 8 common core structures of mucin type glycans, which can be further decorated with highly branched sugars leading to highly complex structures. These glycans are responsible for cell recognition and have roles to play in a variety of cellular functions such as inflammatory responses, angiogenesis, autoimmunity and cancer onset.

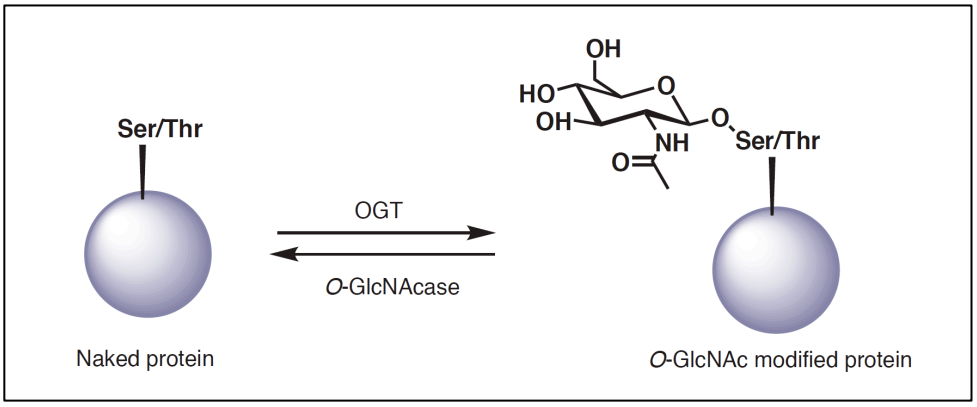

Figure 1.1: The O-GlcNAc modification of serine and threonine residues on proteins, cycled by OGT or O-GlcNAc transferase and OGA or O-GlcNAcase

In contrast to the above two forms of glycosylation, the nuclear and cytosolic *O*-GlcNAc is simple in structure in that only a monosaccharide, namely a β-*N*-acetylglucosamine residue is appended onto the hydroxyl side chains of serine and threonines. This post-translational modification was discovered by Gerald W. Hart and co-workers at John’s

Hopkins University[3,4] while studying the capping of terminal GlcNAc residues with bovine milk galactosyl transferase, on the surface of lymphocytes. They were using a tritium labeled galactose substrate for the enzyme and chanced upon the monosaccharide *O*-GlcNAc modification on several intracellular proteins. This was the first report of such a post-translational modification, immediately distinguishing itself from canonical *O*-linked glycosylation. Besides the location and structure, the other striking difference between *O*-GlcNAc and mucin type glycans is that the *O*-GlcNAc modification is dynamic by virtue of being cycled by two complimentary enzymes: *O*-GlcNAc transferase (OGT) and *O*-GlcNAcase (OGA). In this respect *O*-GlcNAc can be likened to phosphorylation, another wide spread and well studied post-translational modification that is cycled by kinases and phosphatases. Indeed *O*-GlcNAc can be considered more similar to phosphorylation than any other type of glycosylation. The third striking feature of *O*-GlcNAc pertains to its purported function in the cell, given its localization and dynamic nature already discussed above, it is ideal as a signaling modulator.

Role of *O*-GlcNAc in the eukaryotic cell:

Given its dynamic nature *O*-GlcNAc has emerged as an important player in cellular signaling pathways much like phosphorylation. Since its discovery in 1984, a wide variety of intracellular proteins from transcription factors, cytoskeletal proteins, enzymes and metabolic regulators have been identified as being *O*-GlcNAc modified and the list continues to grow. Due to its ubiquitous nature in the eukaryotic cell, the functions of *O*-GlcNAc range from cellular localization, protein-protein interaction mediation, involvement in signaling cascades to mediating protein degradation. In addition to these broad functions based on identification of the types of proteins found to be *O*-GlcNAc modified, there is also mounting evidence that flux in GlcNAcylation patterns often accompany disease onset.

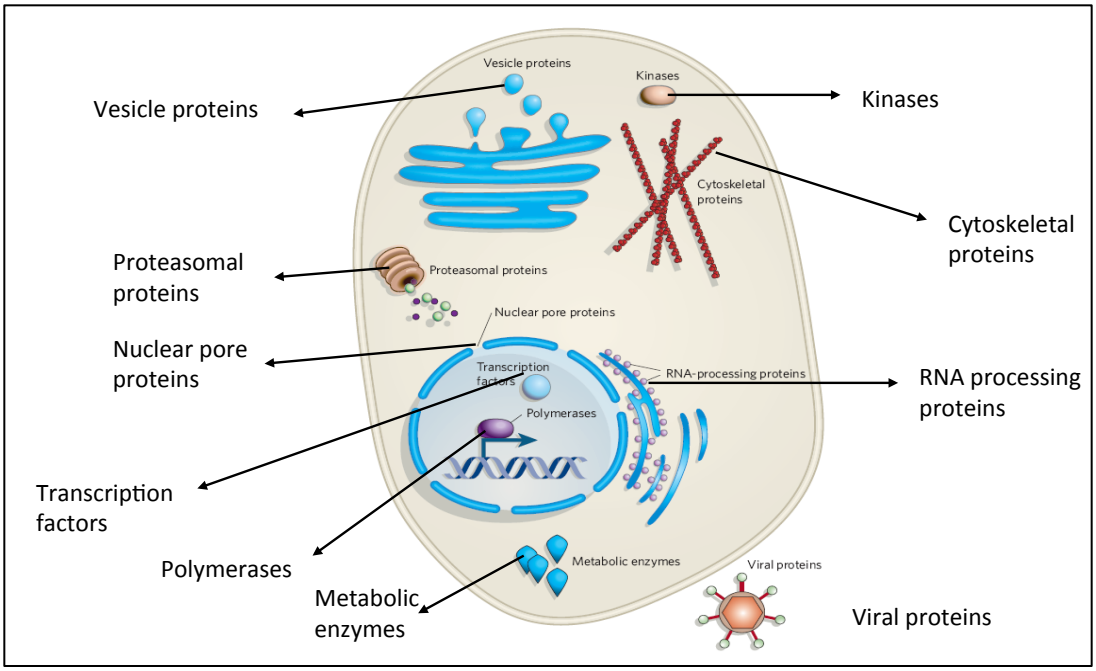

Figure 1.2 Figure adapted with permission from Nature Publishing Group, Macmillan Publishers Ltd: Hart, G.W., Housley, M.P. & Slawson, C. Cycling of O-linked [beta]-N-acetylglucosamine on nucleocytoplasmic proteins. Nature ***446****, 1017-1022 (2007)., Copyright(2007) This figure shows the intracellular distribution of O-GlcNAc in an eukaryotic cell.*

O-GlcNAc: one modification, many roles

The *O*-GlcNAc modification is an ideal modification to act as a sensor of cellular stress and nutrient state, given that the end product of the hexosamine biosynthetic pathway (HBP), namely, UDP-GlcNAc is the donor sugar for OGT to modify proteins. The hexosamine biosynthetic pathway intersects with virtually all metabolic pathways and therefore the cellular concentration of UDP-GlcNAc is mirrored by the cellular state. As is illustrated by the diversity in the types of proteins modified by *O*-GlcNAc, it is understandable that it plays a variety of roles in the cell. Modification on transcription is effected by the fact that the catalytic subunit of RNA polymerase II and numerous transcription factors such as Sp1, NFkB and NFAT are known to be *O*-GlcNAc modified, thereby enabling the regulation of transcriptional activity.[5] GlcNAc is also involved in a regulatory role in cytoskeletal remodeling, protein trafficking and degradation.[6] Given

that both phosphorylation and GlcNAcylation can occur on serine and threonine residues, there has been speculation about their reciprocity. In some cases, the site of modification by O-GlcNAc is also the site for phosphorylation, such as in the case of c-Myc[7] and estrogen receptor[8], but in other cases the sites of modification are close to one another but not at the same site, such as in the case of p53.[9] Therefore, it is more accurate to label the relationship between *O*-GlcNAc and phosphorylation being that of cross-talk, involving nuanced and intersection layers of regulation.

In addition to this, O-GlcNAc has also been implicated in the onset of disease states like cancer, diabetes and neurodegenerative diseases[6]. Several oncogenes, such as c-Myc and p53 have been shown to be modulated via their GlcNAc modiifcations. Therefore, *O*-GlcNAc, by its location, structure and dynamics is poised as a versatile regulator of cellular physiology in tandem with other post-translational modifications like phosphorylation.

OGT and OGA:

OGT or *O*-GlcNAc transferase is the only enzyme known to be able to carry out the O-GlcNAc modification, being able to act on a variety of substrates in intracellular locations. Knock-out of the OGT gene is embryonically lethal in mice[10] signifying the integral nature of OGT and *O*-GlcNAc modifications in the cell. Even though there is no consensus sequence for this modification, OGT recognizes its substrates via protein:protein interactions mediated by several tetratricopeptide repeat motifs.[11] The uridine diphosphate activated donor sugar of GlcNAc, i.e. UDP-GlcNAc is the substrate for OGT which is also the end product of the hexosamine biosynthetic pathway (HBP).[12] This signifies that OGT and O-GlcNAc modifications intersect with nutrient sensing and metabolism of the cell in addition to all the other metabolic pathways that intersect with the HBP.

After the characterization of OGT from rabbit[13] and rat[14] in the 1990's, the crystal structure of OGT was recently solved[15] for OGT in complex with UDP and UDP+peptide substrate which throws more light on the recognition of peptide sequences by OGT.

OGA or O-GlcNAcase is the reciprocal enzyme to OGT, being responsible for the cleavage of the sugar residue from *O*-GlcNAc modified proteins. At this time there is no crystal structure for OGA but two bacterial homologs have been characterized[16,17] which indicate the presence of a C-terminal histone acetyltransferase domain in addition to the N-terminal glycosidase domain. They also aid in the understanding of the mechanism of OGA action which is supposed to proceed via a substrate assisted catalysis mechanism.[18] Inhibitors of OGA include PUGNAc and NAG-thiazoline[19] and GlcNAcstatin[20-22] which have greatly impacted the ability of researchers to study *O*-GlcNAc modifications in cells.

Together, OGT and OGA present a potent combination of enzymes that can moidify protein structure, function and stability via the *O*-GlcNAc modification.

Chemical tools employed for the study of *O*-GlcNAc:

O-GlcNAc modifications are challenging to study as demonstrated by how they evaded discovery until the early eighties. The reason being that the single monosaccharide modification is sub-stoichiometric and therefore challenging to probe via standard analytical techniques, it does not alter protein charge or significantly alter the size therefore migration in gel electrophoresis is not affected. Additionally, on cell lysis, O-GlcNAcase inhibitors are essential to prevent loss of *O*-GlcNAc by OGA cleavage as a response to cellular stress and damage. Furthermore, the *O*-GlcNAc Ser/Thr linkage is labile in traditional mass spectrometric methods.[23]

Historically, the first method used to study *O*-GlcNAc was the use of a GalT galactosyl transferase method [3] which caps any terminal GlcNAc residue with a N-acetylgalactosamine (GalNAc). Based on this method Hseih-Wilson and coworkers developed a chemoenzymatic method for the study of *O*-GlcNAc modified proteins from cell lysates[24] which employed a mutant GalT enzyme that could accept a ketogalactose in the form of a UDP donor sugar. This method was an improvement on the initial GalT capping method because the ketogalactose moiety afforded a chemical handle through which *O*-GlcNAc modified proteins could be enriched for or visualized. However it

suffered from the caveats of needing a mutant GalT with stringent pH requirements for efficient enzymatic reaction and a challenging synthesis of the ketogalactose donor sugar.

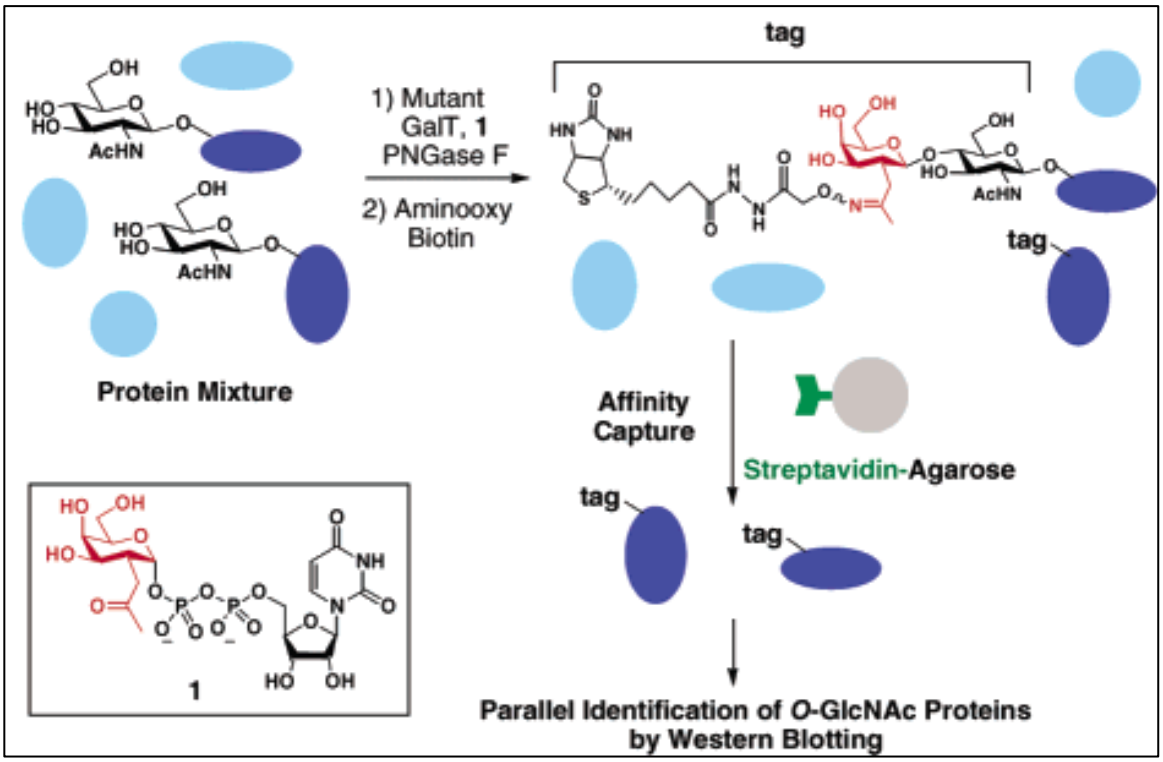

Figure 1.3: Reprinted with permission from (Tai, H.C., Khidekel, N., Ficarro, S.B., Peters, E.C. & Hsieh-Wilson, L.C. Parallel identification of O-GlcNAc-modified proteins from cell lysates. Journal of the American Chemical Society 126, 10500-10501 (2004)). Copyright (2004) American Chemical Society.

.Chemoenzymatic tagging of O-GlcNAc modifications for subsequent identification of modified proteins in cell lysates.

Another approach used for the study of *O*-GlcNAc modifications involves the use of a two-step procedure to identify the site of modification on the protein via mass spectrometric techniques. The first step is a mild β-elimination reaction of the *O*-GlcNAc group resulting in an α,β-unsaturated carbonyl compound that can undergo a Michael addition with a nucleophile. This allows the identification of *O*-GlcNAcylated peptides from trypsin digested proteins because a unique molecular weight tag can be attached in the form of dithiothrietol (DTT). Alternatively, the peptides can be enriched for by

affinity chromatography via a biotin pentyl amine tag (BAP). Tandem mass spectrometry followed by database searches facilitates identification of the exact location of the *O*-GlcNAc moiety on the peptide.

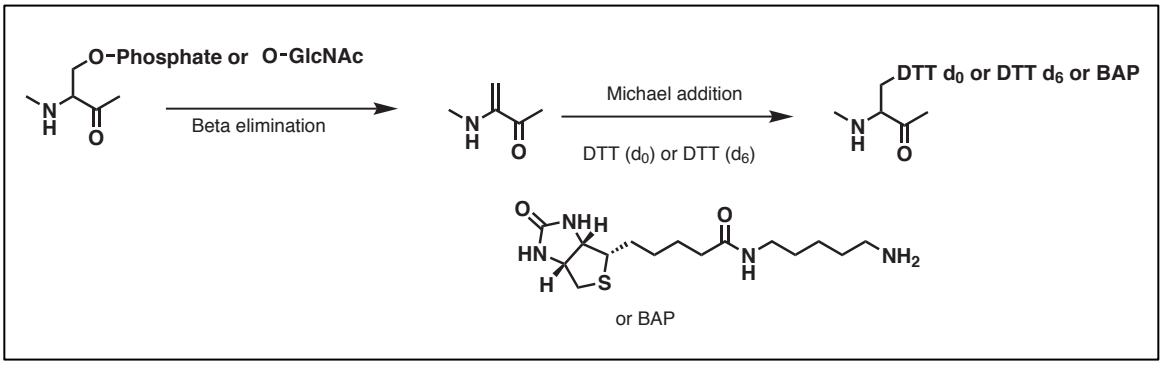

Figure 1.4: BEMAD β-elimination followed by Michael addition marks the site of O-GlcNAc on the peptide by using a unique mass tag, which enables quantitation (when using heavy and light isotope labeled DTT) or enrichment (when using Biotin pentyl amine tag).

One of the chemical approaches has been the incorporation of non-canonical sugar substrates as a means to enrich for and identify GlcNAcylated proteins. The driving principle of this strategy is the installation of an unnatural GlcNAc surrogate via the metabolic machinery of the cell. There is no need for a mutant GalT enzyme in this case, which makes this method easier than the chemoenzymatic strategy described above. The non canonical sugar substrate is accepted by the biosynthetic pathways, in this case the hexosamine biosynthetic pathway[25] that ultimately yields the activated donor sugar (UDP-GlcNAc) bearing the unnatural functionality. Thereafter, OGT transfers the unnatural sugar onto its targets. Once installed, the surrogate sugar, chosen for its capability to undergo one of the bioorthogonal reactions described in Figure 1.6 can be suitably modified. The first attempt at this method was by Bertozzi and co-workers where they incorporated GlcNAz via metabolic labeling with peracetylated N-azidoacetylglucosamine Ac_4GlcNAz[25]. The peracetylated version of the sugar was used to enhance the cell permeability, once inside the cell, intracellular esterases deacetylate the unnatural sugar substrate upon which it gets funneled into the

hexosamine biosynthetic pathway via the the GlcNAc salvage pathway, as shown in Figure 1.5.

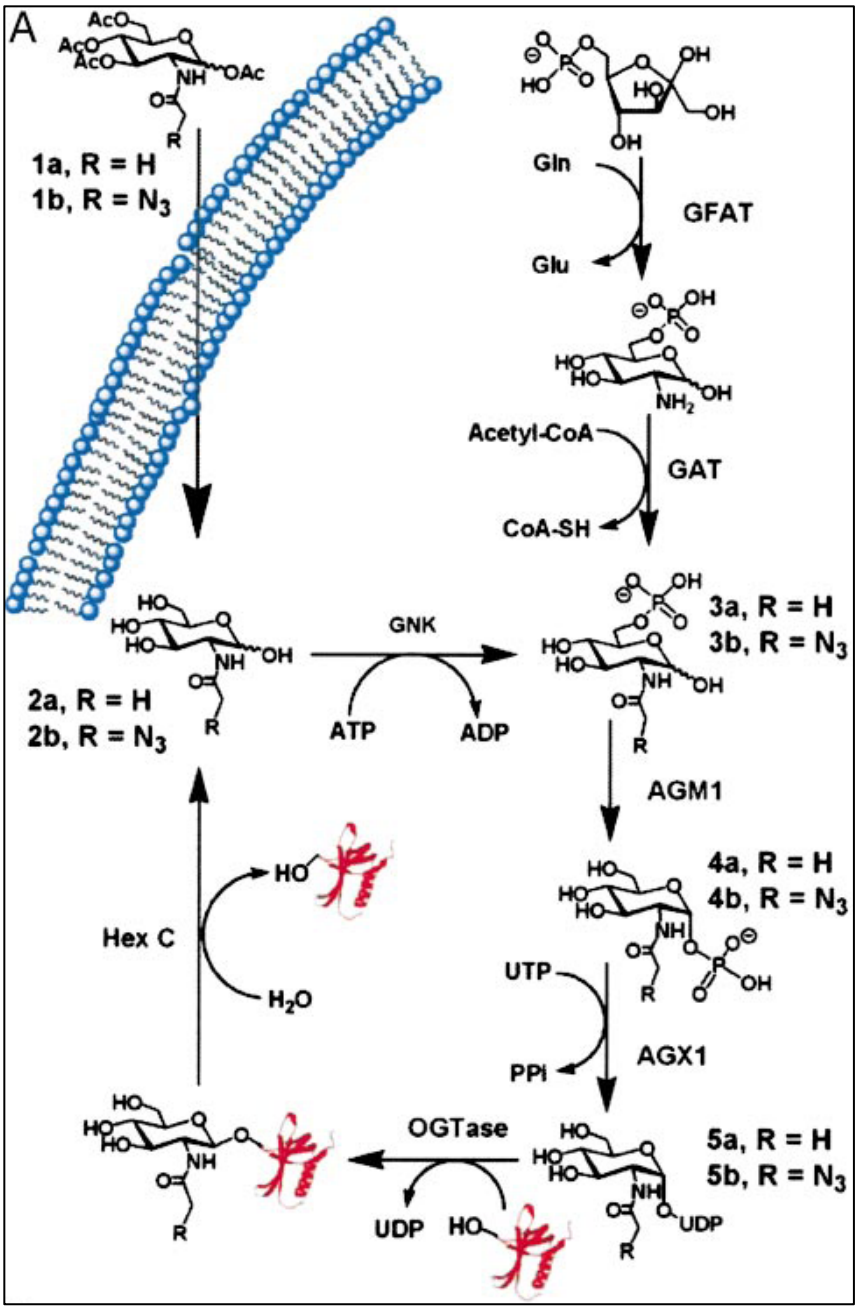

Figure 1.5: Figure reprinted from Vocadlo, D.J., Hang, H.C., Kim, E.J., Hanover, J.A. & Bertozzi, C.R. A chemical approach for identifying O-GlcNAc-modified proteins in cells. Proceedings of the National Academy of Sciences of the United States of America ***100***, *9116-9121 (2003). "Copyright (2003) National Academy of Sciences, USA."*

Hexosamine biosynthetic pathway showing de novo synthesis of UDP-GlcNAc and the salvage pathway through which incorporation of peracetylated GlcNAz occurs. The peracetylated derivative enters the cell via passive diffusion and is deacetylated in the cytosol by esterases.

Azido derivatives of GlcNAc have been used by Zhao and coworkers to survey cell lysates for *O*-GlcNAc modified proteins through a tagging via substrate strategy.[26] They employed Ac_4GlcNAz as a chemical reporter followed by Staudinger ligation with a biotinylated phosphine reagent to aid in enrichment and identification of GlcNAcylated proteins.

Although Ac_4GlcNAz was found to be incorporated into GlcNAcylated proteins, the incorporation level was not high because of the tolerance of the GlcNAc salvage pathway enzymes as demonstrated by Vocadlo et al. [25] Bertozzi and coworkers found that interestingly, Ac_4GalNAz, peracetylated azidogalactosamine, that they were using to label extracellular mucin type *O*-linked glycans was a better suited for *intracellular O*-GlcNAc.[27] The phenomenon was due to Ac_4GalNAz being directed to the GalNAc salvage pathway and converted to the activated donor sugar UDP-GalNAz and then subsequently being epimerized via the UDP-GlcNAc epimerase to UDP-GlcNAz. This apparent “cross-talk” between the GalNAc salvage pathway and the GlcNAc pathways was beneficial for better azido sugar incorporation for GlcNAc protein identification, producing up to three orders of magnitude more UDP-GlcNAz donor sugar from UDP-GalNAz compared to when Ac_4GlcNAz is used as the metabolic label. This can be attributed to the better tolerance of the unnatural azido sugar substrate by the enzymes of the GalNAc salvage pathway rather than the GlcNAc salvage pathway.

Results:

The finding that Ac_4GalNAz provides a better metabolic incorporation of azido sugar than Ac_4GlcNAz was employed to study *O*-GlcNAc modifications in our laboratory.

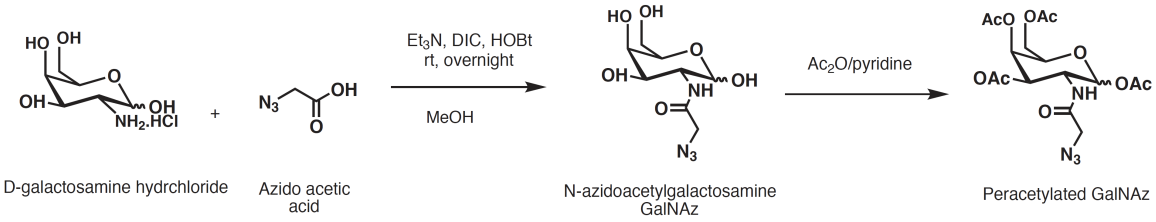

Figure 1.6: Synthesis of Ac_4GalNAz for metabolic labeling to detect O-GlcNAc modifications. The peracetylated sugar was includedd in cell culture media to facilitate metabolic labeling.

The strategy for studying *O*-GlcNAc modifications followed the following scheme:

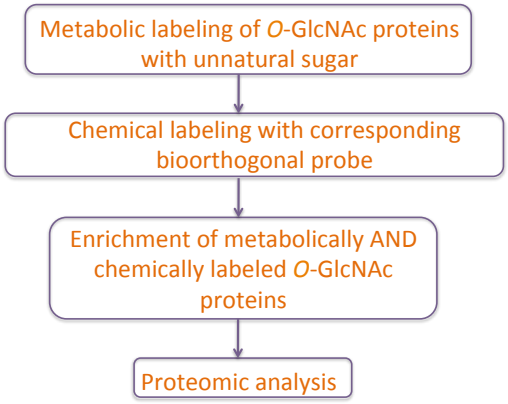

Scheme 1.1:Experimental scheme for study of O-GlcNAc modified proteins from metabolically labeled cell lysates

Given that azides can be modified using a variety of bioorthogonal reactions, we chose two reactions: Copper accelerated Azide Alkyne Cycloaddition (CuAAC) [28]and Staudinger ligation also known as Bertozzi-Staudinger Ligation[29].

However, to serve the objective of enriching for O-GlcNAc modified proteins, probes containing biotin were chosen. Biotin based chemical probes can be used as an affinity purification tag using the affinity between biotin and strept(avidin). The biotin-avidin interaction is a widely used affinity purification strategy but suffers from some drawbacks. The most noticeable one is that very harsh elution conditions are required to break the biotin-(strept)avidin interaction (K_d of 10^{-15} M). To overcome this, a derivative of biotin with lower affinity (K_d 10^{-13} M) called desthiobiotin was considered[30] to aid in the enrichment process. The desthiobiotin-(strept)avidin affinity can be disrupted by using an elution buffer containing free biotin which gently replaces the binding sites on (strept)avidin and affords elution of desthiobiotin labeled and hence O-GlcNAz labeled proteins.

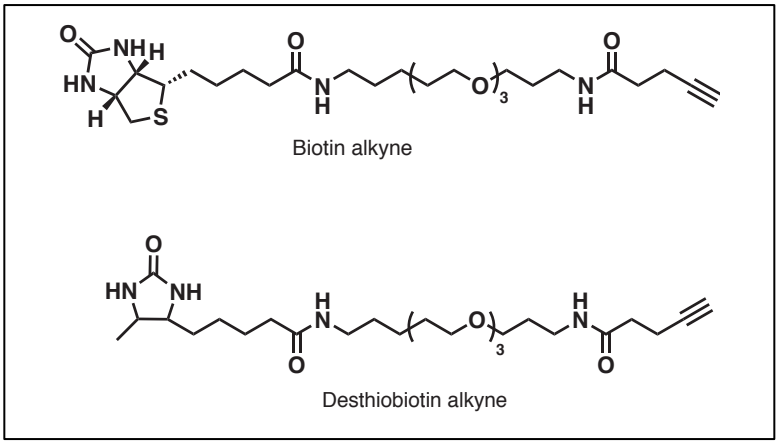

Figure 1.7: Desthiobiotin and biotin alkynes used for CuACC labeling of metabolically azide labeled lysates. Desthiobiotin is a derivative of biotin that has lower affinity for (strept)avidin and hence can be eluted gently using a solution of free biotin.

Using the desthiobiotin alkyne, enrichment of *O*-GlcNAc modified proteins was attempted via affinity capture using streptavidin agarose beads. Briefly, metabolically and chemically labeled lysates were captured over streptavidin beads, washed and eluted using 50 mM solution of free biotin. The eluates should contain *O*-GlcNAz and

desthiobition labeled proteins that can then be analyzed for O-GlcNAz modified proteins.

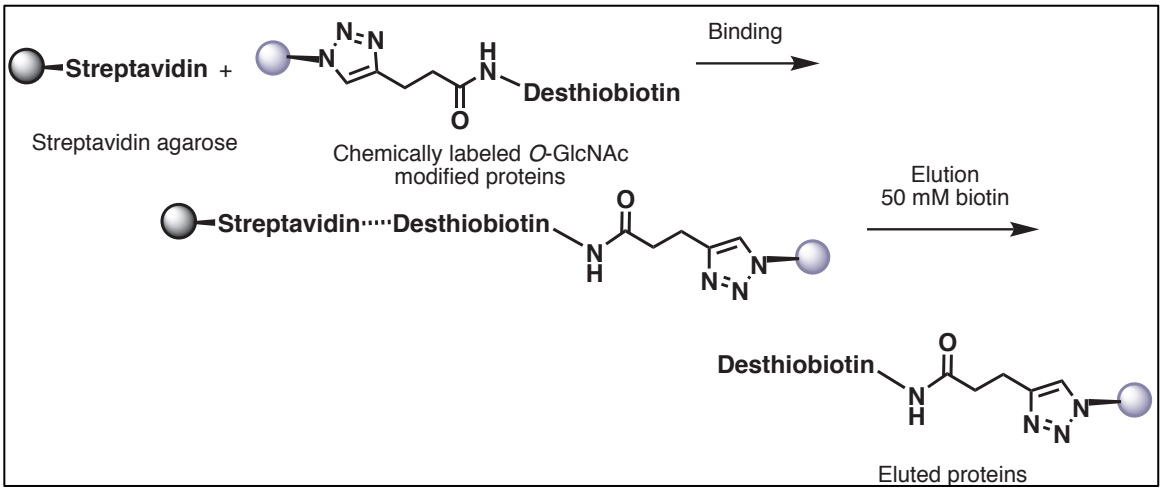

Figure 1.8: Procedure for capture of metabolically and chemically labeled proteins bearing desthiobiotin moieties with streptavidin agarose. The desthiobiotin and streptavidin interaction can be disrupted by a gentle elution buffer containing 50 mM free biotin.

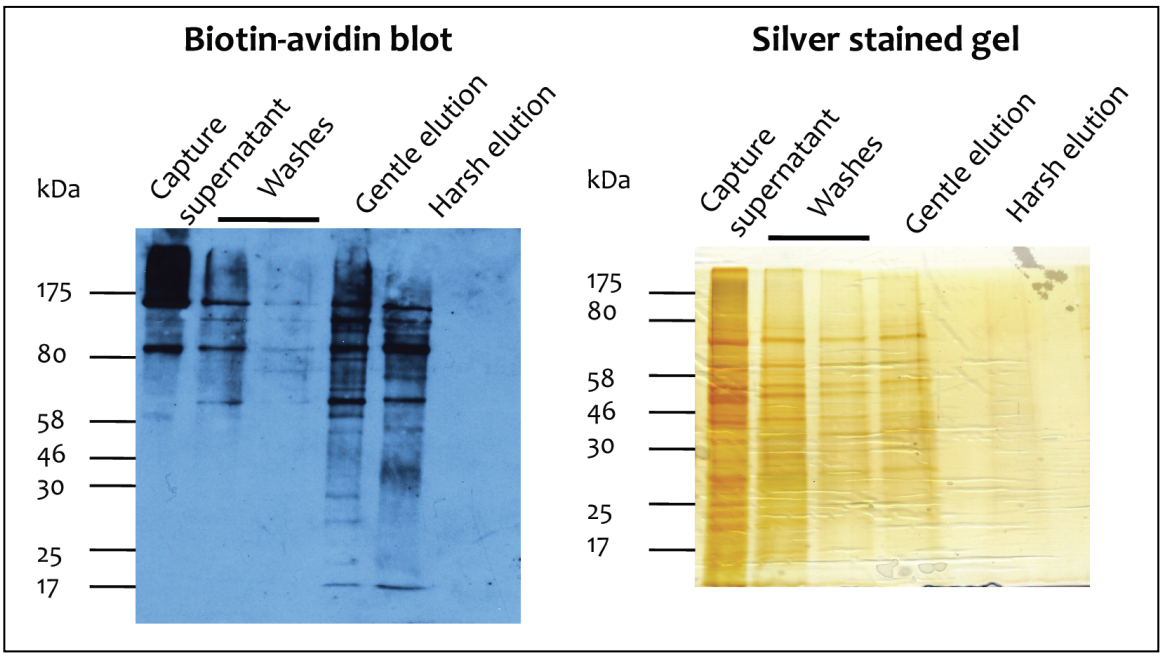

Figure 1.9 Results of enrichment with lysates metabolically labeled with Ac4GalNAz then chemically labeled with desthiobiotin alkyne. A anti-avidin blot shows signal from desthiobiotin labeled proteins and a silver stained gel shows total protein profile for the same samples. Gentle elution refers to 50 mM biotin

solution and harsh elution refers to a denaturing buffer containing urea, SDS and biotin[31] Poor enrichment and overwhelming background is evident form the silver stained gel on the right panel above.

The results of the enrichment show that although there is signal arising from desthiobiotinylated and hence *O*-GlcNAzylated proteins in the eluates on the anti-avidin blot, the protein profile in the silver gel indicates that the background overwhelms the signal. To investigate the cause of this low efficiency of enrichment, we sought to verify that the chemical labeling was proceeding satisfactorily.

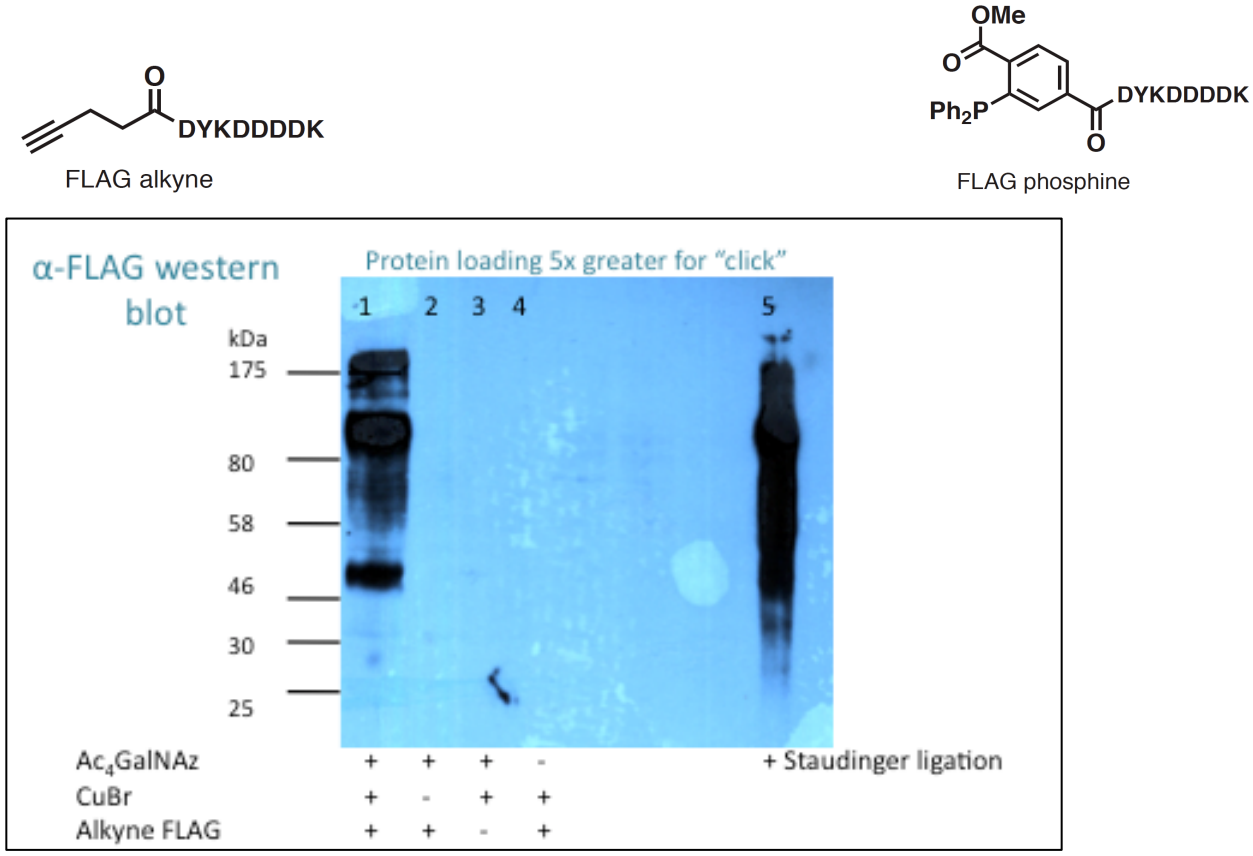

Figure 1.10: Bioorthogonal chemical labeling of azides introduced metabolically onto O-GlcNAc modified proteins. Azide containing cell lysates were chemically labeled with FLAG peptide containing probes via CuAAC or Bertozzi-Staudinger ligation. Subsequently lysates were run on SDS PAGE, followed by Western blotting using an anti-FLAG antibody.

From the above western blot it can be observed that the western signal obtained from CuAAC labeled lysates is significantly lower than that from Bertozzi-Staudinger ligation. The disparity between these two bioorthogonal reactions can be rationalized based on the fact that at the concentration regimes of the metabolically incorporated azide, the Staudinger ligation may be more efficient than the CuAAC. The poor enrichment using the CuAAC reaction was further illustrated by mass spectrometric analysis of eluates from metabolically and chemically labeled lysates and control lysates with no metabolic labeling. There was no enrichment of GlcNAzylated proteins over the background.

To further understand the results above the following rationale can be put forward. Given the incomplete knowledge of the kinetics of the CuAAC reaction in biomolecules, and given that the metabolically incorporated reactant (azido sugar) is always going to be lower in concentration than the exogenously added alkyne, it can be argued that metabolically incorporating an alkyne instead of an azide could significantly affect the reaction rate. Precedents exist for metabolically installed azides showing higher background after chemical labeling due to non specific interaction of the Cu (I) acetylide formed by the alkyne probe.[32] Therefore, exploring the O-GlcNAc modification using a metabolically installed alkyne sugar may prove to be beneficial.

Previously, alkyne analogs of sugars have been used for metabolic labeling. Wong and coworkers have employed alkynyl analogs of fucose and *N*-acetylmannosamine for the study of cell surface oligosaccharides.[33] Interestingly, Lemoine and coworkers have reported that alkynyl derivatives of *O*-GlcNAc were not incorporated into cell lysates.[34] This result is contradictory to our findings that alkynyl analogs are in fact incorporated into cellular proteins which was corroborated by the findings of Pratt and coworkers.[35]

We proceeded to synthesize alkynyl derivatives of both glucosamine and galactosamine, to metabolically label *O*-GlcNAc modified proteins in cells.

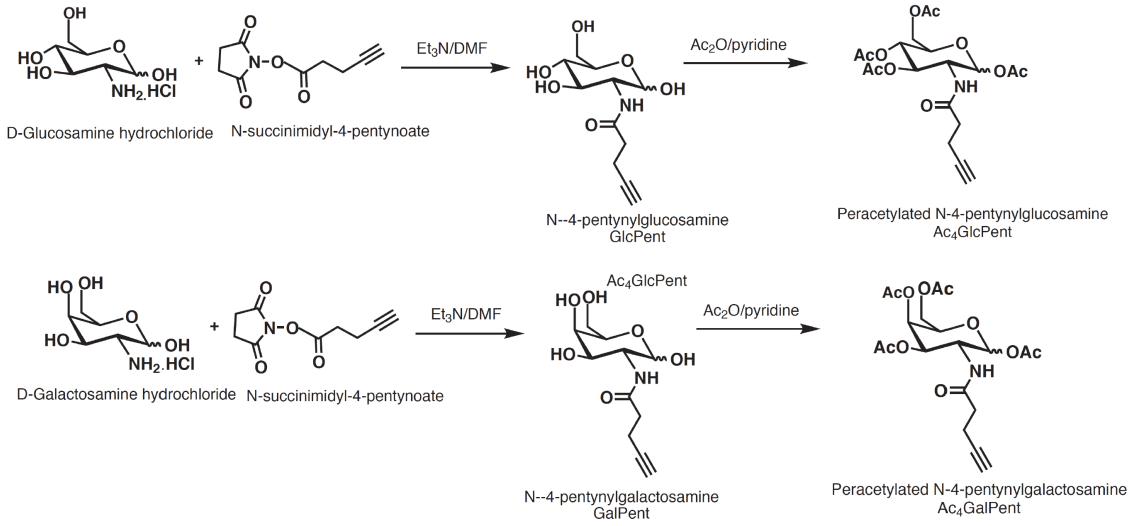

Figure 1.11: Synthesis schemes for alkynyl derivatives of glucosamine and galactosamine.

The alkynyl derivatives were included in cell culture media following the same procedure as the azido sugars, cells were lysed and lysates were chemically labeled with azido probes and analyzed via western blot of in gel-fluorescent scanning.

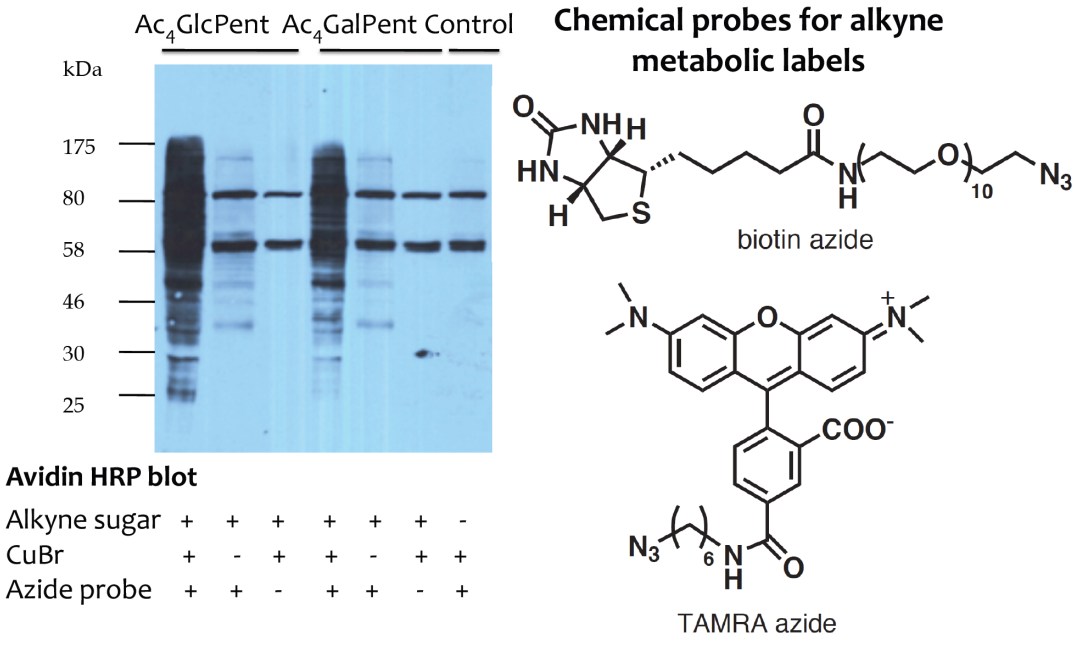

Figure 1.12: Biotin azide was used to chemically label metabolically labeled lysates, after which labeled proteins were detected on an anti-avidin blot. The bands observed in the negative control lanes we attribute to endogenous biotinylated proteins that were detected in all lysates, including metabolically unalabeled lysates. TAMRA (tetramethylrhodamine) azide can be used for in-gel-fluorescent scanning after chemical labeling and SDS PAGE.

Based on our results and those of Pratt and co-workers[35], given both azido and alkynyl chemical reporter mimics of *O*-GlcNAc, we chose the alkynyl analog of glucosamine i.e. Ac_4GlcPent or Ac_4GlcNAlk as the best choice for a metabolic labeling reagent.

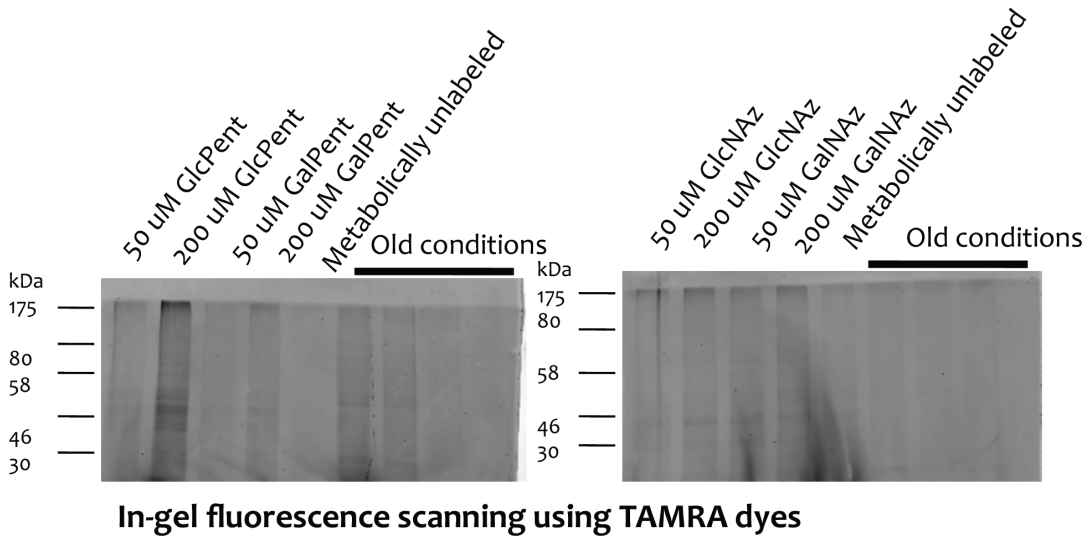

Figure 1.13: A range of concentrations of azido and alkynyl sugar analogs ranging from 50, to 200 μM final concentration for 16 h in cell culture were used, metabolically labeled cells were lysed, chemically labeled with TAMRA azide (see Figure 2.8 for structure) and then subjected to in-gel fluorescence. Old conditions depict 50 μM concentration of alkynl sugar analogs on the gel on the left and azido analogs on the gel on the right. 200 μM GlcPent was chosen as the best analog for metabolic labeling for future experiments.

The concentration of Ac_4GalNAz used by the Bertozzi group[27] was 50 μM with a labeling period of 72 h in cell culture. In contrast the Pratt group[35] used a 200 μM labeling concentration for a period of 16 h in cell culture.

The Pratt group's procedure was adopted for further experiments via a collaboration for enrichment of metabolically and chemically labeled lysates using their cleavable biotin

linker.[35] The enrichment strategy developed by them is detailed below. The results from these studies are detailed in Chapter 2.

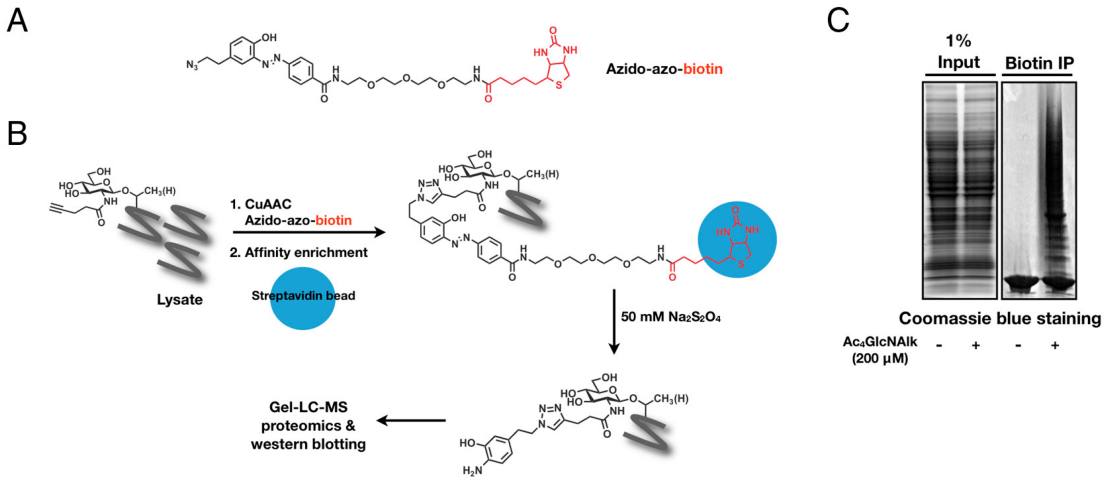

Figure 1.14: Zaro, B.W., Yang, Y.-Y., Hang, H.C. & Pratt, M.R. Chemical reporters for fluorescent detection and identification of O-GlcNAc-modified proteins reveal glycosylation of the ubiquitin ligase NEDD4-1. Proceedings of the National Academy of Sciences *(2011)*

Discussion:

Probing *O*-GlcNAc modifications using azido chemical reporter mimics yielded poor labeling via CuAAC but strong labeling with Bertozzi-Staudinger ligation. This phenomenon can be rationalized based on the fact that given the concentration regime of metabolically installed chemical reporter, i.e. *O*-GlcNAz, the Bertozzi-Staudinger ligation reaction may be more efficient than the CuAAC. Additionally, since the kinetics of the CuAAC in biomolecules are not clearly defined with a rate law, and given the literature precedence[32] showing increased background labeling with exogenous alkyne probe rather than azide probe, the choice of an alkynyl derivative of GlcNAc would be the best choice for probing this modification using chemical reporters.

However, the azido sugars do have the advantage of being accessible via a variety of bioorthogonal reactions, namely CuAAC, Strain promoted alkyne azide cycloaddition (SPAAC) and Bertozzi-Staudinger ligation. The increased background issue is offset by

this versatility and a decision of the best metabolic label has to be made taking into consideration all these factors.

Materials and methods:

Synthesis of *O*-GlcNAc derivatives

Synthesis of Ac_4GalNAz and Ac_4GlcNAz

Procedures detailed in Laughlin *et al.*[36] were used.

GlcNAz and GalNAz:

Azidoacetic acid was synthesized according to Luchansky et al.[37] D-glucosamine hydrochloride or D-galactosamine hydrochloride (1.5 g, 7.0 mmol) was added to a solution of azidoacetic acid (0.98 g, 9.7 mmol) in methanol (70 mL). Triethylamine (2.5 mL, 17 mmol) was added and the reaction mixture was stirred for 5 min at rt. The solution was cooled to 0 °C and N-hydroxybenzotriazole (HOBt, 0.86 g, 7.0 mmol) was added, followed by diisopropylcarbodiimide (1.76 g, 14 mmol). The reaction was allowed to warm to rt overnight, concentrated and the crude GlcNAz or GalNAz was purified using a gradient of 5-20% methanol-dichloromethane. The yield for GlcNAz was 70% and yield for GalNAz was 65%.

Ac_4GlcNAz and Ac_4GalNAz:

Acetic anhydride (1.0 mL, 11 mmol) was added to a solution of GlcNAz or GalNAz (0.025 g, 0.095 mmol) in pyridine (2 mL) and the reaction mixture was stirred overnight at room temperature. The solution was concentrated, resuspended in dichloromethane, washed with 1M HCl, saturated $NaHCO_3$ and saturated NaCl. Then the worked up solution was dried over $MgSO_4$, filtered and concentrated. If necessary, silica gel column chromatography was performed eluting with 2:1 hexanes:ethylacetate. The yield for Ac_4GlcNAz was 40% and yield for Ac_4GalNAz was 42%.

Ac_4GlcNAz

^{1}H NMR: 400 MHz, $CDCl_3$ mixture of anomers d: 1.99-2.16 (6H and 6H, overlap due to mixture of anomers), 3.86 (2H, s), 3.98-4.05 (2H, m), 4.19-4.23 (1H, m), 4.38-4.40 (1H, m), 4.41-4.44 (1H, m), 5.12-5.27 (2H, m), 6.14-6.15 (1H, d), 6.70-6.72 (1H, d)

^{13}C NMR: 400 MHz, $CDCl_3$ d: 20.49-20.79, 51.12, 52.21, 61.50, 67.51, 69.72, 70.32, 90.25, 167.43, 168.92, 169.33, 170.90, 171.02, 171.65

Ac_4GalNAz spectra:

^{1}H NMR: 400 MHz, $CDCl_3$ mixture of anomers d: 2.01-2.02 (6H), 2.16-2.17 (6H), 3.93 (2H, s), 4.06-4.10 (2H, m), 4.23- 4.27 (2H, m), 4.65-4.71 (1H, m), 5.22-5,26 (1H, dt), 5.43-5.44 (1H, d), 6.22 (1H, d) 6.27 (1H, d)

^{13}C NMR: 400 MHz, $CDCl_3$ d: 20.61-20.87, 47.01, 52.45, 61.20, 66.55, 67.60, 68.63, 90.91, 169.92-170.96

Synthesis of Ac_4GlcPent and Ac_4GalPent:

1,3,4,6-tetra-O-acetyl-N-pentynylglucosamine (Ac_4GlcPent):

a) N-succinimidyl 4-pentynoate: to a stirred solution of 4-pentynoic acid (1 g, 10.2 mmol) and *N*-hydroxysuccinimide (1.18 g, 10.2 mmol) in dry dichloromethane (100 mL) at 0 °C, dicyclohexylcarbodiimide (DCC) (2.10 g, 10.2 mmol) was added. The resulting mixture was stirred at room temperature for 5 h. The urea formed was filtered out and the filtrate was concentrated and re-dissolved in ethyl acetate (200 mL). The solution was washed with 5% aqueous $NaHCO_3$ (2 x 50 mL), water (50 mL) and brine (50 mL). The organic layer was separated, dried over anhydrous MgSO4 and concentrated. Recrystallization with dichloromethane and hexanes yielded the desired product with no further purification necessary, yield was 90%

^{1}H NMR: 300 MHz, $CDCl_3$ d 2.03 (1H, t), 2.60 (2H,td), 2.83 (4H, s) 2.87 (2H, t)

b) N-4-Pentynylglucosamine

The scheme provided Hsu *et al*[33] was followed: Briefly, a mixture of d-glucosamine hydrochloride (863 mg, 4.0 mmol), *N*-succinimidyl 4-pentynoate (781 mg, 4.0 mmol),

triethylamine (1.67 ml, 12.0 mmol) in DMF (31 ml) was stirred at room temperature overnight. The reaction mixture was concentrated *in vacuo*, and the residue was purified by flash column chromatography (gradient of 10-20% MeOH/CH_2Cl_2) to give *N*-4-Pentynoylglucosamine (GlcPent), yield 40%

Thereafter, acetic anhydride (1.0 mL, 11 mmol) was added to a solution of GlcPent (0.220 g, 0.849 mmol) in pyridine (2 mL) and the reaction mixture was stirred overnight at room temperature. The solution was concentrated, resuspended in dichloromethane, washed with 1M HCl, saturated $NaHCO_3$ and saturated NaCl. Then the worked up solution was dried over $MgSO_4$, filtered and concentrated. If necessary, silica gel column chromatography was performed eluting with 2:1 hexanes:ethylacetate. The yield for Ac_4GlcPent was 34%.

The same procedure was followed for Ac_4GalPent, substituting galactosamine hydrochloride in the first step. GalPent yield was 35%, Ac_4GalPent was 28%.

Ac_4GlcPent

^{1}H NMR: 400 MHz, $CDCl_3$ (mixture of anomers) d: 1.98-2.13 (13H), 2.13 (3H, s), 2.28-2.31 (2H, m), 2.41-2.42 (2H, m), 3.95-3.99 (2H, m), 4.03-4.08 (1H, m), 4.08-4.19 (1H, td), 4.46-4.49 (2H, m), 5.91-5.93 (1H, d), 6.12-6.13 (1H, d)

^{13}C NMR: 400 MHz, $CDCl_3$ d: 14.52-14.67, 20.40-20.80, 34.40, 35.21, 50.76, 52.52, 61.42, 61.54, 67.45, 67.85, 69.31-69.55, 70.37, 72.31, 72.54, 82.38, 82.48, 90.42, 92.29, 168.52, 169.00, 169.18, 169.37, 170.55, 170.79, 170.89, 171.02, 171.39

Ac_4GalPent

^{1}H NMR: 400 MHz, $CDCl_3$ (mixture of anomers): 1.9-2.1 (12H), 2.35-2.48 (4H, m), 3.44-3.67 (2H, m), 4.10-4.30 (3H, m), 4.74-4.80 (1H, td), 5.23-5.24 (1H,d), 5.72-5.74 (1H,d) 6.20 (1H, d)

^{13}C NMR: 400 MHz, $CDCl_3$ d: 14.19-14.75, 20.74-21.05, 35.23, 46.67, 47.21, 60.41, 60.64, 62.42, 66.85, 67.73, 67.90, 69.56, 69.94, 70.18, 71.47, 82.56, 82.60, 91.29, 91.45, 168.90, 169.00, 171.14- 171.24

FLAG alkyne and phosphine: FLAG peptide was synthesized by Fmoc-protected Solid phase peptide synthesis according to procedures detailed in Laughlin et al.[36] Briefly, all peptides were synthesized by standard Fmoc SPPS protocol using diisopropyl carbodiimide and HOBt to form activated esters. Alkyne functionalized peptides were produced by on-bead *N*-terminal functionalization with propynoic acid. Phosphine FLAG was obtained by on-bead *N*-terminal derivitization with 2-(Diphenylphosphino)terephthalic acid 1-methyl 4-pentafluorophenyl diester (Sigma-Aldrich 679011). During all deblocking steps 0.1 M HOBt was added to the 20% piperidine solution to alleviate aspartamide formation.

Desthiobiotin alkyne and Biotin alkyne were synthesized by Marian S. Fernando

Biotin azide:

This compound was a gift from the Sampson lab at Stony Brook University.

Briefly, the procedure used for synthesis was as follows:

Biotin-NHS: N-hydroxysuccinimide (1.02 µmol, 117 mg), biotin (1.02 µmol, 250 mg) and DCC (1.02 µmol, 211 mg) were dissolved in 7 mL dry DMF, and the reaction was stirred for 16 h at rt. After filtration and evaporation of solvent, the product was precipitated with Et2O, and was washed with a mixture of cold Et2O/2-propanol (1:1).

Biotin-PEG$_{10}$-N$_3$. Biotin-NHS (0.31 mmol, 107 mg) and O-(2-Aminoethyl)-O′-(2-azidoethyl)nonaethylene glycol (0.21 mmol, 110 mg) were dissolved in 1 mL dry DMF. DIEA (0.31 mmol, 56 µL) was added to the mixture, and the reaction was stirred for 16 h at rt. After evaporation of solvent, the product was precipitated with Et2O. Silica gel chromatography eluting with CH_3OH:EtOAc/1:1 yielded Bio-PEG10-N_3. ESI mass spectrometry was used to identify the compound, calculated $[M+H]^+$ was 752.4, experimental was 753.4.

TAMRA-azide and alkyne:

TAMRA-azide was purchased from Lumiprobe LLC, cat # 17130 as a 10 mM stock in DMSO.

TAMRA alkyne was synthesized by Partha S. Banerjee

Cell culture:

Jurkat cell lines (human leukemic cell line) were maintained in a 37 °C/5% CO2 incubator, in RPMI 1640 media supplemented with 10% fetal bovine serum and 1% penicillin-streptomycin antibiotic. Cells were maintained between densities of $1x10^6$ to $2x10^6$.

Metabolic labeling procedure:

Metabolic labeling procedure for initial experiments with azido sugars was followed according to Boyce *et al*. [27] Briefly, 50 µL Ac_4GalNAz stock solution (50 mM) in methanol was coated onto cell culture flasks by allowing methanol to evaporate. Sugar coated cell culture flasks were used to culture Jurkat cells as mentioned above. The final concentration of azido sugar was 50 µM in the media and metabolic labeling was carried out for 72 h. For later experiments comparing the alkynyl sugars Ac_4GlcPent and Ac_4GalPent to azido sugars as in figure 1.13, labeling times were reduced to 16 h and final concentration of alkynyl sugars in cell culture media was increased to 200 µM. Ac_4GlcPent and Ac_4GalPent stock solutions of 200 mM concentration were prepared in DMSO, appropriate volumes of stock solutions were introduced into the cell culture media for metabolic labeling.

Cell lysis procedure:

Jurkat cells were pelleted by centrifugation at 4 °C for 5 min at 5,000 rpm, followed by 2 washes with ice-cold PBS. Cell pellets were then resuspended in 1% NP-40 lysis buffer [1% NP-40, 150 mM NaCl, 50 mM triethanolamine (TEA) pH 7.4] with protease inhibitor cocktail (Calbiochem Cat# 539134, protease inhibitor cocktail set III, EDTA free) for 10 min and then centrifuged at 4 °C for 10 min at 10;000 × g. The supernatant or soluble lysate was used for all chemical labeling experiments.

Chemical labeling procedure:

Staudinger ligation on azido sugar labeled lysates:

Staudinger ligation was carried out by mixing virus samples with final concentration of 500 μM FLAG phosphine reagent and PBS, according to the procedure detailed in Laughlin *et al.*[61] Reactions were allowed to proceed at rt overnight.

CuAAC reaction on azido and alkynyl sugar labeled lysates:

Reactions consisted of metabolically labeled lysates, with a final concentration of 100 μM corresponding alkyne or azide probe, 1 mM sodium ascorbate, 100 μM tris[(1-benzyl-1-H-1,2,3-triazol-4-yl)methyl]amine ligand (TBTA) (10 mM stock in DMSO) and 1 mM $CuSO_4$ in the reaction mixture. Reactions were allowed to proceed for 1h at rt.

In-Gel Fluorescence Scanning:

Metabolically and chemically labeled lysates were separated via SDS-PAGE, the gel was incubated in destaining solution (50% methanol, 40% H2O, 10% glacial acetic acid) for 5 min followed by water for an additional 5 min prior to scanning on a Typhoon scanner with excitation filter at 532 nm and emission filter at 580 ± 15 nm.

NMR Spectra

Ac4GlcNAz

Proton:

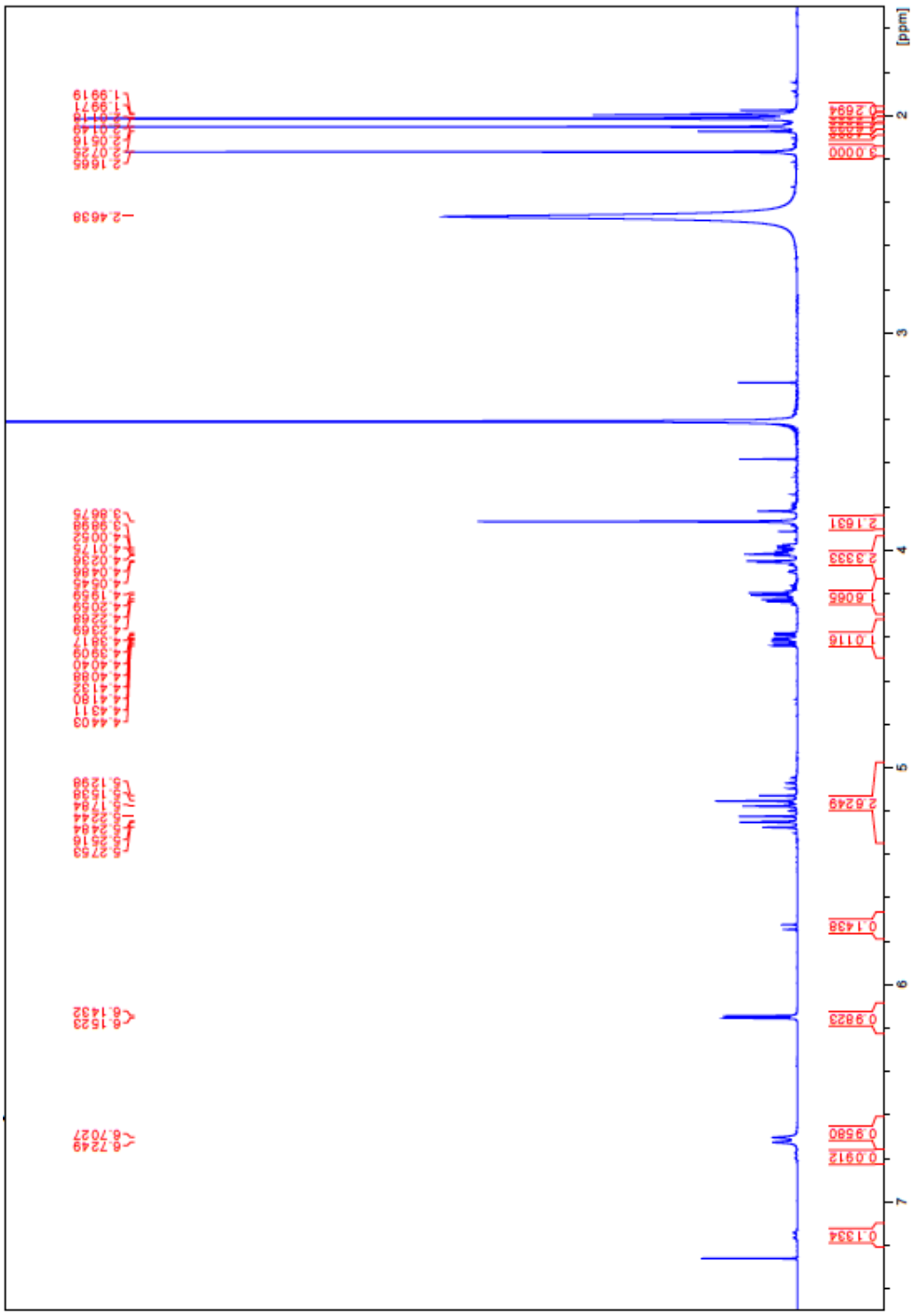

Carbon:

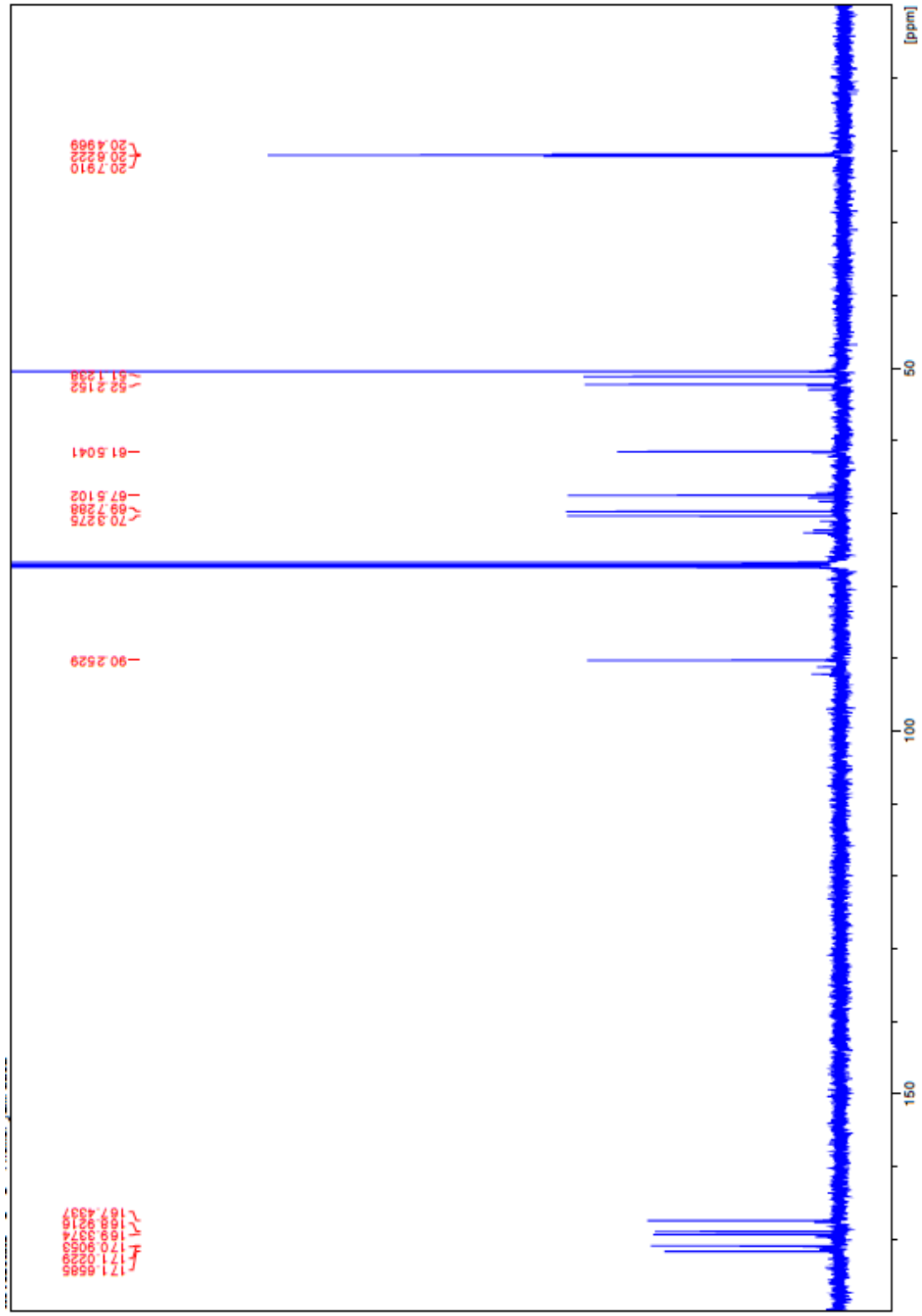
20.7910
20.8222
20.4969
52.2152
51.1238
61.5041
67.5102
69.7288
70.3275
90.2529
171.8586
171.0259
170.9955
168.9374
168.9218
167.4337
[ppm]
50
100
150

Ac4GalNAz

Proton:

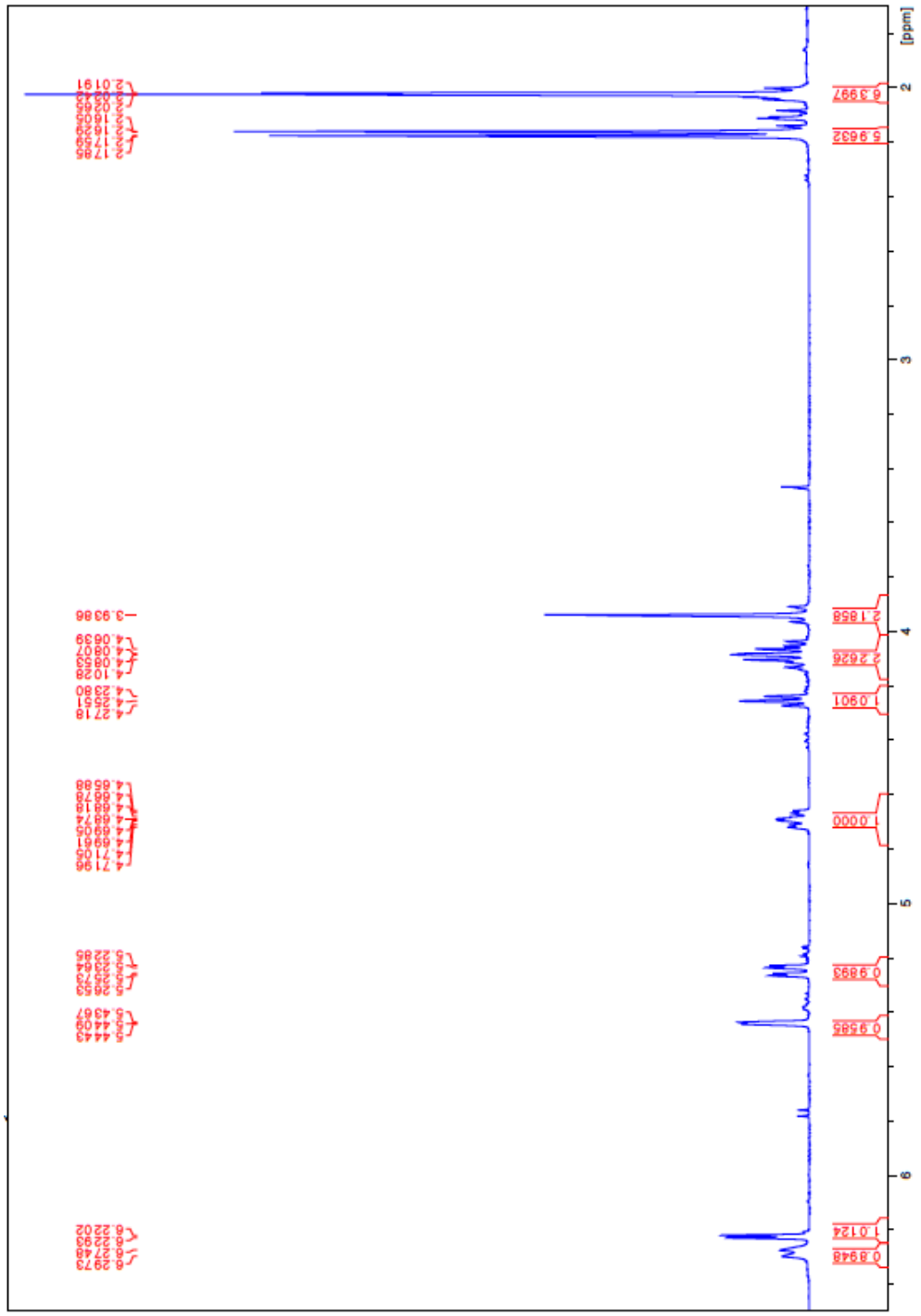

Carbon

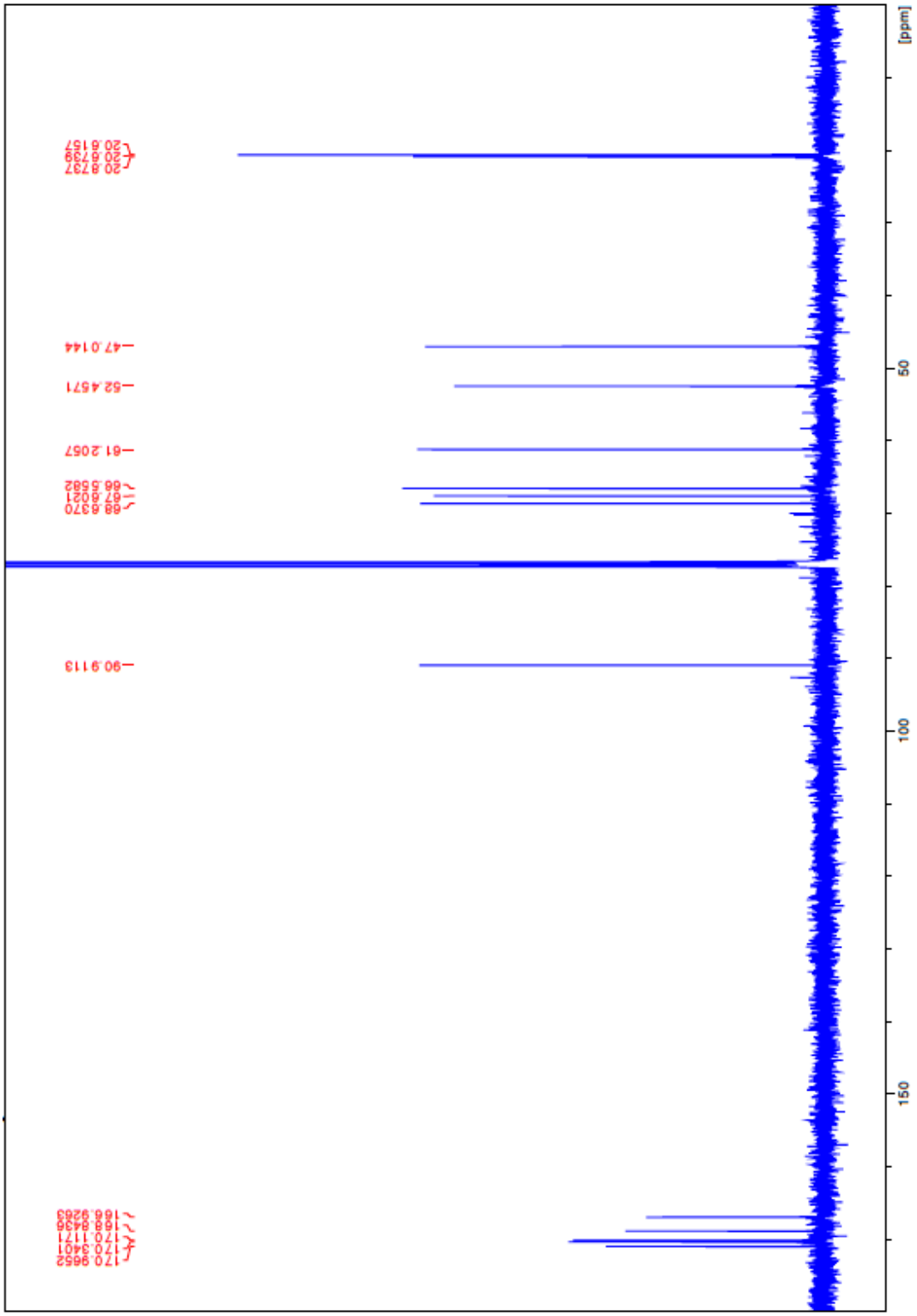
20.8157
20.8739
20.8737
47.0144
52.4571
61.2057
66.5582
67.6021
68.6370
90.9113
166.9263
168.8436
170.1171
170.3401
170.9652
[ppm]
50
100
150

Ac4GlcPent also called Ac4GlcNAlk

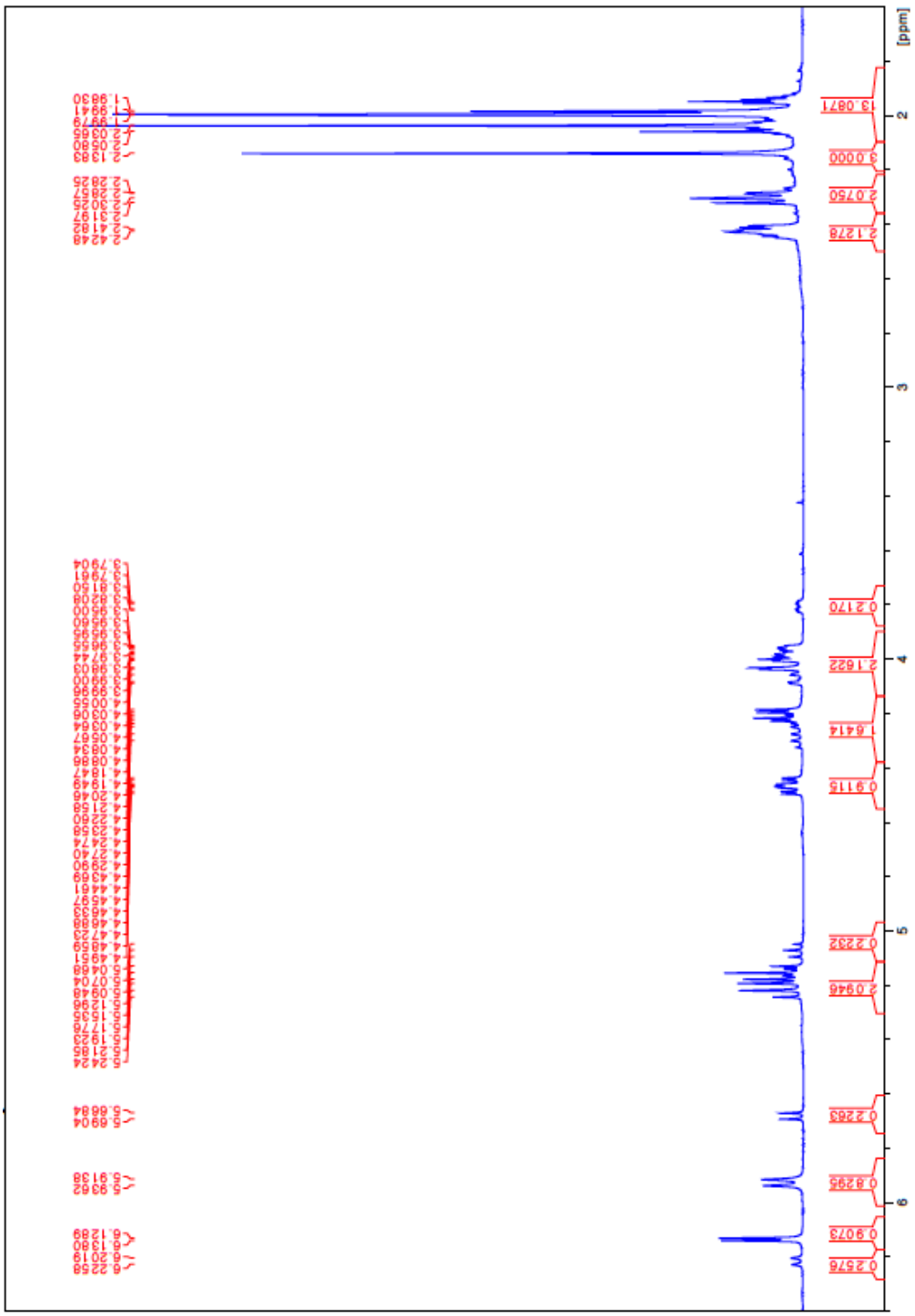

Carbon

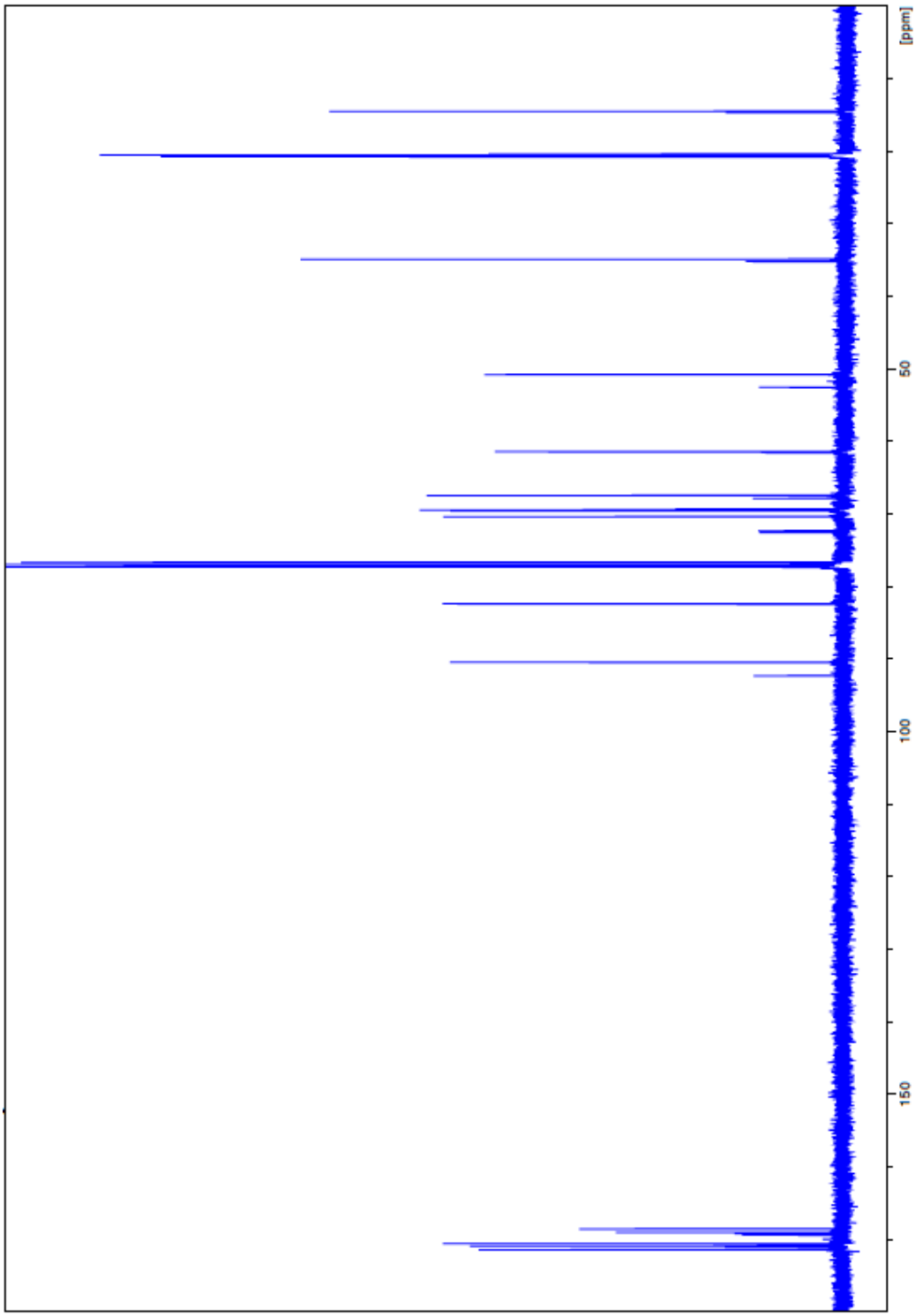

Ac4GalPent also called Ac4GalNAlk

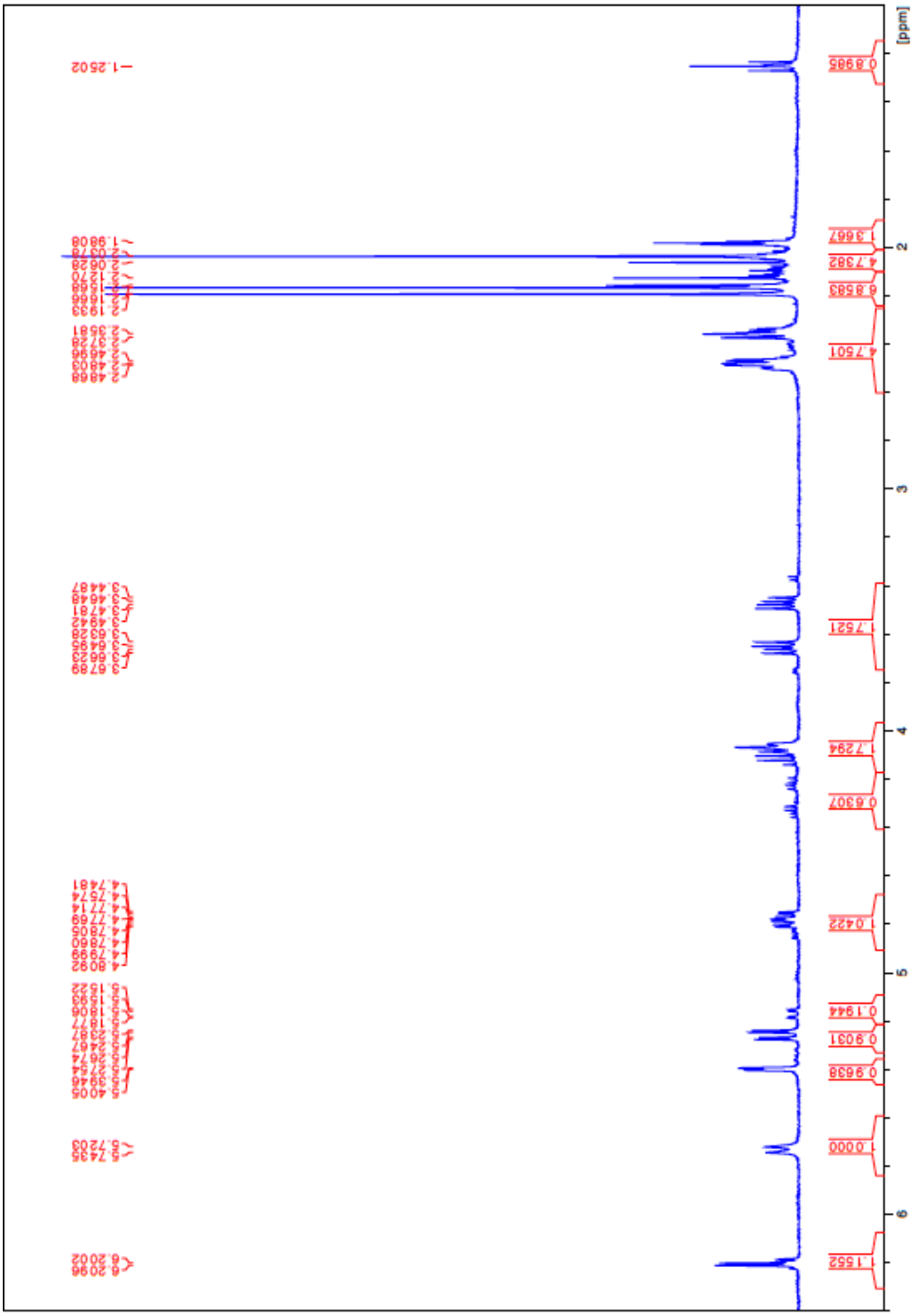

Carbon

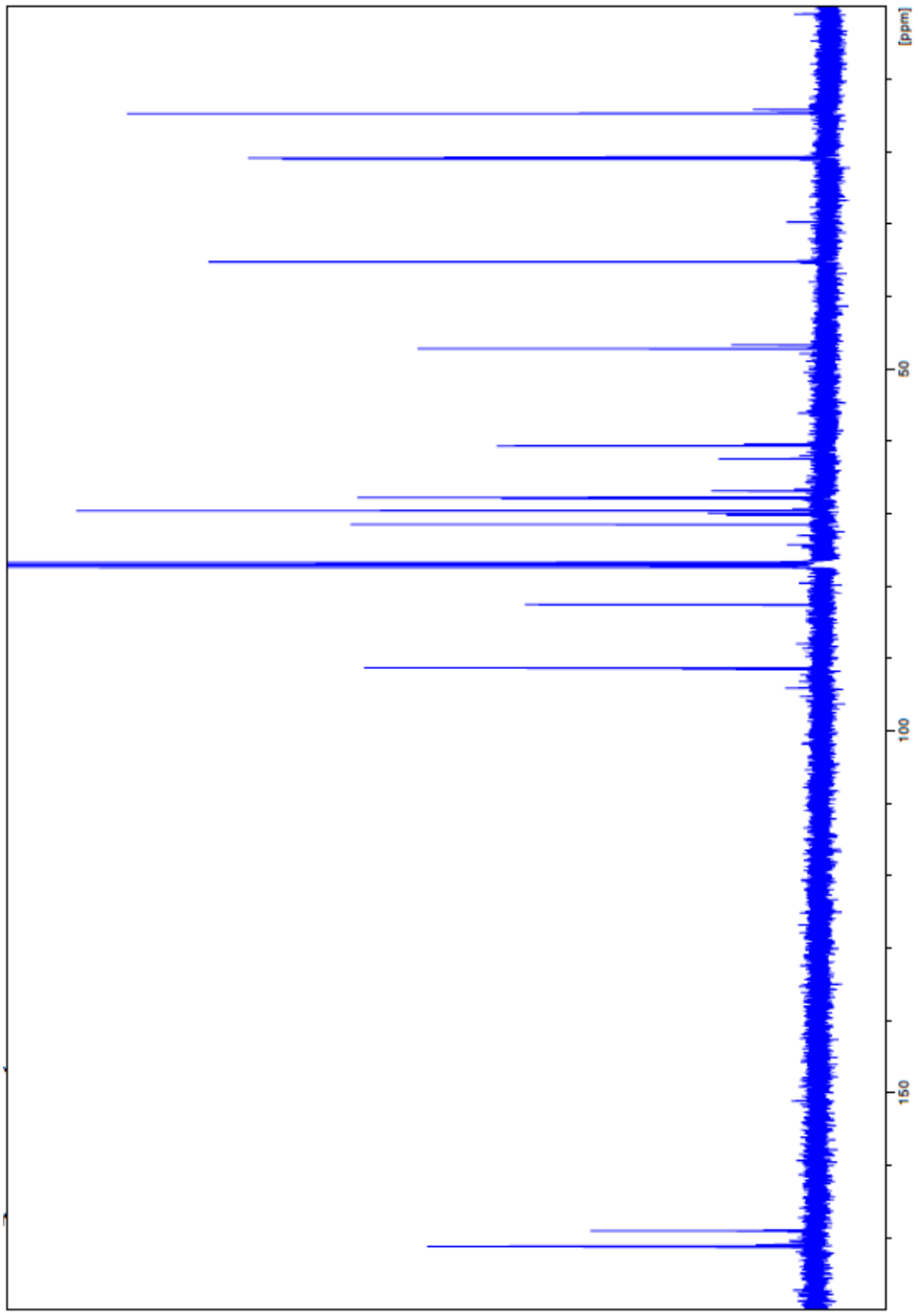

Chapter 2

Probing *O*-GlcNAc modifications during T-cell activation

Introduction:

Linking *O*-GlcNAc modifications to lymphocytes:

The immune system in multi-cellular organisms can be broadly divided into the innate and adaptive arms. The innate immune system provides the first line of defense against a pathogenic infection or any kind of foreign agent. The innate immune response is one that occurs based on the recognition of common patterns and motifs associated with the physical structure of pathogens and is not a specific response. It is mediated by cells that circulate in the vascular system of the organism like monocytes, neutrophils, macrophages etc. and occurs immediately upon infection. On the other hand, the adaptive arm of the immune system requires more time to develop and needs specific gene expression and production of antibodies against the pathogen. T and B lymphocytes are the main cells responsible for regulating the adaptive immune system. They are responsible for interfacing with the innate immune system to process the nature of the infection or pathogen and then undergo changes in gene expression. This in turn triggers a series of chemical and genetic signals that cause maturation and proliferation of specific cells that can eradicate the infection. The process by which this occurs requires a complex and inter-related set of signaling mechanisms. The first step in this process is usually triggered at the cell surface of the T or B lymphocyte conduct information from their cell surface T and B cell receptors (TCR or BCR) to the interior of the cell. After stimulation of the TCR or BCR, a series of phosphorylation and de-phopshorylation events occur via various cytosolic signaling proteins. This signal cascade culminates in a change in transcriptional activity at the nuclear level leading to change in protein expression and hence change in cellular behavior.

Given this scenario, a post-translational modification like *O*-GlcNAc could prove to be versatile and useful in modulating protein structure and function in a dynamic fashion. Therefore, it is plausible that signaling cascades usually involving phosphorylation may also involve *O*-GlcNAc to transmit information based on external stimuli that directs cellular physiology.

The earliest reported instance linking *O*-GlcNAc modifications with lymphocyte activation was from 1991, about 7 years after the discovery of *O*-GlcNAc in 1984. Hart and coworkers observed[38] that there was an rapid change in global levels of *O*-GlcNAc modifications in T lymphocytes that were treated with agents known to cause activation. Known activators of T cells include phorbol 12-myristate 13-acetate (PMA) and ionomycin and concavalin A. The change in *O*-GlcNAc levels with PMA/ionomycin or concavalin A treatment was rapid after activation and returned to control levels after a few hours. Interestingly, after activation while *O*-GlcNAcylated nuclear proteins were increased, returning to control levels after a few hours, there was a concomitant decrease in a subset of cytosolic *O*-GlcNAcylated proteins, which also returned to control values after few hours. This was the first clue that *O*-GlcNAc may have some role to play in the early stages of T cell activation.

Thereafter, the link between *O*-GlcNAc and lymphocyte activation was further strengthened by the finding that the transcription factor NFκB, which controls transcription of a variety of cytokine genes important for T cell activation was *O*-GlcNAc modified.[39] Guerini and coworkers then showed that OGT was required for the activation of T and B lymphocytes[40] with clear evidence that in addition to NFκB, another master regulator of transcription NFAT, was also *O*-GlcNAc modified and that their *O*-GlcNAc state might influence their nuclear translocation and hence control transcriptional activity. These two transcription factors are also phosphorylated and changes in phosphorylation modulate their location and function in the cell. Introducing the *O*-GlcNAc modification into the picture provides a second layer of control and complexity to their regulation that could impact the process of T cell activation. This work remains the strongest link between the *O*-GlcNAc modification and the T cell

activation signaling pathways leaving a lot of unanswered questions as to how the dynamics of these processes is dictated.

Other evidences of *O*-GlcNAc involvement in the immune system include the finding that neutrophils stimulated with a chemotactic peptide show increased *O*-GlcNAc modified proteins[41] and that motility signaling is influenced by *O*-GlcNAc modifications.[42]

These evidences build up a strong case for investigating the dynamics of *O*-GlcNAc modified proteins during T cell activation. To begin to elucidate such a complex network of interlacing signaling pathways, it is important to identify the players i.e. signaling proteins that are *O*-GlcNAc modified. The fact that phosphorylation plays a pivotal role in these signaling pathways provides an added layer of complexity because *O*-GlcNAc and phosphorylation can both target the same amino acid residues. A few key points have to be noted before embarking on investigating the *O*-GlcNAc dynamics of T cell activation: firstly, the flux in *O*-GlcNAc following T cell activation, as first reported[38] was found to be transient and it has also been reported that in Jurkat cells (immature T-lymphocyte cell line) and in primary T cells that *O*-GlcNAc modification on NFAT increases after TCR activation[40,43], lasts for around 15 minutes and then decreases rapidly. The increase in *O*-GlcNAc modification also coincides with nuclear translocation in lymphocytes. Given that traditionally, NFAT is considered to be dephosphorylated to expose a nuclear localization signal, it is possible that *O*-GlcNAc modification of NFAT stabilizes the dephosphorylated form and therefore controls the localization. Therefore, it would be interesting to gain more insight into how *O*-GlcNAc plays into the more characterized phosphorylation dynamics during T cell activation.

Overview of T cell signaling networks:

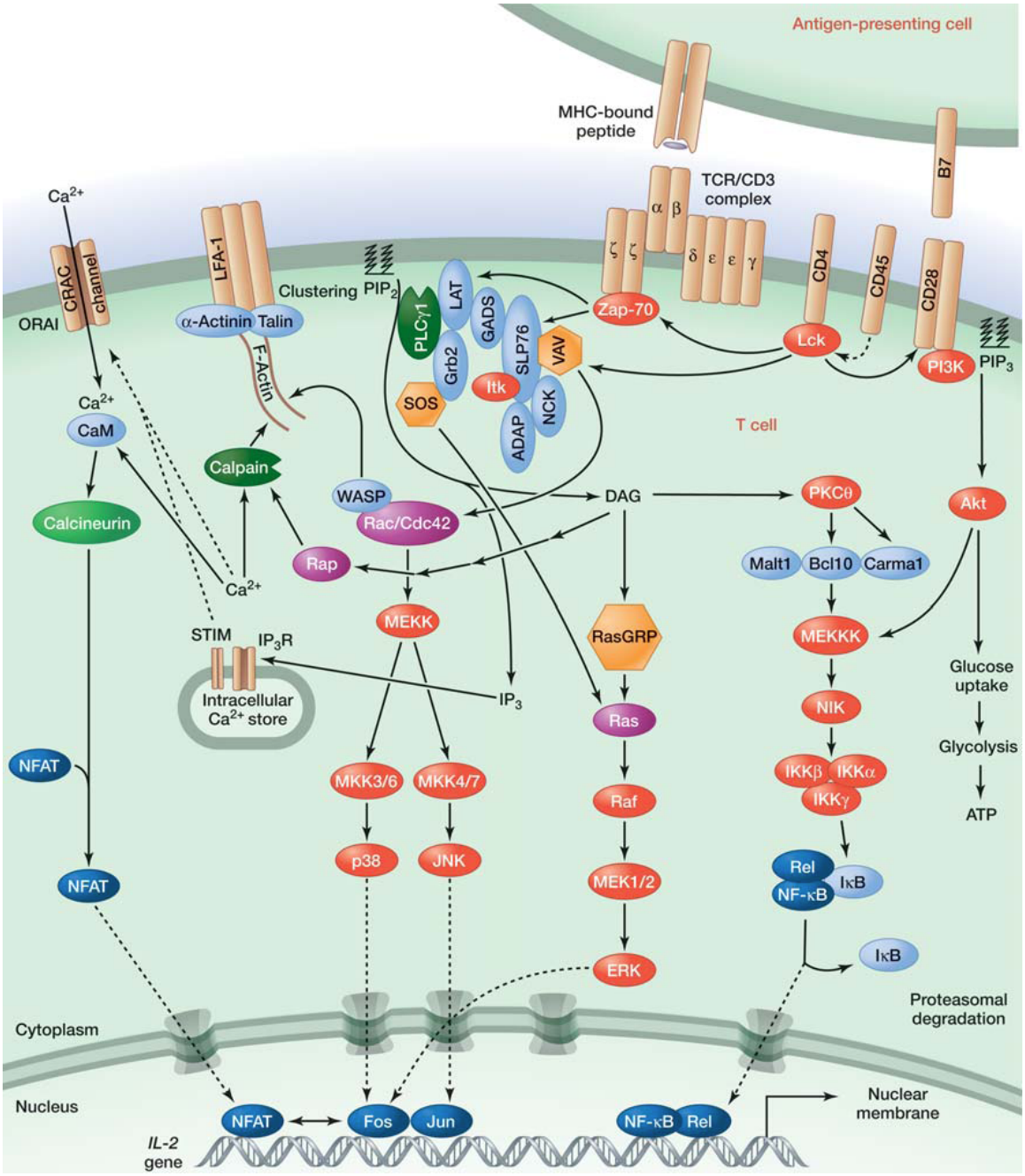

Figure 2.1: Samelson, L.E. Immunoreceptor Signaling. Cold Spring Harbor Perspectives in Biology 3(2011) doi: 10.1101/cshperspect.a011510 Copyright © 2011 Cold Spring Harbor Laboratory Press; all rights reserved.

This figure shows the T cell signaling network from the cell surface T cell receptor to the nucleus with transcription factor recruitment. The phosphorylation events that occur in downstream of TCR activation are also shown.

The signals for T cell activation originate at the cell surface either via engagement of the TCR with an antigen presenting cell or by other receptor activated events. Calcium channel opening can also trigger signaling events that ultimately cause changes in transcriptional activity. The event that occurs first after receptor engagement is activation of tyrosine kinases, which leads to a series of phosphorylation cascades. In the figure shown above NFAT and NFκB are depicted in the nucleus where they perform their role as transcription factors and regulate the transcription of cytokines and other T cell maturation signals. This marks the response to the stimulus received at the cell surface and the fact that *O*-GlcNAc modification of these transcription factors affects their activity underscores the need to understand other targets of *O*-GlcNAc in this complex and multi-layered signaling network.

Activators of T cell signaling:

For T cell activation studies, the most commonly used immortalized cell line is the Jurkat cell line. It is a human leukemic cell line generated from a male subject with leukemia. Common methods to induce T cell activation in cell culture containing Jurkat cells include the use of anti-CD3 antibodies to mimic the receptor engagement process and the use of mitogens like phorbol esters and lectins. The mitogens used by Hart and coworkers[38] to show *O*-GlcNAc flux in cells was the combination of phorbol 12-myristate 13-acetate (PMA) and ionomycin, administered together, or Concavalin A administered alone. The first combination is known to act on T cells by by-passing the signaling cluster proximal to the TCR[44], instead they act on the PLCγ and the calcium channel ORAI. PMA like other phorbol diesters, is known to activate Protein kinase C[45,46] (PKCθ). Ionomycin is a calcium ionophore (i.e. can induce calcium ion transport across a lipid membrane) and therefore also activates PKCθ.[47] Ionomycin also serves as an ionophore for the calcium channel ORAI[48] that leads to activation of Calcineurin, a

phosphatase that ultimately affects NFAT activity. Concavalin A is a plant lectin extracted from jack bean that causes activation of T cells by associating with T-cell receptors.[49] Depending on the mode of activation chosen, different sub-networks in the T-cell signaling network shown in Figure 2.1 can be invoked.

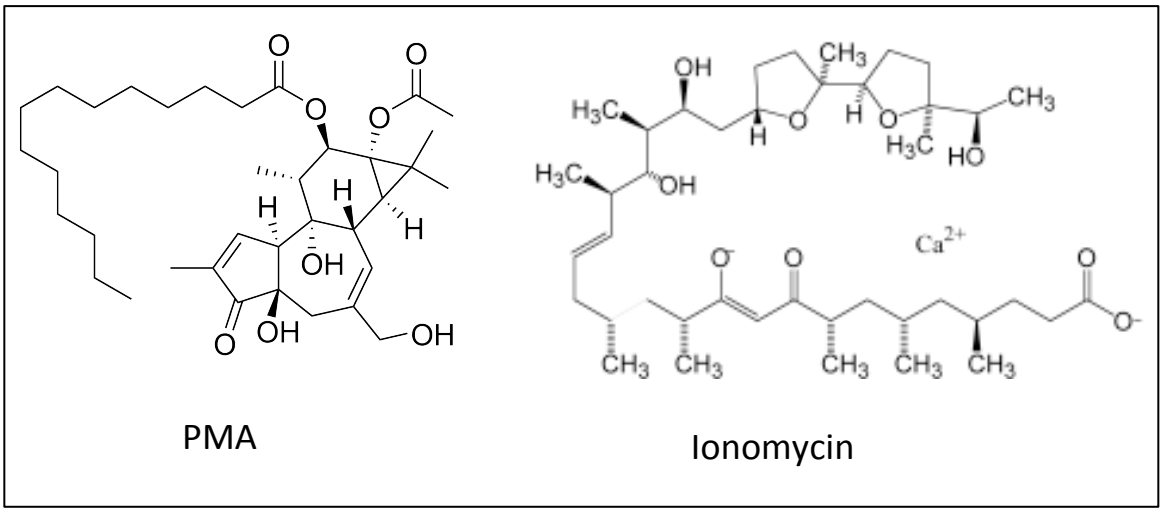

Figure 2.2: Structures of PMA and ionomycin, activators of PKCθ

Chemical approach to investigating the dynamics of *O*-GlcNAc in T cell

Given the evidence of involvement of OGT and *O*-GlcNAc modifications in the T-cell activation process, we sought to use the chemical reporter strategy using unnatural sugar mimics of *O*-GlcNAc to probe the dynamics in the system. The alkynyl reporter GlcNAlk developed by Pratt and coworkers[35] was used as the method for enrichment of *O*-GlcNAc modified proteins from activated Jurkat cells. The question we sought to answer using this strategy was to identify the proteins that are *O*-GlcNAc modified immediately following activation to aid in understanding how this post-translational modification could impact the process and signaling involved in T-cell activation.

Results:

Activation of T cells:

The method of activation of Jurkat cells was chosen based on literature precedence from the work of Hart and coworkers[38] and Guerini and coworkers.[40] A combination of PMA and ionomycin was used in both these studies. The other deciding factor for our experiments was to zoom in on a time window around activation where we could have the most *O*-GlcNAc modifications as this modification has been observed to be transient in T cells. Based on Guerini and coworkers observation[43] that it is likely that *O*-GlcNAc on NFAT undergoes an upsurge immediately following T cell activation to return to basal levels 10-15 minutes afterward directed us to a specific time window of 5-10 minutes after activation to capture the maximum number of *O*-GlcNAc modified proteins. The activation of T cells was performed using 10 ng/mL PMA and 2.5 μM ionomycin as per the work of Guerini et al.[40]

Metabolic labeling and enrichment of *O*-GlcNAc modified proteins:

Jurkat cells were metabolically labeleld by introducing the peracetylated alkynyl sugar analog Ac_4GlcNAlk or AC_4GlcPent for 16 hours according to the Pratt laboratory protocol[35] at the end of which activation reagents were introduced into the cell culture medium. The activated and control cells were incubated with 10 ng/mL PMA and 2.5 μM ionomycin for 5 minutes before lysis. Chemical labeling via CuAAC on metabolically labeled lysates and control lysates was done using a fluorescent azide probe azido-rhodamine[35] (Az-Rho) to check for any discernable differences between labeling pattern of activated and unactivated cells.

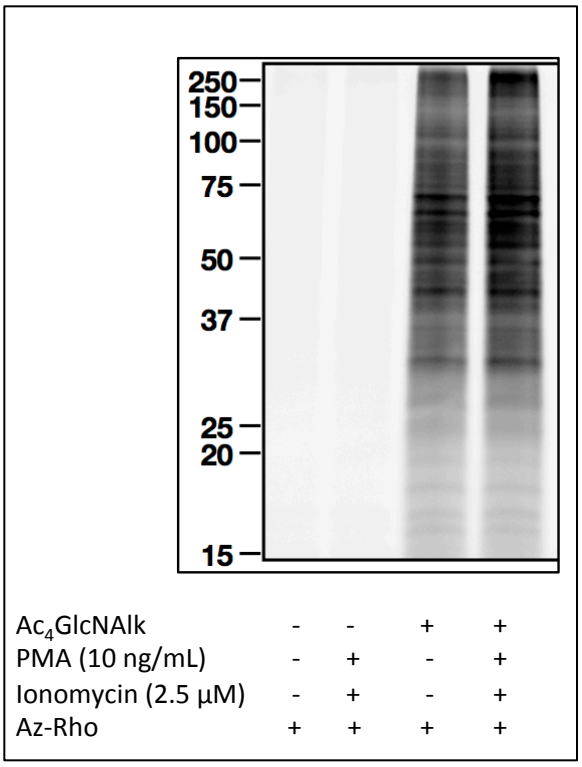

Figure 2.3: In-gel fluorescence scanning on metabolically labeled and unlabeled Jurkat cell lysates with and without activation with PMA/ionomycin

The chemical labeling profile shows no discernable difference between the activated and unactivated cell lysates in terms of banding pattern. This could be due to the fact that the changes may not be detectable in a gross survey like a fluorescence scan of a gel. In addition, due to the short time frame of the activation the manifested differences may require a more sensitive and subtle technique to highlight differences between activated and unactivated cell sets. Thereafter the metabolically labeled and activated lysates were subjected to enrichment by chemically labeling with azo-azido-biotin followed by in gel LC MS

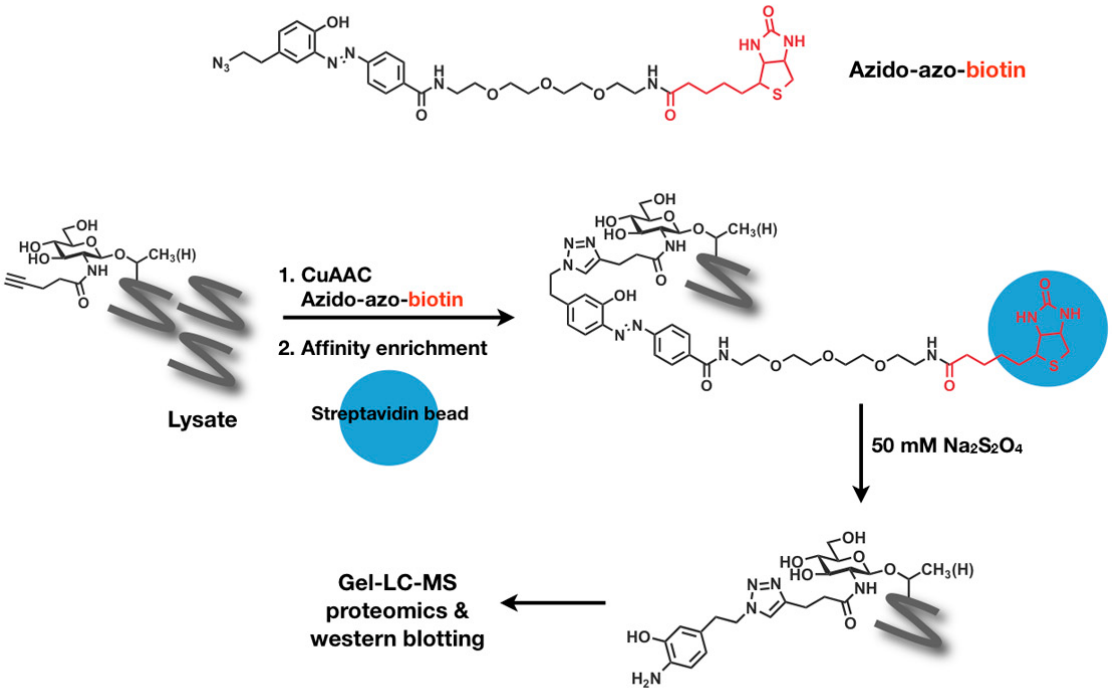

Figure 2.4: Zaro, B.W., Yang, Y.-Y., Hang, H.C. & Pratt, M.R. Chemical reporters for fluorescent detection and identification of O-GlcNAc-modified proteins reveal glycosylation of the ubiquitin ligase NEDD4-1. Proceedings of the National Academy of Sciences (2011)

There were four possible types of samples that could have been used for the mass spectrometry experiments namely: Ac_4GlcNAlk labeled and activated, Ac_4GlcNAlk labeled and unactivated, metabolically unlabeled and activated, metabolically unlabeled and unactivated. We however only chose to run in gel-LC/MS on Ac_4GlcNAlk labeled and activated and metabolically unlabeled and activated lanes. The reason for this decision to omit the unactivated samples irrespective of whether they were metabolically labeled or not was due to the fact that without doing isotopic labeling (e.g. SILAC or iTraq) the comparison of protein level between activated and unactivated samples could be difficult. Therefore we chose to probe *O*-GlcNAc modified proteins only in the activated samples to then follow up on interesting proteins via traditional biochemical methods.

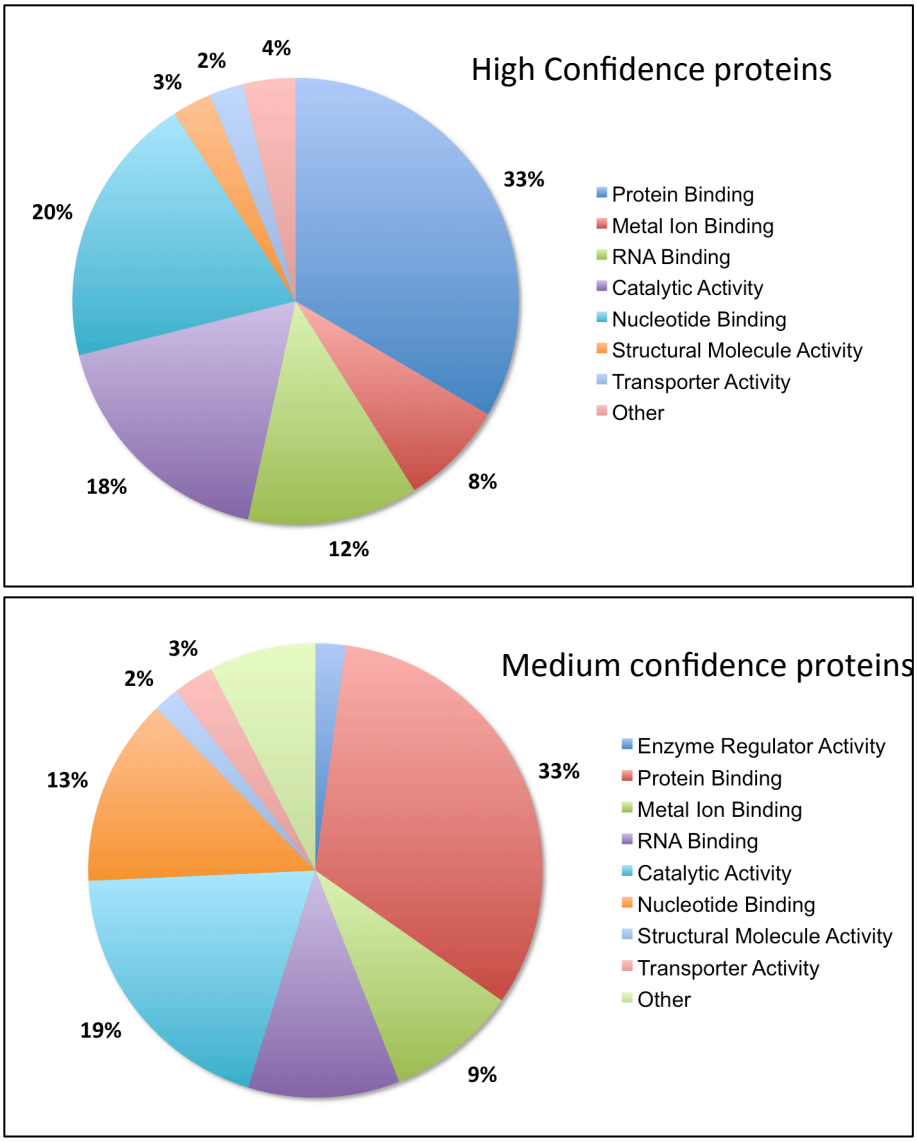

Figure 2.5: Chart showing the approximate percentages of different proteins based on their cellular function. This is not a quantitative representation because most of the proteins identified were annotated with 2 or more known cellular functions. The label "Other" signifies protein functions that were too small in percentage to be assigned a unique color.

The chart above shows proteins identified via the enrichment procedure detailed in Figure 2.4. A total of 1069 proteins were identified which were then grouped in to high (234), medium (332) and low (366) confidence proteins. This rating was given by the following criteria: high is if a protein had at least 5 peptides in the GlcNAlk labeled

sample and at least 2X as many peptides in GlcNAlk versus the unlabeled samples. Similarly, medium is at least 2 peptides in the GlcNAlk lane and at least 2X as many peptides in GlcNAlk versus unlabeled samples. Low confidence proteins were deemed so if there is at least 1 peptide in the GlcNAlk sample and 0 peptides in the control i.e. unlabeled sample.

Selecting targets to validate from mass spectrometric data:

We chose to scrutinize the high confidence list of proteins to determine if proteins known to be involved in T cell activation were identified. At first glance, (see table 3.1 on the following page) the T cell receptor glycoprotein CD3 epsilon and delta chains were found in the high confidence list. Additionally, Zap-70 and Receptor type tyrosine protein phosphatase C, also called CD45, were found in the list. Referring to Figure 2.1 detailing the T cell signaling network, these are all components that are proximal to the T cell receptor and are hence separated from the sub-networks activated by PMA/ionomycin. It is plausible that there may be some sort of feed-back from those TCR-distal networks to components of the TCR-proximal networks. Regardless of whether these identified proteins were *O*-GlcNAc modified in response to PMA/ionomycin treatment or by a feedback mechanism or are constitutively *O*-GlcNAc modified, we chose to pursue these targets for their impact on T cell activation. Interestingly, CD45 and Zap-70 are part of the initial phosphorylation cascade that occurs proximal to the TCR: CD45 de-phosphorylates Lck, which in turn phosphorylates Zap-70. Although Zap-70 and CD45 were found on our high confidence list, Lck was found in the medium confidence list. The prospect of all three of these signaling proteins being O-GlcNAc modified was very interesting and further exploration would be useful to gain insight on how their *O*-GlcNAcylation state affects their activity.

Accession#	Description	Unlabeled	GlcNAlk	Molecular Function
Q12906	Interleukin enhancer-binding factor 3	1	29	DNA binding; protein binding; RNA binding
P08575	Receptor-type tyrosine-protein phosphatase C or CD45		24	Catalytic activity; protein binding; receptor activity; signal transducer activity
Q9UIG0	Tyrosine-protein kinase BAZ1B		20	catalytic activity; metal ion binding; nucleotide binding; protein binding; structural molecule activity
Q9Y277	Voltage-dependent anion-selective channel protein 3		13	nucleotide binding; transporter activity
P45880	Voltage-dependent anion-selective channel protein 2]		12	nucleotide binding; transporter activity
Q9NYF8	Bcl-2-associated transcription factor 1 OS=Homo sapiens		10	DNA binding; protein binding
P18031	Tyrosine-protein phosphatase non-receptor type 1		7	catalytic activity; metal ion binding; protein binding
Q12905	Interleukin enhancer-binding factor 2		7	catalytic activity; DNA binding; nucleotide binding; protein binding; RNA binding
P07766	T-cell surface glycoprotein CD3 epsilon chain		7	protein binding; receptor activity; signal transducer activity; structural molecule activity
P43403	Tyrosine-protein kinase ZAP-70		7	catalytic activity; nucleotide binding; protein binding
Q99986	Serine/threonine-protein kinase VRK1	2	6	catalytic activity; nucleotide binding; protein binding
Q96HS1	Serine/threonine-protein phosphatase]		6	catalytic activity
P04234	T-cell surface glycoprotein CD3 delta chain		5	protein binding; receptor activity; signal transducer activity
P21796	Voltage-dependent anion-selective channel protein 1		5	protein binding; transporter activity
P18031	Tyrosine-protein phosphatase non-receptor type 1		7	catalytic activity; metal ion binding; protein binding
P06239	Tyrosine-protein kinase Lck		4	catalytic activity; nucleotide binding; protein binding

Table 2.1 This table shows the curated list of high confidence proteins that were chosen based on their intimate involvement with the T cell signaling process. The only exception is the protein tyrosine kinase Lck, highlighted in red, which is a medium confidence protein. The four proteins highlighted were chosen for further validation experiments.

The sequence of experiments to validate hits from the mass spectrometric data was as follows:

1. Immunoprecipitate target from activated and metabolically labeled Jurkat cell lysates
2. Confirm incorporation of unnatural sugar (azido sugar Ac_4GalNAz or alkynyl sugar Ac_4GlcPent/Ac_4GlcNAlk). The alkynyl sugar was used for the enrichment strategy as per the Pratt lab procedure[35] but for confirming the presence of *O*-GlcNAc on the target, we chose to use lysates metabolically labeled with Ac_4GalNAz followed by Bertozzi-Staudinger ligation with FLAG-Phosphine.
3. The next step was to treat the *O*-GlcNAcylated target protein with a glycosidase to remove *O*-GlcNAc, or in this case the metabolically incorporated *O*-GlcNAz residue. After de-GlcNAcylation chemical labeling with FLAG phosphine should show loss of azide dependent signal. The glycosidase of choice was first jack bean β-*N*-acetylhexosaminadase (HexC), which has been used by Bertozzi, and coworkers[25] for the treatment of azido labeled *O*-GlcNAc modified proteins. Another alternative to HexC, which is more specific for the O-GlcNAc modification, is CpNagJ, a bacterial analog of human *O*-GlcNAcase, which has shown to be highly effective as an O-GlcNAc stripper.[17,50] CpNagJ, however has not been used on azido substrates so our experiments with *O*-GlcNAz labeled proteins and CpNagJ were exploratory.

Target 1: CD45

Brief overview:

CD45 is a receptor type protein phosphatase (PTP) that is also called leukocyte common antigen due to being expressed ubiquitously on all leukocytes. CD45 can exist in several isoforms ranging in molecular weight between 180-220 kD. The extracellular domain of this protein is extensively glycosylated with *N*- and *O*-linked glycans and the glycosylation state of which varies based on the state of the T cell.[51] The tyrosine

phosphatase activity comes from a membrane proximal phosphatase domain whose substrates are mainly Src kinase family members crucial to T cell signaling, namely Lck[52] from T cells and and Lyn in B cells[53]. CD45 dephosphorylation of these kinases is important for triggering T-cell proliferative and cytokine secretion signaling mechanisms.[54]

Immunoprecipitation of CD45 from activated Jurkat cell lysates:

CD45 was immunoprecipitated from Ac_4GalNAz labeled and activated Jurkat cell lysates, that were chemically labeled with FLAG-phosphine.

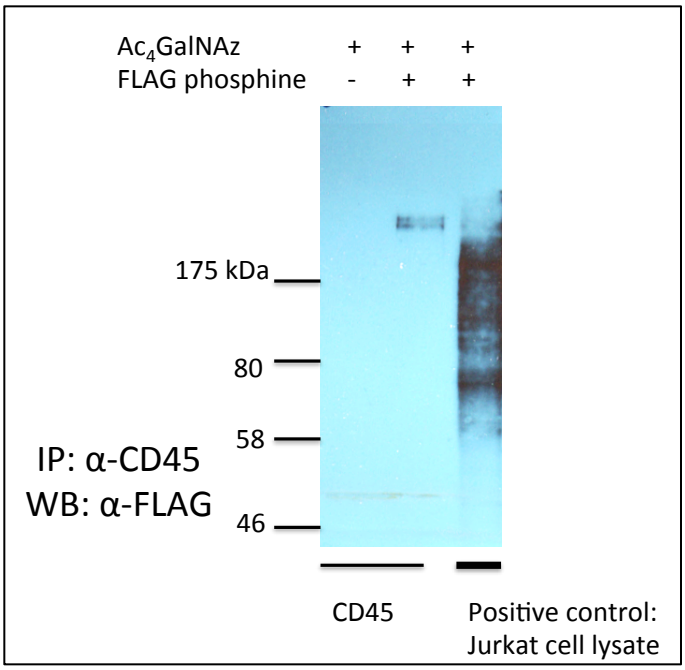

Figure 2.6: CD45 shows FLAG phosphine and hence azide dependent signal on immunoprecipitation at the correct molecular weight 180-220 kD. This confirms that CD45 has an azido sugar incorporated on it metabolically, which is accessible to FLAG phosphine.

This experiment was a preliminary one to ascertain if CD45 was indeed *O*-GlcNAc modified. However, there was an added complication in interpreting this result because CD45 is known to be both *N* and *O*-linked glycosylated. From the Pratt lab results[35] it was indicated that GlcNAlk was incorporated into N-linked glycans, intracellular *O*-

GlcNAc but not in the core structure of O-linked glycans. The azido sugar GalNAz, has been shown to be predominantly in intracellular *O*-GlcNAc by Boyce *et al.*[27] However, it may be incorporated into the mucin type O-glycans to a lesser extent. Therefore to truly understand the nature of the glycosylation that CD45 seems to exhibit, we chose to enzymatically treat it with 2 speciifc enzymes, CpNagJ specific for intracellular *O*-GlcNAc, and PNGase F (peptide: *N*-glycosidase F) specific for *N* -linked glycans. After treating metabolically labeled CD45 with these two enzymes, we should be in a better position to comment on the nature of the glycosylation and ultimately determine if it is in fact *O*-GlcNAc modified.

Treatment of CD45 with CpNagJ and PNGase F

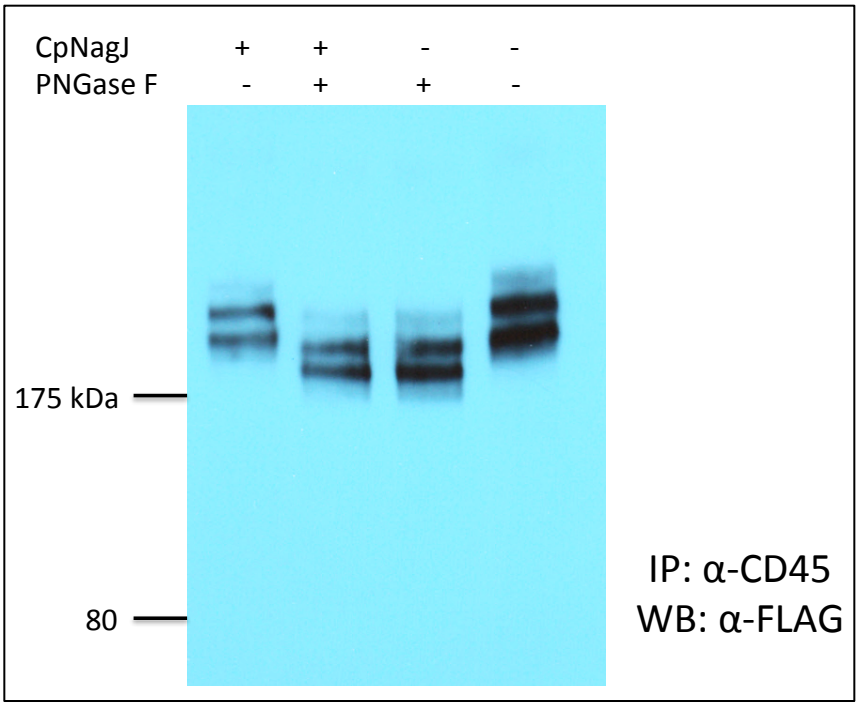

Figure 2.7: The anti-FLAG western blot above shows immunoprecipitated, azido sugar labeled CD45 treated in succession with CpNagJ and PNGase F to remove O-GlcNAz and N-linked glycans. Chemical labeling with FLAG phosphine was done post enzymatic treatment and FLAG and hence azide dependent signal was assayed by western blot.

For the above experiment, CD45 from metabolically labeled lysates was immunoprecipitated, eluted and then enzymatically treated. The result of CpNagJ and

PNGase F treatment followed by FLAG phosphine labeling shows that CpNagJ treatment does reduce the signal significantly from the untreated lane on the extreme right, however, PNGase F treatment does not diminish the azide dependent signal, although it does reduce the molecular weight of the protein, as demonstrated by the higher mobility on the gel and western shown above. This result confirms that CD45 is in fact *O*-GlcNAc modified and that CpNagJ treatment reduces that modification although it does not completely remove it. This can be reasoned as being due to the incomplete treatment of CD45, i.e. the amount of CpNagJ added was insufficient or that the fact that CD45 had *O*-GlcNAz instead of O-GlcNAc, reduced the efficiency of the enzyme. As mentioned before, this is the first instance of CpNagJ being used to cleave an azido derivative of GlcNAc.

We next chose to determine if inhibition of CpNagJ with a small molecule transition state mimic inhibitor PUGNAc would ablate the ability of CpNagJ to remove O-GlcNAz from CD45.

Treatment of CD45 with CpNagJ with and without PUGNAc inhibition

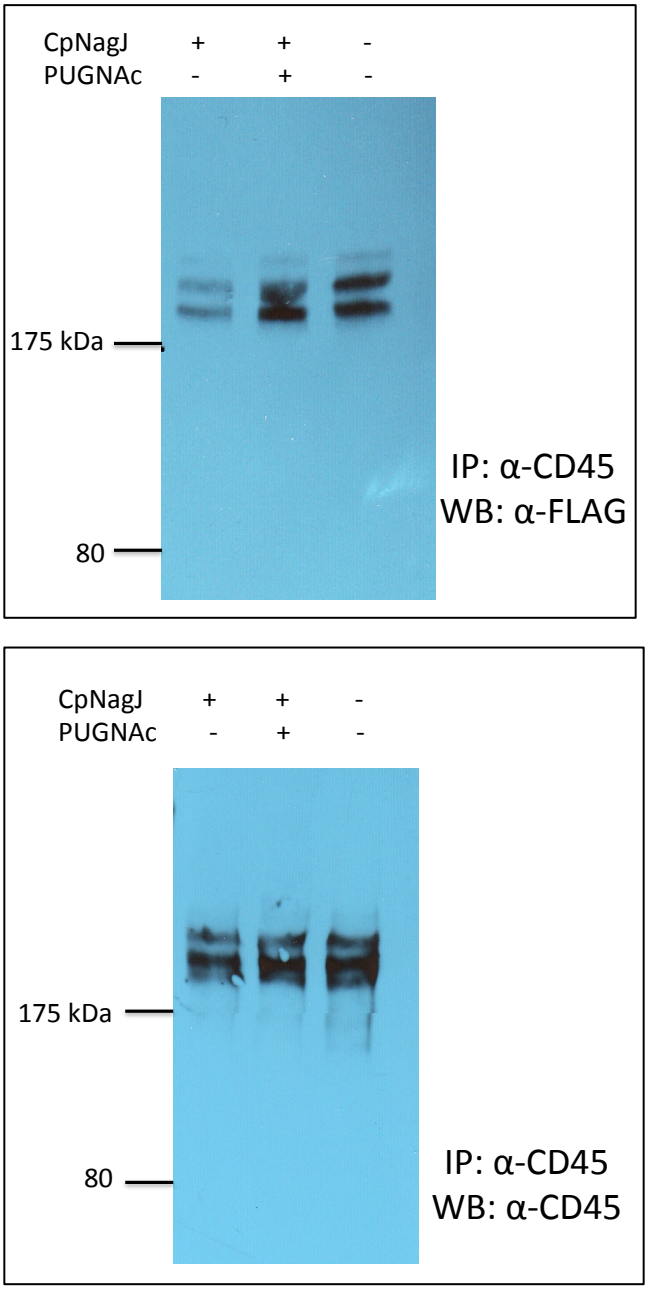

Figure 2.8: Treatment of CD45 with CpNagJ with and without PUGNAc shows that PUGNAc prevents digestion of O-GlcNAz from CD45 as demonstrated by the chemical labeling with FLAG phosphine.

The above result convinced us that CD45 is *O*-GlcNAc modified and that it can be de-GlcNAcylated using CpNagJ. To determine the impact of the *O*-GlcNAc modification on its functional activity as a phosphatase, we chose to do an in vitro phosphatase assay.

CD45 functional assay: phosphatase activity based on presence or absence of *O*-GlcNAc.

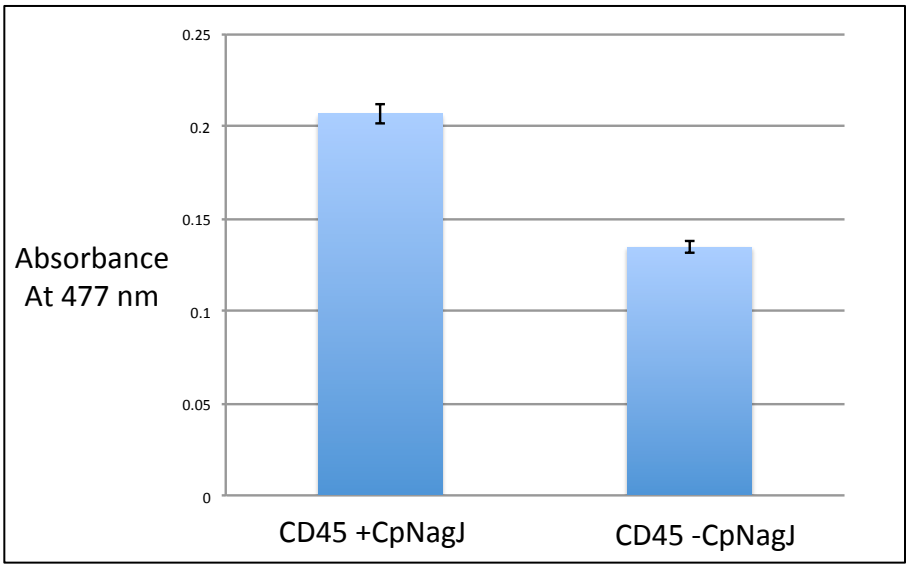

Figure 2.9: Phosphatase activity assay on CD45 treated with and without CpNagJ measured by the dephosphorylation of OMFP. CD45 was incubated with CpNagJ prior to assaying phosphatase activity, PUGNAc was included in all samples to block background hydrolase activity of CpNagJ, values shown are in triplicate with blank correction.

The above experiment was carried out on metabolically unlabeled CD45 to understand the true impact of CpNagJ mediated de-GlcNAcylation. The in vitro phosphatase assay was carried out by incubating immunoprecipitated CD45 with and without CpNagJ treatment in a phosphatase reaction buffer, containing a small molecule phosphatase substrate, o-methyl-fluorecscein phosphate (OMFP). OMFP is routinely used as a phosphatase substrate for alkaline phosphatases and protein tyrosine phosphatases (PTPs) and the read out of the assay is absorbance at 477 nm. This assay shows that de-GlcNacylated CD45 shows more than 50% increase in phosphatase activity, which is significant. The implications of this on CD45's activity are discussed in the Discussion section.

Target 2: Zap-70

Brief overview:

Zap-70 or T cell receptor zeta associated protein gets its name due to its 70 kD molecular weight. Zap-70 is a soluble tyrosine kinase that is crucial player in the TCR proximal phosphorylation cascade that determines T cell activation.[55] Zap-70 is recruited to the TCR zeta chian when the immunoreceptor tyrosine based activation motifs (ITAMS) on the TCR are phosphorylated by tyrosine kinases like Lck. Recruitment of Zap-70 is a key step to ensure propagation of the signaling mechanism. Like many Src family kinases, Zap-70 undergoes autophosphorylation and can also be phosphorylated by Lck during the signaling process. Phosphorylated Zap-70 is also responsible for recruitment of other adaptor proteins, which act as its substrate in the phosphorylation cascade.

Immunoprecipitation of Zap-70 from activated Jurkat cell lysates:

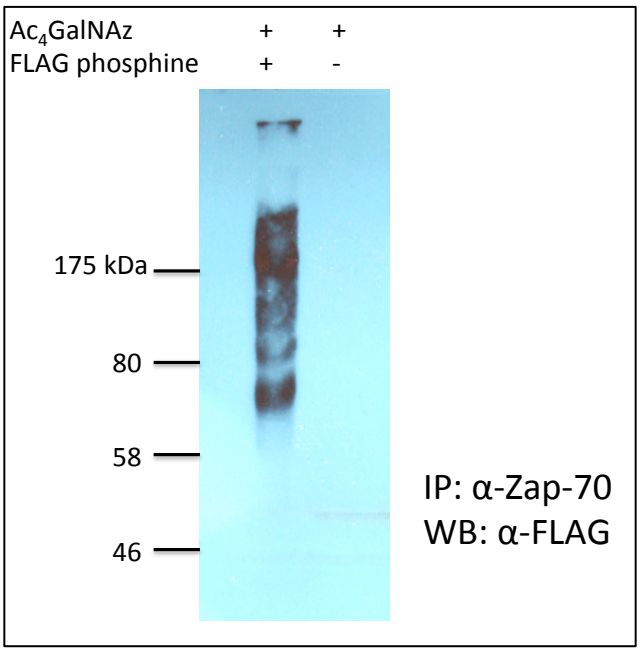

Figure 2.10: This figure shows Zap-70 immunoprecipitated from metabolically and chemically labeled lysates shows azide dependent signal. This confirms that Zap-70 is O-GlcNAc modified but the banding pattern shows bands leading up to the correct molecular weight of 70 kDa.

The preliminary experiment on immunoprecipitation of Zap-70 from metabolically labeled and chemically FLAG labeled lysates showed that Zap-70 shows azide dependent signal, in addition being an intracellular soluble kinase, Zap-70 does not contain other forms of *O*- or *N*-linked glycosylation. Therefore the signal can be attributed to intracellular *O*-GlcNAc. However, the laddering of bands up to the correct molecular weight is a phenomenon that has been observed previously[56] by other researchers working with Staudinger ligation of FLAG phosphine on metabolically incorporated azides. Thus, there may be multiple sites of O-GlcNAc on Zap-70 that could lead to such a laddering pattern.

Treatment of Zap-70 with CpNagJ:

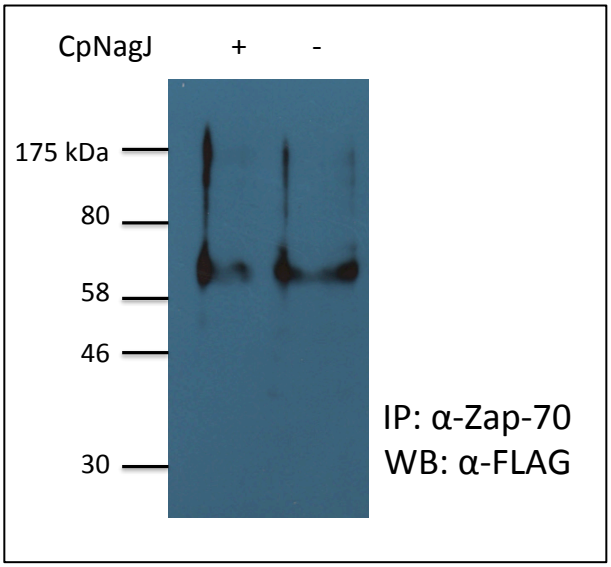

Figure 2.11: Treatment of Zap-70 with CpNagJ shows no difference between treated and untreated lanes by anti-FLAG western blot.

The next step was to determine if the O-GlcNAc on Zap-70 could be stripped by treatment with CpNagJ. Interestingly, Zap-70 showed no signs of CpNagJ dependent

loss of signal which can only be attributed to the poor processing of the azido sugar by CpNagJ for de-GlcNAcylation. The prospect that such a regulatory modification, as we believe O-GlcNAc to be, to be “buried” in the interiors of the protein may be implausible.

Target 3: Lck

Brief overview:

Lck or lymphocyte specific protein tyrosine kinase is a 56 kDa member of the src family of kinases and displays characteristic Src homology 2 (SH2) and SH3 domains. Lck is localized to the cell membrane via N-terminal myristoylation or palmitoylation of amino acid residues. Lck activity is maintained by a delicate balance between kinases like C-terminal Src kinase (CSK) that inhibit and phosphatases such as CD45 that activate it.[57] Lck is capable of autophosphosphorylation and is responsible for phosphorylating ITAMs on the CD3 and zeta chains of the T cell receptor, which eventually causes recruitment of Zap-70.

Immunoprecipitation and treatment of Lck with CpNagJ:

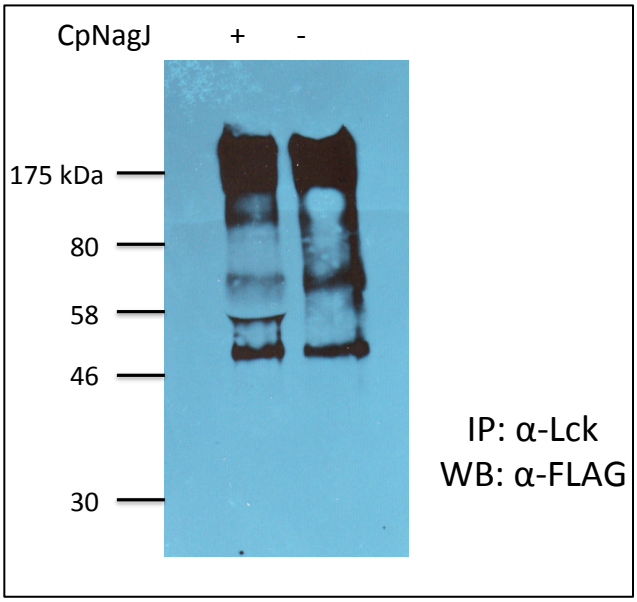

Figure 2.12: This figure shows immunoprecipitated Lck with and without CpNagJ treatment, banding pattern leading up to the correct molecular weight of 56 kDa. Again, like Zap-70, Lck is O-GlcNAc modified but there is no reduction in azide dependent signal on CpNagJ treatment.

The results for Lck mirrored that for Zap-70, Lck showed O-GlcNAc modification but was impermeable to the treatment with CpNagJ, which we attribute to the poor processing of the azido sugar by CpNagJ in the context of Lck.

Target 4: PTP1B

Brief overview:

PTP1B is one of many protein tyrosine phosphatases (PTP) that has an N terminal catalytic domain and a C-terminal domain that targets it to the cytoplasmic face of the endoplasmic reticulum.[58] PTP1B is believed to be regulated via phosphorylation of serine as well as tyrosine residues. Protein kinase C has been shown to phosphorylate PTP1B on treatment with phorbol esters.[59] The substrates of PTP1B dephosphorylation interact with this ER tethered enzyme via a protein:protein interaction regulatory domain. PTP1B was the only target chosen with no direct link to the TCR signaling pathway, however the fact that protein kinase C (which is activated by PMA/ionomycin treatment) modulates PTP1B, could prove interesting for our studies.

Immunoprecipitation and treatment of PTP1B with CpNagJ:

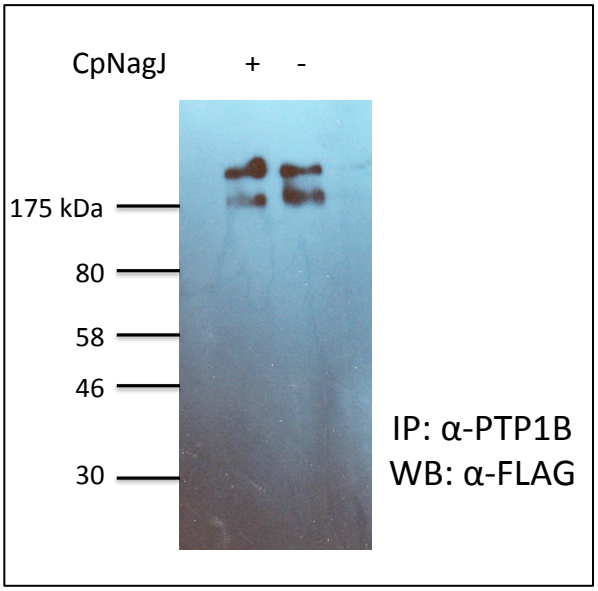

Figure 2.13: Immunopreciptated PTP1B showed azide dependent signal but at a very high molecular weight. The correct molecular weight of PTP1B is 50 kDa, however two bands close to 175 kDa and above were observed on all immunopreciptates. Additionlly, there was no reduction in signal for the CpNagJ treated samples.

Discussion:

From our results, all four targets we chose to validate via immunoprecipitation showed presence of *O*-GlcNAc modifications as seen by azide dependent signal in anti-FLAG blots. However, there was no difference between the azide dependent signal on targets pulled down from unactivated and activated lysates (data for unactivated lysates not shown, there was no observable difference between the azide dependent signal on immunoprecipitates from activated and inactivated cells). This indicates that the targets we chose may be constitutively *O*-GlcNAc modified, in fact our mass spectrometry data queried only activated lysates for *O*-GlcNAc, unactivated lysates with or without metabolic labeling were not included in the enrichment experiment. Regardless of this, our finding that these targets are *O*-GlcNAc modified is still relevant and provides interesting insight into the effect of *O*-GlcNAc on T cell signaling proteins.

The second interesting feature about our results is that out of the four targets, only CD45 seemed susceptible to CpNagJ de-glycosylation. Admittedly, our experiments with CpNagJ were carried out on metabolically labeled CD45, Zap-70, Lck and PTP1B, which has never been reported or attempted before. It is not very plausible that the O-GlcNAc modifications on these proteins are inaccessible but it is indeed plausible that CpNagJ is unable to "fit" *O*-GlcNAz on Zap-70, Lck and PTP1B in its active site to deglycosylate them. Furthermore, the site of glycosylation on these proteins are as yet unknown and identification of these sites may improve our ability to predict the local environment and three dimensional accessibility of the *O*-GlcNAc modification for CpNagJ treatment.

Thirdly, the FLAG modified Zap-70, Lck and PTP1B demonstrate some unique features. In the case of anti-FLAG blots on azido sugar labeled Zap-70 and Lck, they are marked by a regular banding pattern, leading up to the right molecular weight, which presumably is due to discreet sub-populations of the protein that have varying number of FLAG moieties attached. This has been reported previously in proteins carrying azidohomoalanine[56] that were modified via Staudinger ligation. On the other hand, the PTP1B blots show two distinct bands around 175 kDa, even though the molecular weight of the protein is 50 kD. The only explanation that fits this observation is that either PTP1B has extensive *O*-GlcNAcylation and hence multiple FLAG modifications causing the low mobility upon gel electrophoresis.

Regarding the results obtained for CD45, we have been able to show that not only is CD45 *O*-GlcNAc modified, but it is also susceptible to *O*-GlcNAc stripping via treatment with CpNagJ and subject to inhibition by PUGNAc. Most interestingly, the phosphatase activity of CD45 shows a more than 50% increase upon *O*-GlcNAc stripping. This phenomenon has exciting implications for the regulation of the activity of CD45 by the *O*-GlcNAc modification. In 1991, Ostergaard *et al.*[60] reported that ionomycin had a negative regulatory effect on the phosphatase activity of CD45 from mouse T cells. Interestingly, this reduction in phosphatase activity was accompanied by reduced

phosphorylation on serine residues on CD45. Our results that CD45 is *O*-GlcNAcylated and that removal of *O*-GlcNAc sharply increases its phosphatase activity could be a plausible explanation for the negative regulatory effect of ionomycin. At the time this report was published, the authors did not consider the possibility of a modification like *O*-GlcNAc as a factor that could regulate CD45 activity. However, today, in the light of all the information about the nuanced mechanisms by which O-GlcNAc and phosphorylation can interact, it is indeed a distinct possibility that serines on CD45 may be both *O*-GlcNAc and phosphorylated. This explanation also corroborates with the evidence for increased O-GlcNAc levels immediately after activation which happens on ionomycin treatment. However we did not carry out studies on CD45 from unactivated cells due to our observation that both activated and unactivated cells showed similar azide dpendent signal and hence GlcNAc modification. The details of this phenomenon of ionomycin mediated reduction in CD45 phosphatase activity[60] and *O*-GlcNAc mediated reduction in phosphatase activity needs to be explored in further detail.

Conclusion and Future directions:

Using the alkynyl chemical reporter mimic GlcNAlk or GlcPent we have identified 234 high confidence proteins that are potentially *O*-GlcNAc modified. Out of those 234, we chose 3 high confidence proteins (CD45, Zap-70, PTP1B) and 1 medium confidence protein (Lck) to validate via traditional biochemical methods. Upon immunoprecipitation, all four targets showed the presence of the O-GlcNAc modification via azide dependent western signal. The fact that we used the alkynyl reporter for the mass spectrometric experiments but the azido reporter for our confirmatory experiments with correlating results, proves the versatility of the chemical reporter strategy and validates the principle behind using this tool to probe GlcNAc dynamics. Furthermore, our results with CD45 demonstrate the impact of the *O*-GlcNAc modification on its function and open up exciting avenues for the regulation of this ubiquitously expressed protein tyrosine phosphatase in TCR based signaling.

Having established that these four targets are in fact *O*-GlcNAc modified, the next challenge is to identify the sites of modification, which can shed more light on how their *O*-GlcNAc modification interfaces with their phosphorylation state.

Materials and methods:

Cell culture and metabolic labeling:

Jurkat cell culture was done as previously described in Chapter 1. Metabolic labeling was done according to Zaro et al[35] Briefly, 50 µL DMSO stock solutions (200 mM) of Ac_4GlcPent or Ac_4GlcNAlk were introduced into cell culture media at a final concentration of 200 µM. Control flasks were administered with only DMSO. For azido sugar labeling for immmunoprecipitation experiments for target validation, flasks were coated with stock solution (50 mM) in methanol of Ac_4GalNAz. By letting the methanol stock solution evaporate in the flasks, a final concentration of 200 µM was achieved. For both types of sugars, metabolic labeling was allowed to proceed for 16 hours prior to lysis and/or activation.

T cell activation:

Phorbol 12-myristate 13-acetate was obtained from Calbiochem, Cat# 524400, 1mg/mL stock solution was prepared in DMSO and stored at -20 °C. Ionomycin was obtained from Calbiochem, cat# 407950, 1 mg/mL stock solution was prepared in DMSO and stored at -20 °C. For activation experiments, to Jurkat cells metabolically labeled for 16 hours, 10 ng/mL of PMA and 2.5 µM of ionomycin was introduced into the cell culture flask and incubated in the 37 °C incubator for 5 minutes after which cells were spun down and washed for lysis.

Cell lysis and immunoprecipitation:

Jurkat cells after metabolic labeling and activation were spun down, washed 2X with ice cold PBS before resuspending in lysis buffer. Lysis buffer consisted of 50 mM Tris pH 7.6, 150 mM NaCl, 5 mM EDTA, 1 mM EGTA, 1% NP-40 and 1x protease inhibitor cocktail (Calbiochem Cat# 539134, protease inhibitor cocktail set III, EDTA free) and 0.05 mg/mL PMSF. Cells were resuspended in lysis buffer and vortexed every few minutes and kept on ice for 20 min before spinning down in a microcentrifuge at 13,500 rpm for 20 min to pellet insoluble material. The supernatant form this was used for all immunoprecipitation and flash frozen in liquid nitrogen for short term storage at -20 °C, or at -80 °C for longer term storage.

Immunoprecipitations were carried out on lysates obtained above, the antibody for the desired protein was added to the lysate following manufacturer's instructions and rocked at 4 °C. Antigen-antibody complex was allowed to form for a minimum of 2h up to a maximum of 12 h, after which Protein-G agarose beads (Santa Cruz Biotechnology, #sc-2002) was added to pull down immune complexes. Protein G beads were allowed to rock with the immune complex for at least 1 hour up to a maximum of 6 hours. At the end of that period, the samples were spun down at 3000 rpm in a microcentrifuge, and washed 3 to 6 times with a wash buffer containing 20 mM Tris pH7.6, 300 mM NaCl, 2 mM EDTA, 0.1% NP-40, 1X protease inhibitor cocktail (see lysis buffer for Cat# and details) and 0.05 mg/mL PMSF. After washes, the immune complex was eluted with 5X Laemmli buffer for blots in figures 2.6 and 2.10 where FLAG labeled lysates were used for IP. However, for all other IPs where chemical labeling and enzymatic treatment had to be done on eluate, a pH 2.9 100 mM glycine buffer was used. Elution was carried out by incubating washed protein G beads with immune complex with 50 to 100 µL of glycine elution buffer with rocking at room temperature for 15 min. At the end of 15 min, the beads were spun down, the eluate collected and immediately neutralized with 1 M MES buffer pH 6.5. The elution process was repeated 2 more times; elautes from all

three elutions were combined and used for chemical labeling and/or enzymatic treatment as required.

Staudinger ligation:

Metabolically labeled lysates carrying azido sugars were subjected to Staudinger ligation by mixing lysates, with a FLAG phosphine reagent and PBS, according to the procedure detailed in Laughlin *et al.*[61] Reactions were allowed to proceed at room temperature overnight.

Enzymatic treatments: CpNagJ and PNGase treatment

CpNagJ treatment was carried out according to procedures described by Rao *et al*.[17] CpNagJ was obtained from Glycobiochem, Dundee, Scotland, cat# GBC00001. Briefly, for treatment of azido sugar labeled mmunoprecipitated proteins, 100 mM glycine pH2.9 eluates neutralized with 1 M MES pH 6.5 were taken, 20-30 µL reaction volumes were used with 1-2 uL of 1 mg/mL CpNagJ enzyme. The eluates and enzyme were incubated in a 37 °C water bath for 4 hours. The same procedure was used for the PUGNAc treated samples, except that 50 mM PUGNAc stock solution in DMSO was added to a final concentration of 100 µM. Samples marked untreated with PUGNAc received just DMSO as a control. The same procedure was used for metabolically unlabeled CD45 eluate used for the phosphatase assay (Figure 2.9)

PNGase F peptide:*N*-glycosidase F treatment was obtained from New England Biolab, cat# P0704S according to the instructions provided by the manufacturer. Briefly, CD45 eluates from immunoprecipitation were treated with the G7-glycosidase-reaction buffer and PNGase F enzyme and incubated at 37°C water bath for 1 hour after which chemical labeling was carried out with FLAG phosphine.

In vitro phosphatase assay for CD45:

CD45 glycine/MES eluates from immunoprecipitations were used as is for this assay without any concentration or buffer exchange. Phosphatase reaction mixtures were

prepared with a final concentration of MES of 83 mM, 50 mM NaCl, mM EDTA, mM DTT, 0.1 mg/mL BSA and 100 µM OMFP. 50 mM PUGNAc stock solution in DMSO was added to a final concentration of 100 µM in all samples, including the blank to inhibit the CpNagJ and therefore reduce any background hydrolase activity that may be observed. The CD45 phosphatase reaction mixtures were allowed to incubate in a 37°C water bath for 2-3 hours before absorbance was read at 470 nm in a US-Vis spectrometer. All readings were taken in triplicate and blank corrected.

Antibodies and reagents:

Antobodies for CD45, Zap-70, Lck and PTP1B were purchased from Santa Cruz Biotechnology, Texas. Catalog# sc-1178, sc-32760, sc-433, sc-133259 respectively. PUGNAc for inhibition of CpNagJ was obtained from Tocris Bioscience, cat # 3384

Western blots:

FLAG labeled samples were boiled at 95°C for 6 minutes with 5X loading dye. The samples were run on a 5% (for CD45 blots) or 10% (for all other blots) polyacryamide electrophoresis gel and transferred onto nitrocellulose at 40V over 2 hours in western transfer buffer (25 mM tris, 192 mM glycine, 0.5% SDS and 10% methanol). Anti-FLAG blots were blocked in 5% milk in PBST and treated with anti-FLAG M2 HRP conjugate at a dilution of 1:12000 in 5% milk in PBST. Blots were washed with milk and PBST and developed by chemiluminescence (Millipore Immobilon Western kit). For anti-CD45 blots, incubation with primary antibody anti-CD45 was carried out at a dilution of 1:1000 in 5% milk/PBST for 4 hours at rt. After 4 washes in PBST, blots were incubated with secondary anti-mouse HRP antibody at a dilution of 1:1000 for 1 h at rt. Blots were washed 4x with PBST before exposing to HRP substrate and development.

Biotin Enrichment:

Jurkat cells labeled with Ac4GlcNAlk (200 µM) or DMSO were resuspended in 200 µL H2O, 60 µL PMSF in H2O (250 mM), and500 µL 0.05% SDS buffer (0.05% SDS, 10 mM TEA, pH 7.4,150 mM NaCl) with Complete Mini protease inhibitor cocktail (Roche Biosciences). To this was added 8 µL Benzonase (Sigma), and the cells were incubated

on ice for 30 min. At this time, 4%SDS buffer (2000 µL) was added and the cells were briefly sonicatedin a bath sonicator and collected by centrifugation at 20;000 × g for 10 min at 15 °C. Protein concentration was normalized by BCA assay (Pierce, ThermoScientific) to 1 mg⁄mL(10 mg total cell lysate). The appropriate amount of click chemistry cocktail was added and the reaction was allowed to proceed for 1 h, after which time 10 volumes of ice-cold methanol were added. Precipitation proceeded overnight at −80 °C. Precipitated proteins were centrifuged at 5,200 × g for 30 min at 0 °C and washed three times with 40 mL ice-cold MeOH, with resuspension of the pellet each time. The pellet was then air dried for 1 h. To capture the biotinylated proteins by streptavidin beads, the air-dried protein pellet was resuspended in 4 mL of Hepes buffer (6 M urea, 2 M thiourea, 10 mM Hepes, pH 8.0) by bath sonication. The captured proteins were incubated with freshly made 1 mM dithiothreitol (100 mM stock solution) for 40 min to reduce cystienes. Cystiene capping was achieved after further incubation with freshly prepared 5.5 mM iodoacetamide (550 mM stocksolution) for 30 min in the dark. The beads were then washed twice with PBS (250 µL) once with 4% SDS buffer. Beads resuspended in Hepes buffer were then incubated on a rotator for 2 h, washed twice with Hepes buffer, twice with PBS, and twice with 1% SDS in PBS (10 mL per wash, 2;000 × g, 2 min). Samples were then transferred to 2-mL dolphin-nosed tubes. Beads were then incubated in 250 µL of sodium dithionite solution (1% SDS, 25 mM sodium dithionite) for 30 min at RT to elute captured proteins. The beads were centrifugated for 2 min at 2;000 × g and the eluent collected. The elution step was repeated, and the eluents combined. Protein was concentrated using a YM-10 Centricon (Millipore), washed with 300 µL PBS and centrifuged at 10;000 × g for 30 min. The concentrated eluent was transferred to a microcentrifuge tube and dried by SpeedVac. Dried pellets were resuspended in 1x SDS-free loading buffer (10% glycerol, 0.1% bromophenol blue, 0.7% β-mercaptoethanol) and boiled for 5 min.

LC-MS Analysis

Each lane of the SDS-PAGE gel was sliced into 10 fractions, and each excised gel slice was placed in a microcentrifuge tube. The gel slices were washed twice with 50 mM

ammonium bicarbonate (ABC, 300 µL, 15 min), destained twice with a 1 : 1 solution of 50 mM ABC/acetonitrile for 30 min, and then dehydrated in 100% acetonitrile. After drying the gel pieces in a SpeedVac, gel pieces were rehydrated in a trypsin solution (2 µg of trypsin per gel slice) and incubated at 37 °C in a water bath for 18 h. The peptides were eluted in 50% acetonitrile in H2O with 0.1% TFA (200 µL, twice), and SpeedVac dried. Samples were then subjected to nano-HPLC/MS/MS analysis (Thermo Linear Trap Quadrupole- Orbitrap in the Proteomic Resource Center at Rockefeller University). LC-MS analysis was performed with a Dionex 3000 nano-HPLC coupled to an Linear Trap Quadrupole-Orbitrap ion trap mass spectrometer (ThermoFisher). Peptides were pressure loaded onto a custom-made 75-µm–diameter, 15-cm C18 reverse phase column and separated with a gradient running from 95% buffer A [HPLC water with 0.1% (vol*/*vol) formic acid] and 5% buffer B [HPLC-grade CH3CN with 0.1% (vol*/*vol) formic acid] to 55% B over 30 min, next ramping to 95% B over 10 min and holding at 95% (vol*/*vol) B for 10 min. One full MS scan (300–2,000 MW) was followed by three data-dependent scans of the nth most intense ions with dynamic exclusion enabled. Peptides were identified using MASCOT 2.3.02 in this case and the data was compared against the Uniprot database. A total of 1069 proteins were identified which were then grouped in to high (234), medium (332) and low (366) confidence proteins. This rating was given by the following criteria: high for a protein that had at least 5 peptides in the GlcNAlk labeled sample and at least 2X as many peptides in GlcNAlk versus the unlabeled samples. Similarly, medium for a protein that had at least 2 peptides in the GlcNAlk lane and at least 2X as many peptides in GlcNAlk versus unlabeled samples. Low confidence proteins were deemed so if there was at least 1 peptide in the GlcNAlk sample and 0 peptides in the control i.e. unlabeled sample. A qualitative representation of the approximate percentages of different proteins based on their cellular function is depicted in Figure 2.5. This is not a quantitative representation because most of the proteins identified were annotated with 2 or more known cellular functions. The label “Other” signifies protein functions that were too small in percentage to be assigned a unique color.

Chapter 3

Modification of the surface of poliovirus with an unnatural amino acid

Abstract:

Modification of the surface of viruses commonly used in gene therapy, such as adenoviruses and lentiviruses, is an attractive strategy to manipulate their function and efficacy. In the Carrico lab, successful incorporation of unnatural sugar and amino acid analogs have been demonstrated in adenoviruses and lentiviruses with minimal perturbation to viral fitness and titer. The unnatural analogs contain “click” chemistry or CuAAC compatible functional groups such as azides and alkynes that can be chemoselectively modified. The modification of the surface of polioviruses is an attractive avenue that we sought to explore to manipulate the surface for novel anti-polio vaccine development. The first step towards achieving this was to evaluate if poliovirus production was affected by inclusion of azidohomoalanine in the growth medium and how it impacts viral fitness and titer. The poliovirus production was severely hampered by azidohomolanine with a loss in infectivity as measured by plaque forming units per mL when compared to the wild type control grown in regular media. Therefore the two-step method of metabolically introduced azidohomoalanine thereafter reacted with an exogenously added CuAAC probe to produce novel polio vaccines was not feasible.

Introduction:

The poliovirus is one of best studied and characterized human viruses. Poliovirus belongs to the genus *Enterovirus* from the family Picornaviridae, the name derives form the Latin word for small, namely “pico” and the picornavirus family includes small, non enveloped RNA viruses. Poliovirus is the cause for poliomyelitis, which affects the

central nervous system causing motor neuron destruction that results in paralysis, or even death by respiratory failure. Poliovirus eradication in the developed world has been possible due to the discovery of two vaccines, the inactivated virus vaccine by Salk and the live attenuated virus vaccine by Sabin[62]. This along with the World Health Organization's (WHO) stringent polio eradication program has lead to the decline of poliomyelitis as a global threat. However, there still remains interest in generating novel attenuation schemes to generate anti-polio vaccines. Poliovirus has also been exploited as an anti-tumor therapy agent.[63] Therefore engineering the surface of the poliovirus via incorporation of unnatural amino acid functionalities presents an attractive avenue. With the results obtained from incorporation of unnatural sugar[64] and amino acid[65] functionalities onto the surface of we sought to apply the same principles towards engineering the surface of poliovirus. Azidohomoalanine (Aha) was chosen as a surrogate for methionine, which has been shown to be incorporated onto the adenoviral capsid with minimal perturbation to viral fitness and infectivity.

Results:

Effects of inclusion of azidohomoalanine during production of poliovirus type 1:

Azidohomoalanine (Aha) at 4 mM and 32 mM concentrations was added into the growth medium of HeLa cells used to produce Poliovirus type 1. Briefly, cells were infected with a stock of poliovirus type 1, to a final concentration of 10^8 pfu/plate. To measure the production of virus at t= 0, 2, 4, 6, 9 and 24 hours, cells infected with poliovirus were frozen at the specified time points. Lysis of cells from all plates was achieved by 3 cycles of freeze and thaw. After which the lysates containing virus were used for infectivity assays.

These concentrations of Aha were chosen to compare to existing protocols for the modifications of adenoviral surfaces. The 32mM Aha treated HeLa cells were unable to produce any virus and 4 mM Aha caused a drop in viral titer of 10^8 plaque forming units/mL from 10^9 pfu/mL for control HeLa cells. Furthermore, the production of viruses in Aha treated cells was significantly lower than the control/wild type as demonstrated

by poor recovery after purification by ultra-centrifugation. The results are depicted below.

Effect on Infectivity (fitness):

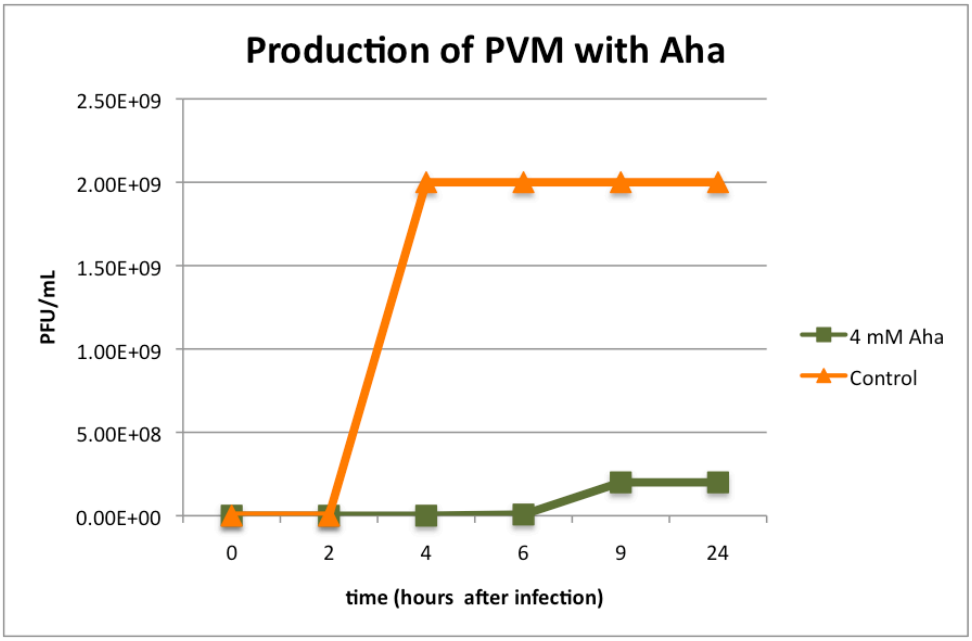

Figure 3.1: Viral fitness as measured by its ability to infect cells to form plaques was measured for the 4 mM Aha treated samples and untreated control. A drop in pfu/mL of 1 order of magnitude was observed compared to wild type.

The procedure used for poliovirus production was taken from the literature[66,67] with the only modification of Aha addition to the production cell line (HeLa) media. For the plaque assay data shown above, no purification of virus was performed; cell lysate containing a suspension of virus was used.

Effect on particle count (production):

To determine the effect of Aha inclusion on the particle count of poliovirus, virus purification via a sucrose cushion followed by ultracentrifugation was performed according to literature procedures.[66,67]

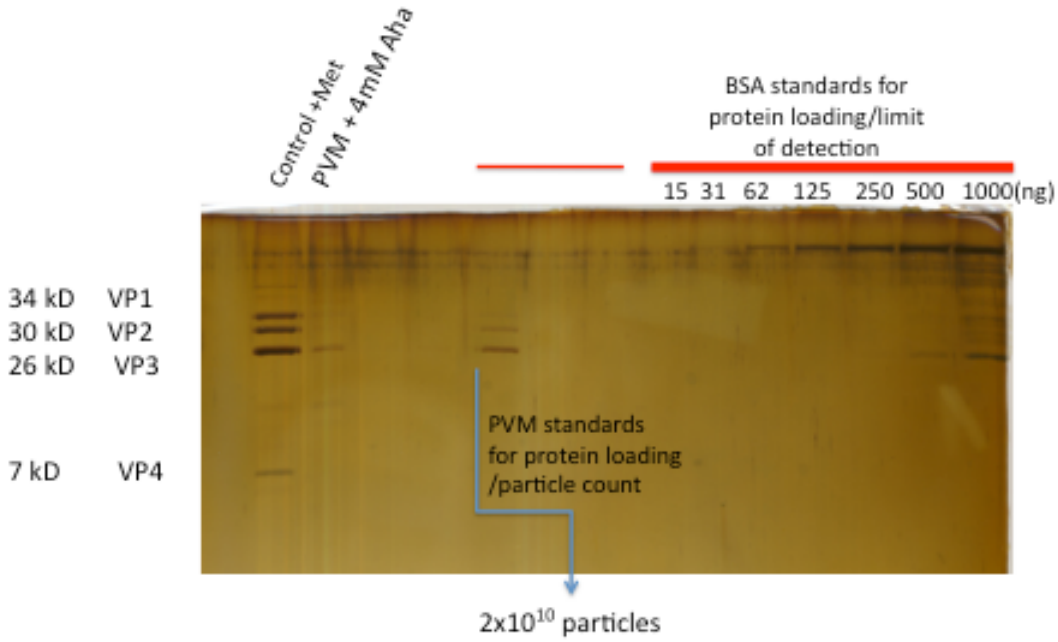

Figure 3.2: Viral production titer in terms of particle/mL was measured after concentrating HeLa lysate from infected cells and subjecting it to ultracentrifugation under a sucrose gradient. Concentrated samples were run on SDS PAGE and stained using silver stain. The control virus showed predicted bands for 4 viral capsid proteins while 4 mM Aha treated virus showed very faint bands for viral capsid proteins indicating low titer. Measurement of the RNA/protein absorbance in a Nanodrop spectrophotometer showed that a particle count of $1x10^{12}$ particles/mL was obtained for the 4 mM Aha treated, purified virus and $8x10^{12}$ particles/mL for the control/wild type virus.

The low infectivity (pfu/mL) observed with Aha inclusion in poliovirus production was accompanied by low particle/mL number as demonstrated by the silver stained gel above.

Attempt at chemical modification with azide compatible biorthogonal reactions (Click reaction and Staudinger ligation):

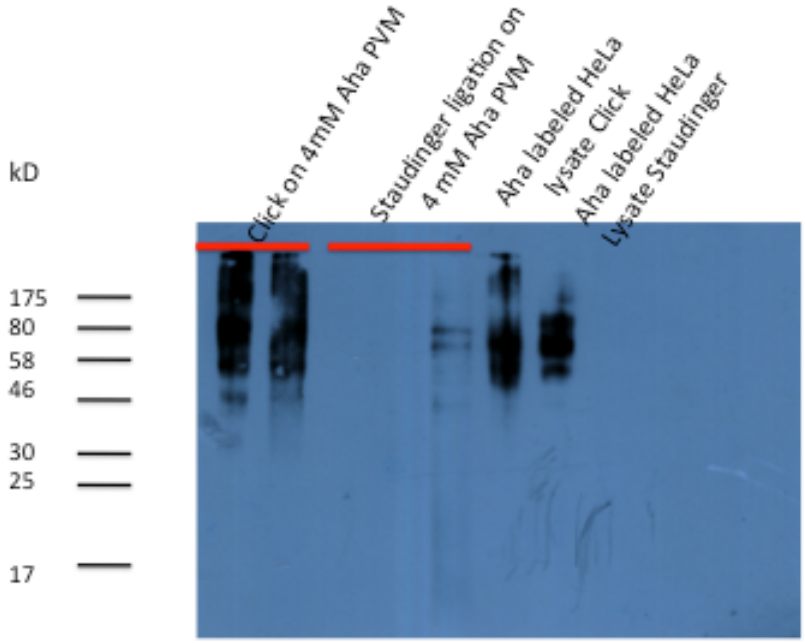

Figure 3.3: Anti-FLAG western blot: since the primary aim of this project was to understand if Aha can be incorporated onto the poliovirus surface, purified virus samples of 4 mM Aha treated were reacted with 2 bioorthogonal reactions: "click" with FLAG alkyne and Staudinger ligation with FLAG phosphine (see Figure 2 for structures). No bands for the viral capsid proteins in the 34 kD to 7 kD region were observed and comparison with HeLa lysate metabolically labeled with Aha showed a similar banding pattern indicating that some cellular protein contaminants may be accounting for the observed FLAG specific western signal. Inclusion of Aha modified adenovirus type 5 (Ad5) as a positive control on a similar anti-FLAG western blot (data not shown) showed banding pattern corresponding to the Ad5 capsid proteins as expected therefore proving that the western signal obtained for poliovirus samples could not be attributed to incorporation of Aha in the viral capsid but due to cellular contaminants in the virus sample that may have leached in due to the low particle number of virus produced.

Lastly, an attempt at chemically modifying poliovirus grown in the presence of Aha with was made. The results of the biorothogonal reactions are depicted in Figure 3.3. The results showed that contaminant azide proteins from HeLa cell lysate chemically modified with FLAG (alkyne or phosphine reagent) dominated the western signal in an anti-FLAG western blot.

Materials and Methods:

Production of Poliovirus with Aha:

Poliovirus type 1 (Mahoney) production was carried out according to literature procedures[66,67] with inclusion of azidohomoalanine (Aha) in the growth medium. Briefly, HeLa R19 cells were maintained as a mono-layer culture in DMEM supplemented with 10% Bovine Calf Serum (BCS). HeLa cells were washed 3x with Met free DMEM media after which infection was carried out with Poliovirus type 1 Mahoney at a multiplicity of infection (MOI) of 5 pfu/cell. Cells were rocked with infection buffer/inoculum for 30 minutes at rt after which inoculum was aspirated out. The cells were allowed to incubate at 37°C in an incubator with 2% BCS and 4 or 32 mM Aha containing Met free DMEM medium. Control plates were incubated with 4 mM Met supplemented Met free DMEM medium. Plates were incubated at 37°C for 2, 4, 6, 9 and 24 hours, at the end of each time point cells were frozen by placing in the -80°C freezer. At the end of the last time point (24 h) three cycles of freeze/thaw were used to lyse cells (from all time points) followed by centrifugation to remove cell debris. This cell lysate containing viral particles was used to determine infectivity via plaque assay, as depicted in Figure 3.1

Purification of Poliovirus and determination of particle number by OD_{260} absorbance:

Literature procedures were followed for the purification of virus particles via a sucrose cushion and ultracentrifugation.[66,67] Briefly, cell lysates produced after 3 freeze/thaw cycles after 24h of infection were clarified by centrifugation for 10 min at 2,000 × *g* followed by a second 10 min centrifugation at 14,000 × *g*. Supernatants were incubated

for 1 h at room temperature in the presence of 10 µg/ml RNase A (Roche) to digest any extraviral or cellular RNA. Thereafter, addition of 0.5% sodium dodecyl sulfate (SDS) and 2 mM EDTA was followed by overlaying virus-containing supernatants on a 6-ml sucrose cushion (30% sucrose in Hanks balanced salt solution [HBSS]; Invitrogen). Virus particles were sedimented by ultracentrifugation for 4 h at 28,000 rpm using an SW28 swinging bucket rotor. Supernatants were discarded and centrifuge tubes were rinsed twice with HBSS while leaving the sucrose cushion intact. After removal of the last wash and the sucrose cushion, virus pellets were resuspended in PBS containing 0.2% SDS and 5 mM EDTA.

Virus titers were determined with a NanoDrop spectrophotometer (NanoDrop Technologies) at the optical density at 260 nm (OD_{260}) and calculated using the formula 1 OD_{260} unit = 9.4×10^{12} particles/mL.

Plaque assay to determine infectivity:

Literature procedures were followed for the protocol.[63,66] Briefly, serial 1:10 dilutions of virus containing lysate or purified virus were used to infect HeLa R19 cells. Post infection, cells were overlaid with a semisolid overlay of 0.6% tragacanth gum (Sigma-Aldrich) in minimal Eagle medium and allowed to incubate undisturbed in a 37°C incubator. At the end of 3 days, the overlay and cell culture media were discarded and the monolayers stained with Crystal Violet to visualize plaques and calculate virus infectivity in pfu/mL.

Western blots:

FLAG labeled samples were boiled at 95°C for 6 minutes with 5X loading dye. The samples were run on a 10% polyacryamide electrophoresis gel and transferred onto nitrocellulose at 40V over 2 hours in western transfer buffer (25 mM tris, 192 mM glycine, 0.5% SDS and 10% methanol). Anti-FLAG blots were blocked in 5% milk in PBST and treated with anti-FLAG M2 HRP conjugate at a dilution of 1:12000 in 5% milk in PBST. Blots were washed with milk and PBST and developed by chemiluminescence (Millipore Immobilon Western kit).

Staudinger ligation:

Staudinger ligation was carried out by mixing virus samples with final concentration of 500 μM FLAG phosphine reagent and PBS, according to the procedure detailed in Laughlin *et al.*[61] Reactions were allowed to proceed at rt overnight.

CuAAC reaction:

CuAAC reactions were carried out according to literature detailed in Agard *et al.*[68] Reactions consisted of virus samples mixed with 100 μM final concentration of FLAG alkyne, with final concentrations of 1 mM sodium ascorbate, 100 μM tris[(1-benzyl-1-H-1,2,3-triazol-4-yl)methyl]amine ligand (TBTA) (10 mM stock solution in DMSO) and 1 mM $CuSO_4$ overnight at rt.

Conclusion:

From the preliminary experiments attempting to incorporate azidohomoalanine on poliovirus, it was observed that a severe loss of infectivity as measured by plaque forming units/mL was observed. In addition to the loss of infectivity, there was also crippling loss in the particle number of virions as shown by the low particle number obtained and the very faint bands in the silver stained gel. This result was not expected by us, given the seamless incorporation of azidohomoalanine on the surface of adenovirus type 5 (Ad 5), with minimal loss in infectivity and particle production.

Chapter 4

Poliovirus antigenic display on the surface of azide enabled adenovirus

Abstract:

When a vaccine against poliovirus is administered, specific regions of the virus capsid are found to stimulate the immune system. These regions present amino acid sequences that are called antigenic epitopes[69] and stimulate production of antibodies that neutralize the virus and therefore protect the vaccinated organism from future infections. The concept of taking these antigenic peptide epitopes, presenting it to the immune system by simply attaching it to a carrier protein and then eliciting an immune response without exposure to whole virus has been explored.[70,71] Although the concept is an attractive one, the results have been less than favorable. The immunity produced by the peptide epitopes alone was weak and not long lived enough to be a viable alternative. This was attributed to the inability of linear (and cyclic) peptide epitopes in replicating the three dimensional conformation presented by the intact virus to the cells of the immune system. As a continuation of this concept, one of the first genetic modifications of the adenovirus capsid protein was performed[72] by incorporating a poliovirus type 3 antigenic epitope.[73] The premise was that the presentation of the epitope on the surface of the adenovirus should mimic the regular three dimensional pattern required by the immune system to trigger antibody production. However the genetically displayed epitope on adenovirus caused antibody production but not a protective immune response.

The aim of this project was to revisit the concept of using antigenic peptide epitopes to elicit an immune response using two modern tools. Firstly, the display of these antigenic peptide epitopes “clicked” onto the capsid of an adenovirus equipped with azides[65] can provide the regular, repetitive arrangement with versatility and flexibility, lacking in the genetic method described above, to potentially stimulate the immune system. Additionally, transgenic mice bearing the receptor required for poliovirus infection are available now that are infected with polio in a facile manner. Such animal models are

important because of the ability to do challenge tests after vaccination to check for protection against infection.

Specific Aims:

The main principle behind this project was to use our lab's azide equipped adenoviruses as a platform for the display of antigenic epitopes towards poliovirus. For this, the procedure we followed was:

1. Design peptide motifs for chemical labeling of azide modified adenovirus, based on knowledge of what antigenic epitopes are most potent for poliovirus
2. Attach said peptide epitopes to adenovirus via "click" reaction
3. Assay the ability of antigenic epitope displaying adenovirus to elicit an immune response in mice susceptible to poliovirus infection. This was to be assayed in two ways: firstly via the production of neutralizing anitbodies and secondly via the challenge test in mice for protective immunity.

Experimental Design:

Design of antigenic peptide epitopes:

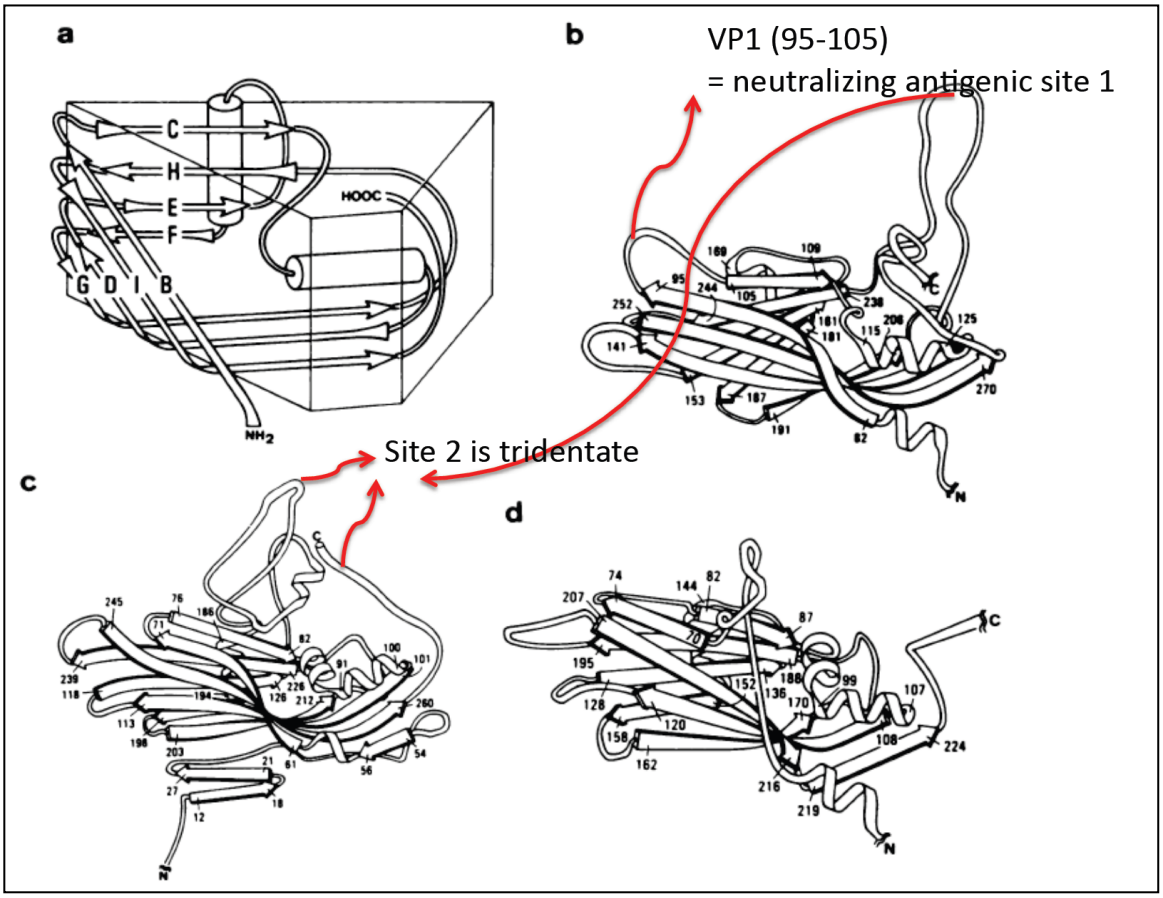

Figure 4.1: Figure adapted from Hogle, J.M. & Filman, D.J. THE ANTIGENIC STRUCTURE OF POLIOVIRUS. Philosophical Transactions of the Royal Society of London Series B-Biological Sciences 323, 467-& (1989) Philosophical Transactions of the Royal Society of London. Series B, Biological Sciences © 1989 The Royal Society

Antigenic peptide epitopes on the surface of Poliovirus type 1 were mapped based on mutants in a virus population that escaped neutralization by antibodies produced in immunized animals. The structural determinants that differentiated these "escape mutants" from the regular population helped determine which residues on the viral capsid were important for inducing a neutralizing antibody response. Since VP1 residue 95-105 forms a contiguous monodentate antigenic epitope it was chosen: PASTTNKDKLF

The genetic introduction of a poliovirus type 3 peptide on adenovirus[72] was used as an inspiration for this project and the peptide EVDNEQPTTRAQKLFA[73] was selected as the second antigenic epitope to covalent “click” on to adenovirus.

The azide enabled (azidohomoalanine or Aha labeled) adenovirus type 5 (Ad5) was produced as described in literature[65]. Briefly, adenovirus was produced in HEK 293 cells with inclusion of azidohomoalanine in the cell culture medium. Thereafter, adenovirus particles equipped with azides were purified via standard ultracentrifugation procedures over a CsCl gradient.

Antigenic peptides equipped with Strain Promoted Alkyne Azide Cycloaddition (SPAAC) functionalities for reaction with azidohomoalanine labeled adenovirus type 5 (Ad5):

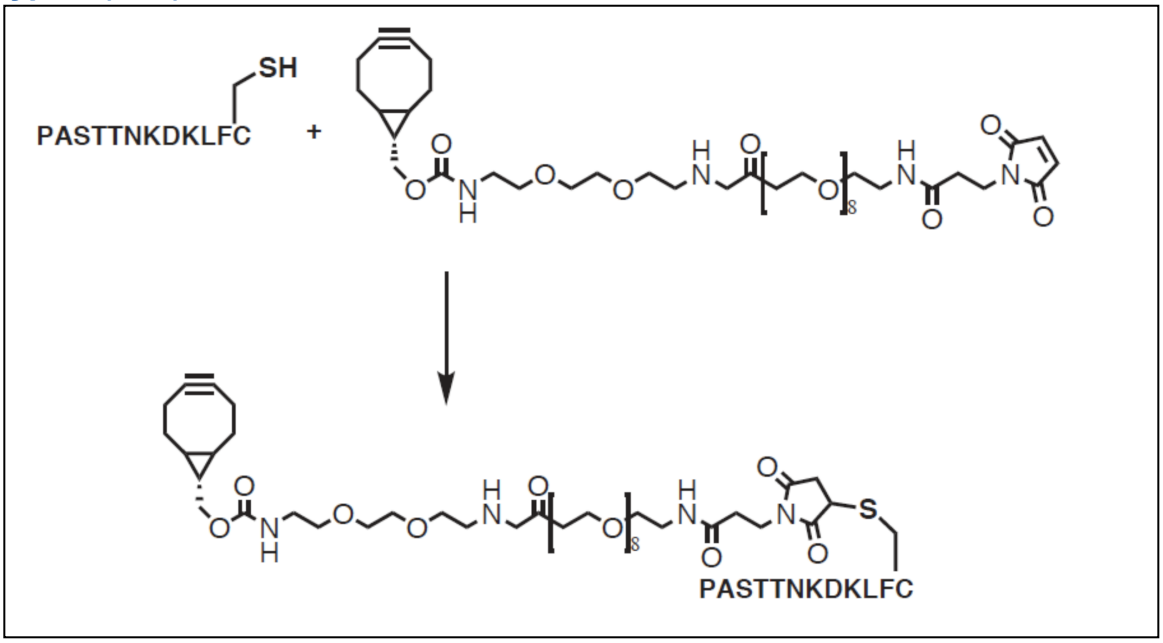

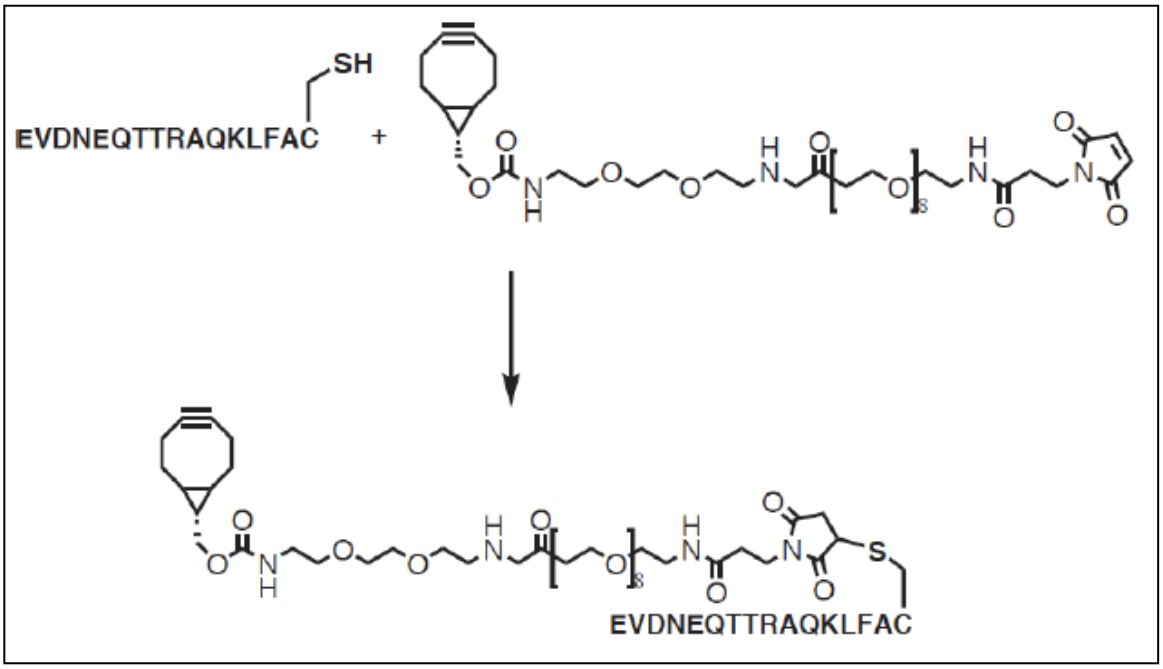

Figure 4.2: Peptide epitopes chosen were synthesized in a microwave assisted peptide synthesizer and equipped with a bicyclononyne based Strain promoted alkyne azide cycloaddition (SPAAC) moiety via a C terminal Cys residue.

The "click" reaction chosen for attachment of peptide to the Ad5 particles was the Strain Promoted Alkyne Azide Cycloaddition (SPAAC) containing a bicyclononyne (BCN) functionality.[74] In order to conjugate the cleaved peptide to the bicyclononyne fragment, a maleimide based coupling method was chosen as per literature precedence[75] due to lability of the strained alkyne under the TFA conditions used for cleavage of peptide from solid synthesis support.

Vaccination scheme:

To determine if antigenic peptides displayed on Ad5 via SPAAC were able to elicit an immune response, polio infection susceptible mice were vaccinated with formalin inactivated, peptide conjugated Ad5. Suitable controls included metabolically unalabed i.e. azide deficient Ad5 treated with peptide-BCN as a negative control. The human oral polio vaccine was chosen as a positive control.

Vaccinations were carried out in the following groups by intramuscular injection in the thigh according to literature procedures.[66]

Group 1: vaccinated with 32 mM Aha -Ad-PV1 peptide
Group 2: vaccinated with 32 mM Aha-Ad-PV3 peptide
Group 3: vaccinated with metabolically unlabeled Ad, treated with BCN-PV1 peptide (negative control)
Group 4: vaccinated with metabolically unlabeled Ad, treated with BCN-PV3 peptide (negative control)
Group 5 and 6: treated with a 1/10 dose of human oral polio vaccine (positive control)
Group 7 and 8: vaccination with formalin inactivated PV1 and PV3

The vaccination schedule adopted was as follows[66]

First dose 10^8 particles per mouse

+4 weeks 2nd dose (booster 1)

+2 weeks 3rd dose (booster 2)

Wait 2 weeks then challenge with a Poliovirus infection to check for immunity

Wait up to 21 days after challenge

Neutralization assay:

To determine if the antigenic epitopes attached to Ad5 were able to elicit an immune response, an assay of neutralizing antibody titer in the serum of vaccinated animals was performed. Basically, blood from vaccinated animals was taken, the serum separated and assayed for the ability to block poliovirus infection in cell culture. The neutralization assay was carried out according to the literature[66]. Briefly, an overlay of HeLa cells were exposed to increasing dilutions of antisera from vaccinated mice, followed by exposure to the corresponding poliovirus (type 1 or type 3 based on antigenic peptide used for vaccination). Thereafter, the cells were allowed to incubate in a 37 °C incubator for 3-4 days and then stained with Crystal Violet to check for neutralizing antibody response.

Results:

Neutralization assay

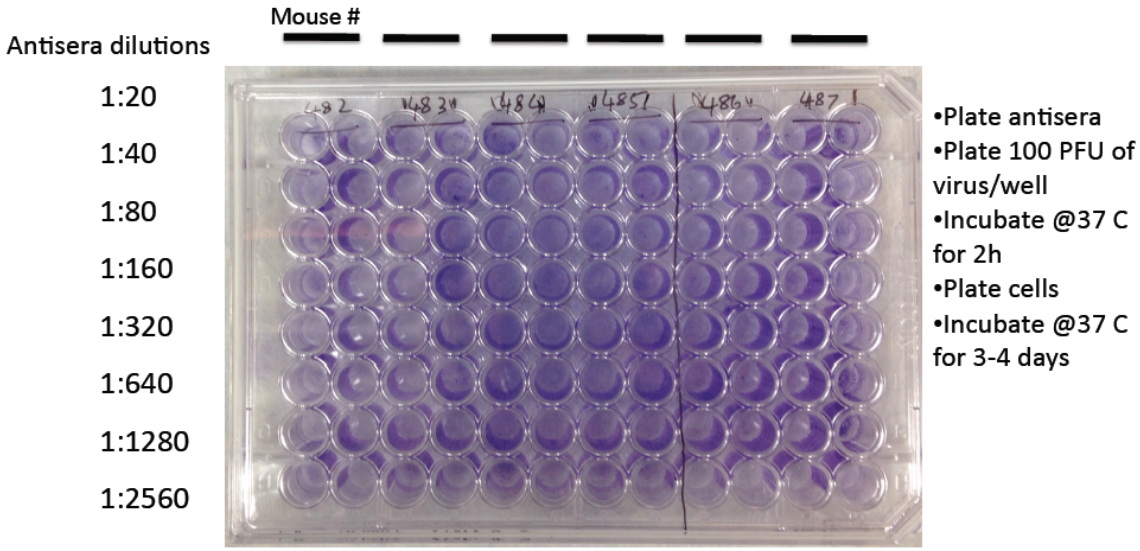

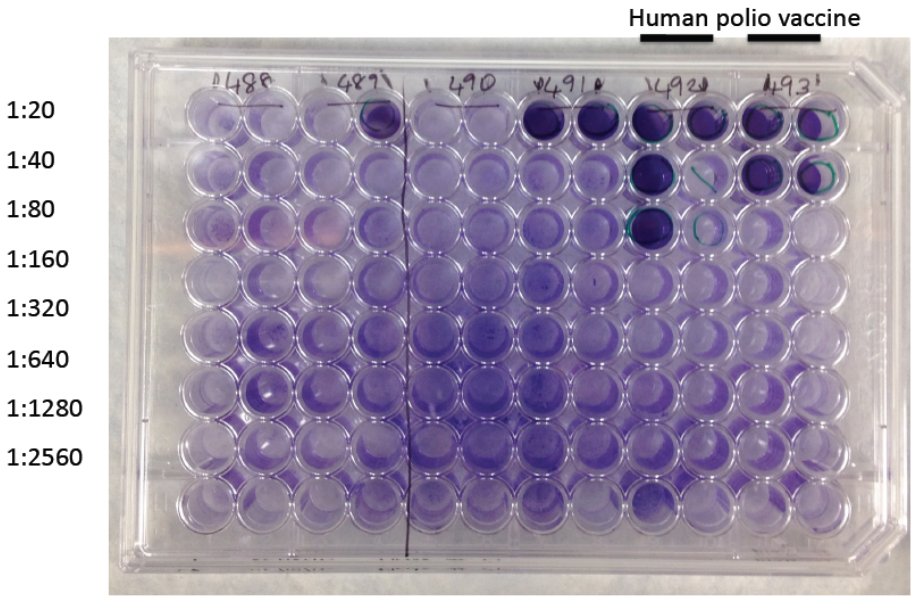

Figure 4.3: the neutralization assay shown above queries the neutralizing antibody titer in the sera from vaccinated mice. Neutralizing antibodies if present in the sera, blocks infection by poliovirus on an overlay of cells. The steps involved are outlined in the figure. The result was that none of the Ad-Poliovirus peptide conjugates produced any neutralizing antibody titer. The positive controls which were vaccinated with dilutions of the Human Polio vaccine were the only ones to produce neutralizing antibodies and therefore block infection, shown by the blue wells with intact monolayer of cells.

Challenge test:

Infection method: intramuscular injection of PV1 in the hind limb = Day 1

Day 3: all Ad vaccinated mice (peptide conjugated and negative controls) began to show paralysis in the hind limbs (stronger on the side injected) 1 mouse in Group 1 (Ad-PV1 peptide) showed delayed onset of paralysis.

Day 4: All Ad-peptide and negative control mice are severely paralyzed, i.e. No protective immunity from vaccination, they were sacrificed

2 out of 8 positive control mice vaccinated with human polio vaccine were protected till day 21.

Therefore the result of these experiments show that the antigenic peptide epitopes when conjugated to Ad5 via SPAAC were unable to produce a neutralizing response.

Conclusion:

On examining the results from the neutralization assay and challenge tests, all indications were that the antigenic epitopes attached to Ad5 were unable to elicit an immune response in vaccinated mice. There are however a few caveats to this interpretation. The chemical labeling of the Ad5 with antigenic epitopes was not rigorously characterized due to technical limitations. An attempt at characterizing the peptide conjugated Ad5 particles was made but was unsuccessful because the only available technique was western blotting and both the anti-VP1 antibody (antibody raised against the viral capsid protein 1) and the anti-poliovirus antibody (antibody raised against whole, intact poliovirus) were not able to recognize the Ad-peptide conjugate. This may be partly due to the fact that the anti-VP1 antibody recognizes the VP1 protein in denatured virus, and the anti-poliovirus antibody (against whole intact poliovirus) had never been used in a western blotting platform (originally having been developed for neutralization assays). Therefore, the chemical labeling via BCN-antigenic peptide conjugates was not characterized completely. In addition, there was no positive control available for the chemical labeling that could be used in a western blotting format: for example, FLAG-BCN conjugate to Ad5 would have served as a suitable positive control.

Materials and methods:

Peptide synthesis:

PASTTNKDKLFC and EVDNEQTTRAQKLFAC

0.5 g of Fmoc-Cys(Trt)-Wang Resin 100-200 mesh (Novabiochem) with a substitution of 0.5 mmole/g was used in a 0.25 mmol scale synthesis reaction using instrument specifications detailed in Marek, P., et al. [76] Double coupling was used for S, T, V and

P. All side chain protected Fmoc amino acids were obtained from Anaspec or EMD Biochemicals. All reactions were performed in N-Methylpyridine (NMP) unless where noted. 0.45M HBTU in DMF and 2M DIPEA in NMP were used to form the activated ester of amino acids. Deprotection was performed using a 20% v/v solution of piperidine in DMF (40 W power, 75°C for 30 s in the first cycle and 180 s in the second cycle).

Synthesis of BCN-peg-maleimide:

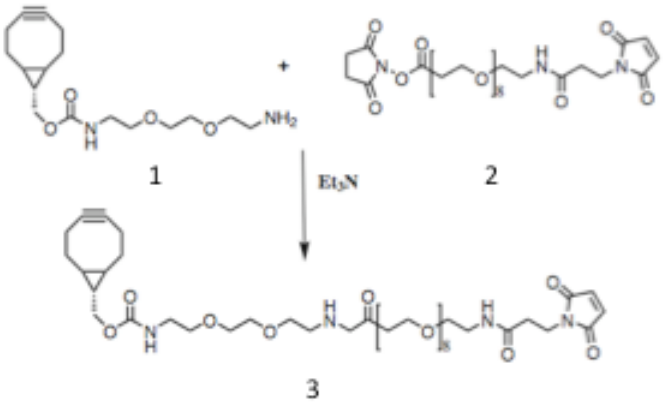

BCN-peg-amine **1** was synthesized by YHO and FAR[74], **2** was obtained from Thermo Scientific catalog # 22108. Briefly a solution of 7.7 µmol of 1 in acetonitrile was added to a 7.8 µmol of 2 in acetonitrile, argon was bubbled through the reaction mixture and the reaction allowed to rotate on the Labquake rotator overnight. Acetonitrile was evaporated and then the crude reaction mixture was purified by HPLC and identity confirmed by LC/MS. Calculated $[M+H]^+$ mass was 899.15, experimental masses observed were 899.35 and 1011.31 for $[M+H]^+$ and $[M+TFA]^-$ peaks respectively.

Synthesis of C-terminal Cysteine tagged synthetic poliovirus epitopes:

Polio type 1 peptide BCN Peg Maleimide conjugate

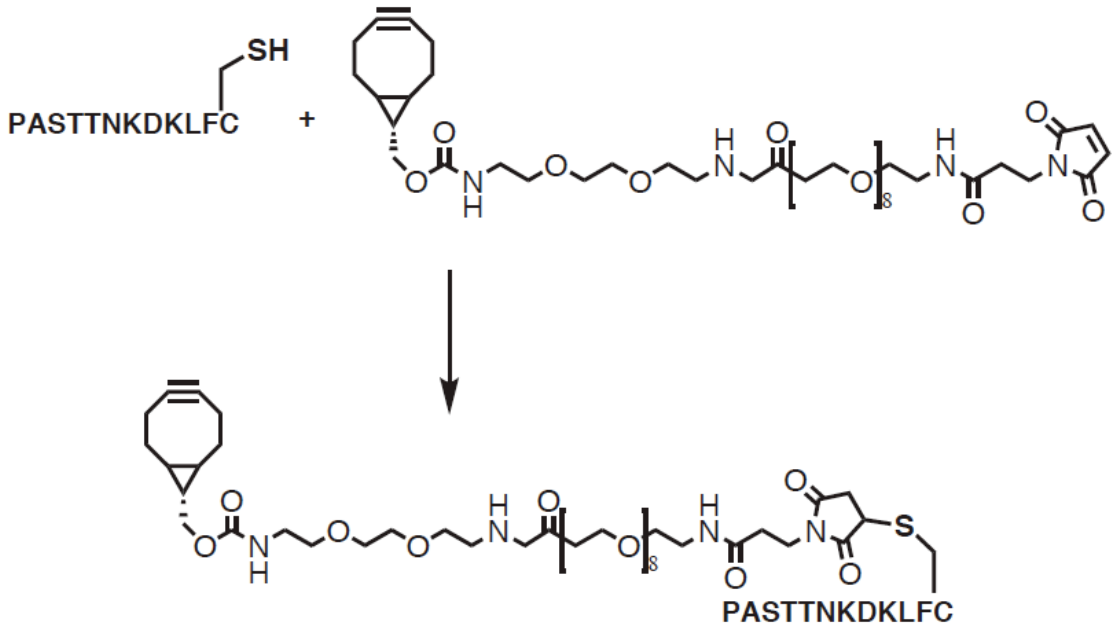

To a solution of Polio type 1 peptide (7.6 mg, 5.74 µmol) in water, reducing buffer consisting of 20 mM EDTA, 10 mM TCEP, 50 mM sodium phosphate pH 7.0 was added to a final volume of 400 µL and rotated at rt for 1 hour on a Labquake rotator. Thereafter a 200 µL of a 22.5% acetonitrile/water solution of BCN-Peg-Maleimide (5.35 mg, 5.951 µmol) was added and coupling allowed to take place overnight at rt with rotation on the Labquake machine. The resulting reaction mixture was concentrated in a speedvac and purified by HPLC with 33% yield. Identification of the BCN-peptide conjugate was confirmed by MALDI spectrometry, calculated mass for $[M+H]^+$ was 2224.5, experimental mass was 2224.0 for $[M+H]^+$.

Polio type 3 peptide BCN Peg Maleimide conjugate

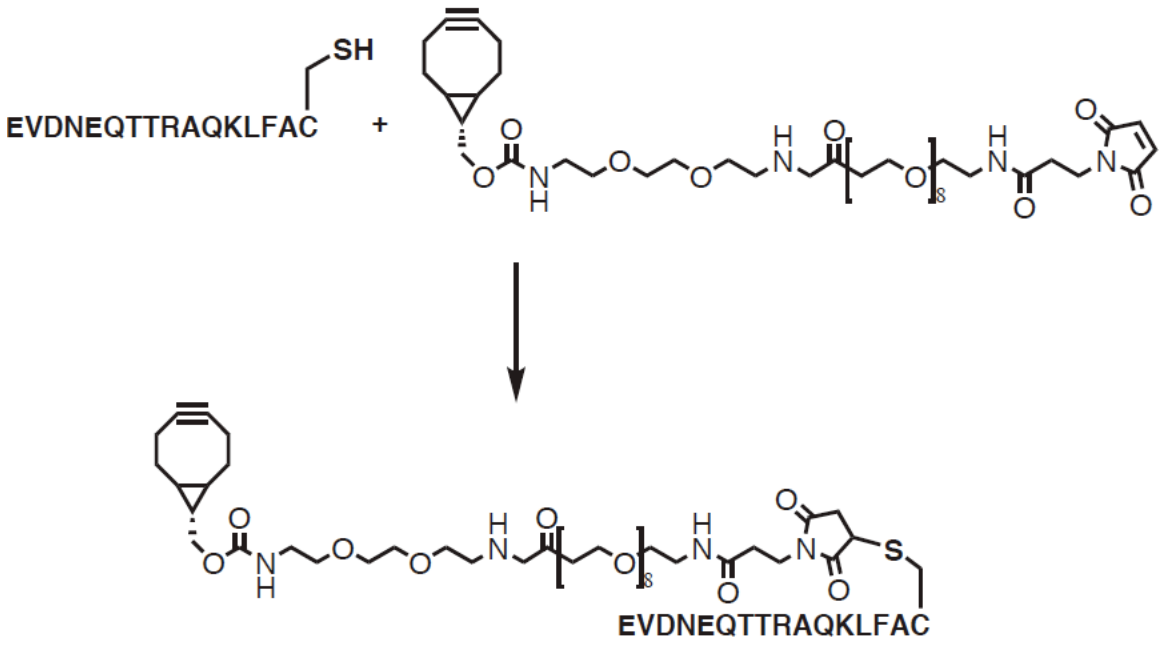

To a solution of Polio type 3 peptide (11.1 mg, 5.69 µmol) in water, reducing buffer consisting of 20 mM EDTA, 10 mM TCEP, 50 mM sodium phosphate pH 7.0 was added to a final volume of 400 µL and rotated at rt for 1 hour on a Labquake rotator. Thereafter a 200 µL of a 22.5% acetonitrile/water solution of BCN-Peg-Maleimide (5.35 mg, 5.951 µmol) was added and coupling allowed to take place overnight at rt with rotation on the Labquake machine. The resulting reaction mixture was concentrated in a speedvac and purified by HPLC with 17% yield. Identification of the BCN-peptide conjugate was confirmed by MALDI spectrometry, calculated mass for $[M+H]^+$ was 2848.8, experimental mass was 2850.9 for $[M+H]^+$ and 2832.5 for $[M-18+H]^+$.

Chemical labeling of azide equipped Ad5:

Azide (32 mM Aha) labeled Ad5 was reacted with 500 µM final concentration of the appropriate BCN-poliovirus Type 1or 3 peptide conjugate in PBS overnight.

An attempt at characterizing the peptide conjugated Ad5 particles was made but was unsuccessful because the only available technique was western blotting and both the anti-VP1 antibody (antibody raised against the viral capsid protein 1) and the anti-poliovirus antibody (antibody raised against whole, intact poliovirus) were not able to recognize the Ad-peptide conjugate. Additionally, the anti-VP1 antibody recognizes the

VP1 protein in denatured virus, the anti-poliovirus antibody (against whole intact poliovirus) had never been used in a western blotting platform (originally having been developed for neutralization assays). Therefore, the chemical labeling via BCN-antigenic peptide conjugates was not characterized rigorously. In addition, there was no positive control available for the chemical labeling that could be used in a western blotting format: for example, FLAG-BCN conjugate to Ad5 would have served as a suitable positive control.

Preparation of peptide epitope bearing Ad5 samples for vaccination:

Inactivation of Ad5 conjugated to BCN-polio epitope peptide prior to vaccination was achieved in accordance with literature procedures.[77] Briefly, Ad5 virus particles after SPAAC reaction with BCN-poliovirus Type 1 or 3 peptide were treated with formalin at a final concentration of 0.01%, at 37 °C for 1 h.

References:

1. Schwarz, F. & Aebi, M. Mechanisms and principles of N-linked protein glycosylation. *Current Opinion in Structural Biology* **21**, 576-582 (2011).
2. Jensen, P.H., Kolarich, D. & Packer, N.H. Mucin-type O-glycosylation – putting the pieces together. *FEBS Journal* **277**, 81-94 (2010).
3. Torres, C.R. & Hart, G.W. Topography and polypeptide distribution of terminal N-acetylglucosamine residues on the surfaces of intact lymphocytes - evidence for O-linked GlcNAc. *Journal of Biological Chemistry* **259**, 3308-3317 (1984).
4. Holt, G.D. & Hart, G.W. The subcellular distribution of terminal N-acetylglucosamine moieties. Localization of a novel protein-saccharide linkage, O-linked GlcNAc. *Journal of Biological Chemistry* **261**, 8049-8057 (1986).
5. Jackson, S.P. & Tjian, R. O-Glycosylation of Eukaryotic transcription factors - implications for mechanisms of transcriptional regulation. *Cell* **55**, 125-133 (1988).
6. Hart, G.W., Slawson, C., Ramirez-Correa, G. & Lagerlof, O. Cross Talk Between O-GlcNAcylation and Phosphorylation: Roles in Signaling, Transcription, and Chronic Disease. in *Annual Review of Biochemistry, Vol 80*, Vol. 80 (eds. Kornberg, R.D., Raetz, C.R.H., Rothman, J.E. & Thorner, J.W.) 825-858 (Annual Reviews, Palo Alto, 2011).
7. Chou, T.Y., Hart, G.W. & Dang, C.V. C-Myc is glycosylated at Threonine-58, a known phosphorylation site and a mutational hot-spot in lymphomas. *Journal of Biological Chemistry* **270**, 18961-18965 (1995).
8. Cheng, X.G. & Hart, G.W. Alternative O-glycosylation/O-phosphorylation of serine-16 in murine estrogen receptor beta - Post-translational regulation of turnover and transactivation activity. *Journal of Biological Chemistry* **276**, 10570-10575 (2001).
9. Yang, W.H. et al. Modification of p53 with O-linked N-acetylglucosamine regulates p53 activity and stability. *Nature Cell Biology* **8**, 1074-U53 (2006).
10. Shafi, R. et al. The O-GlcNAc transferase gene resides on the X chromosome and is essential for embryonic stem cell viability and mouse ontogeny. *Proceedings of the National Academy of Sciences of the United States of America* **97**, 5735-5739 (2000).
11. Iyer, S.P.N. & Hart, G.W. Roles of the tetratricopeptide repeat domain in O-GlcNAc transferase targeting and protein substrate specificity. *Journal of Biological Chemistry* **278**, 24608-24616 (2003).
12. Hanover, J.A., Krause, M.W. & Love, D.C. The hexosamine signaling pathway: O-GlcNAc cycling in feast or famine. *Biochimica Et Biophysica Acta-General Subjects* **1800**, 80-95 (2010).
13. Haltiwanger, R.S., Holt, G.D. & Hart, G.W. Enzymatic addition of O-GlcNAc to nuclear and cytoplasmic proteins -identification of a uridine diphospho-N-acetylglucosmamine-peptide beta-N-acetylglucosaminyl transferase. *Journal of Biological Chemistry* **265**, 2563-2568 (1990).
14. Haltiwanger, R.S., Blomberg, M.A. & Hart, G.W. Glycosylation of nuclear and cytoplasmic proteins - purification and characterization of a uridine diphospho-N-

acetylglucosamine-polypeptide beta-N-acetylglucosaminyltransferase. *Journal of Biological Chemistry* **267**, 9005-9013 (1992).
15. Lazarus, M.B., Nam, Y., Jiang, J., Sliz, P. & Walker, S. Structure of human O-GlcNAc transferase and its complex with a peptide substrate. *Nature* **469**, 564-U168 (2011).
16. Dennis, R.J. et al. Structure and mechanism of a bacterial beta-glucosaminidase having O-GlcNAcase activity. *Nature Structural & Molecular Biology* **13**, 365-371 (2006).
17. Rao, F.V. et al. Structural insights into the mechanism and inhibition of eukaryotic O-GlcNAc hydrolysis. *Embo Journal* **25**, 1569-1578 (2006).
18. Macauley, M.S. & Vocadlo, D.J. Increasing O-GlcNAc levels: An overview of small-molecule inhibitors of O-GlcNAcase. *Biochimica Et Biophysica Acta-General Subjects* **1800**, 107-121 (2010).
19. Whitworth, G.E. et al. Analysis of PUGNAc and NAG-thiazoline as transition state analogues for human O-GlcNAcase: Mechanistic and structural insights into inhibitor selectivity and transition state poise. *Journal of the American Chemical Society* **129**, 635-644 (2007).
20. Dorfmueller, H.C. et al. Substrate and product analogues as human O-GlcNAc transferase inhibitors. *Amino Acids* **40**, 781-792 (2011).
21. Dorfmueller, H.C. et al. GlcNAcstatin: A picomolar, selective O-GlcNAcase inhibitor that modulates intracellular O-GlcNAcylation levels. *Journal of the American Chemical Society* **128**, 16484-16485 (2006).
22. Dorfmueller, H.C., Borodkin, V.S., Schimpl, M. & van Aalten, D.M.F. GlcNAcstatins are nanomolar inhibitors of human O-GlcNAcase inducing cellular hyper-O-GlcNAcylation. *Biochemical Journal* **420**, 221-227 (2009).
23. Greis, K.D. & Hart, G.W. Analytical methods for the study of O-GlcNAc glycoproteins and glycopeptides. *Methods in molecular biology (Clifton, N.J.)* **76**, 19-33 (1998).
24. Khidekel, N., Ficarro, S.B., Peters, E.C. & Hsieh-Wilson, L.C. Exploring the O-GlcNAc proteome: Direct identification of O-GlcNAc-modified proteins from the brain. *Proceedings of the National Academy of Sciences of the United States of America* **101**, 13132-13137 (2004).
25. Vocadlo, D.J., Hang, H.C., Kim, E.J., Hanover, J.A. & Bertozzi, C.R. A chemical approach for identifying O-GlcNAc-modified proteins in cells. *Proceedings of the National Academy of Sciences of the United States of America* **100**, 9116-9121 (2003).
26. Sprung, R. et al. Tagging-via-substrate strategy for probing O-GlcNAc modified proteins. *Journal of Proteome Research* **4**, 950-957 (2005).
27. Boyce, M. et al. Metabolic cross-talk allows labeling of O-linked beta-N-acetylglucosamine-modified proteins via the N-acetylgalactosamine salvage pathway. *Proceedings of the National Academy of Sciences of the United States of America* **108**, 3141-3146 (2011).
28. Hong, V., Presolski, S.I., Ma, C. & Finn, M.G. Analysis and Optimization of Copper-Catalyzed Azide–Alkyne Cycloaddition for Bioconjugation. *Angewandte Chemie International Edition* **48**, 9879-9883 (2009).

29. Sletten, E.M. & Bertozzi, C.R. From Mechanism to Mouse: A Tale of Two Bioorthogonal Reactions. *Accounts of Chemical Research* **44**, 666-676 (2011).
30. Hirsch, J.D. et al. Easily reversible desthiobiotin binding to streptavidin, avidin, and other biotin-binding proteins: uses for protein labeling, detection, and isolation. *Analytical Biochemistry* **308**, 343-357 (2002).
31. Rybak, J.N., Scheurer, S.B., Neri, D. & Elia, G. Purification of biotinylated proteins on streptavidin resin: A protocol for quantitative elution. *Proteomics* **4**, 2296-2299 (2004).
32. Speers, A.E. & Cravatt, B.F. Profiling enzyme activities in vivo using click chemistry methods. *Chemistry & Biology* **11**, 535-546 (2004).
33. Hsu, T.L. et al. Alkynyl sugar analogs for the labeling and visualization of glycoconjugates in cells. *Proceedings of the National Academy of Sciences of the United States of America* **104**, 2614-2619 (2007).
34. Gurcel, C. et al. Identification of new O-GlcNAc modified proteins using a click-chemistry-based tagging. *Analytical and Bioanalytical Chemistry* **390**, 2089-2097 (2008).
35. Zaro, B.W., Yang, Y.-Y., Hang, H.C. & Pratt, M.R. Chemical reporters for fluorescent detection and identification of O-GlcNAc-modified proteins reveal glycosylation of the ubiquitin ligase NEDD4-1. *Proceedings of the National Academy of Sciences* (2011).
36. Laughlin, S.T. & Bertozzi, C.R. Metabolic labeling of glycans with azido sugars and subsequent glycan-profiling and visualization via Staudinger ligation. *Nature Protocols* **2**, 2930-2944 (2007).
37. Luchansky, S.J. et al. Constructing azide-labeled cell surfaces using polysaccharide biosynthetic pathways. *Recognition of Carbohydrates in Biological Systems Pt A: General Procedures* **362**, 249-272 (2003).
38. Kearse, K.P. & Hart, G.W. Lymphocyte-activation induces rapid chnages in nuclear and cytoplasmic glycoproteins. *Proceedings of the National Academy of Sciences of the United States of America* **88**, 1701-1705 (1991).
39. James, L.R. et al. Flux through the hexosamine pathway is a determinant of nuclear factor kappa B-dependent promoter activation. *Diabetes* **51**, 1146-1156 (2002).
40. Golks, A., Tran, T.T.T., Goetschy, J.F. & Guerini, D. Requirement for O-linked N-acetylglucosaminyltransferase in lymphocytes activation. *Embo Journal* **26**, 4368-4379 (2007).
41. Kneass, Z.T. & Marchase, R.B. Neutrophils exhibit rapid agonist-induced increases in protein-associated O-GlcNAc. *Journal of Biological Chemistry* **279**, 45759-45765 (2004).
42. Kneass, Z.T. & Marchase, R.B. Protein O-GlcNAc modulates motility-associated signaling intermediates in neutrophils. *Journal of Biological Chemistry* **280**, 14579-14585 (2005).
43. Pappa, A. & Guerini, D. Immune Regulation by the Posttranslational Modification O-GlcNAc. *Current Signal Transduction Therapy* **5**, 41-48 (2010).
44. Truneh, A., Albert, F., Golstein, P. & Schmittverhulst, A.M. Early steps of lymphocyte-activation bypassed by synergy between calcium ionophores and phorbol ester. *Nature* **313**, 318-320 (1985).

45. Niedel, J.E., Kuhn, L.J. & Vandenbark, G.R. Phorbol diester receptor copurifies with protein kinase C. *Proceedings of the National Academy of Sciences* **80**, 36-40 (1983).
46. Vangsted, A., Neisig, A., Wallin, H., Zeuthen, J. & Geisler, C. Induction of CD3δεω) by phorbol 12-myristate 13-acetate. *European Journal of Immunology* **23**, 1351-1357 (1993).
47. Chatila, T., Silverman, L., Miller, R. & Geha, R. Mechanisms of T cell activation by the calcium ionophore ionomycin. *The Journal of Immunology* **143**, 1283-9 (1989).
48. Hogan, P.G., Lewis, R.S. & Rao, A. Molecular Basis of Calcium Signaling in Lymphocytes: STIM and ORAI. in *Annual Review of Immunology, Vol 28*, Vol. 28 (eds. Paul, W.E., Littman, D.R. & Yokoyama, W.M.) 491-533 (2010).
49. Palacios, R. Concavalin A triggers lymphocytes-T by directly interacting with their receptors for activation. *Journal of Immunology* **128**, 337-342 (1982).
50. Schimpl, M., Schuttelkopf, A.W., Borodkin, V.S. & van Aalten, D.M.F. Human OGA binds substrates in a conserved peptide recognition groove. *Biochemical Journal* **432**, 1-7 (2010).
51. Earl, L.A. & Baum, L.G. CD45 Glycosylation controls T-cell life and death. *Immunology and Cell Biology* **86**, 608-615 (2008).
52. Ostergaard, H.L. et al. Expression of CD45 alters phosphorylation of the Lck-encoded tyrosine protein-kinase in murine lymphoma T-cell lines. *Proceedings of the National Academy of Sciences of the United States of America* **86**, 8959-8963 (1989).
53. Katagiri, T. et al. CD45 negatively regulates Lyn activity by dephosphorylating both positive and negative regulatory tyrosine residues in immature B cells. *Journal of Immunology* **163**, 1321-1326 (1999).
54. Trowbridge, I.S. & Thomas, M.L. CD45 - An emerging role as a protein-tyrosine-phosphatase required for lymphocyte-activation. *Annual Review of Immunology* **12**, 85-116 (1994).
55. Wang, H.P. et al. ZAP-70: An Essential Kinase in T-cell Signaling. *Cold Spring Harbor Perspectives in Biology* **2**(2010).
56. Kiick, K.L., Saxon, E., Tirrell, D.A. & Bertozzi, C.R. Incorporation of azides into recombinant proteins for chemoselective modification by the Staudinger ligation. *Proceedings of the National Academy of Sciences of the United States of America* **99**, 19-24 (2002).
57. Salmond, R.J., Filby, A., Qureshi, I., Caserta, S. & Zamoyska, R. T-cell receptor proximal signaling via the Src-family kinases, Lck and Fyn, influences T-cell activation, differentiation, and tolerance. *Immunological Reviews* **228**, 9-22 (2009).
58. Yip, S.-C., Saha, S. & Chernoff, J. PTP1B: a double agent in metabolism and oncogenesis. *Trends in Biochemical Sciences* **35**, 442-449 (2010).
59. Flint, A.J., Gebbink, M., Franza, B.R., Hill, D.E. & Tonks, N.K. Multisite phosphorylation of the protein-tyrosine phsphatase, PTP1B - identification of cell-cycle regulated and phorbol ester stimulated sites of phosphorylation. *Embo Journal* **12**, 1937-1946 (1993).

60. Ostergaard, H.L. & Trowbridge, I.S. Negative regulation of CD45 protein tyrosine phosphatase-activity by ionomycin in T-cells. *Science* **253**, 1423-1425 (1991).
61. Laughlin, S.T. & Bertozzi, C.R. Metabolic labeling of glycans with azido sugars and subsequent glycan-profiling and visualization via Staudinger ligation. *Nat. Protocols* **2**, 2930-2944 (2007).
62. Mueller, S., Wimmer, E. & Cello, J. Poliovirus and poliomyelitis: A tale of guts, brains, and an accidental event. *Virus Research* **111**, 175-193 (2005).
63. Toyoda, H., Yin, J., Mueller, S., Wimmer, E. & Cello, J. Oncolytic treatment and cure of neuroblastoma by a novel attenuated poliovirus in a novel poliovirus-susceptible animal model. *Cancer Research* **67**, 2857-2864 (2007).
64. Banerjee, P.S., Ostapchuk, P., Hearing, P. & Carrico, I. Chemoselective Attachment of Small Molecule Effector Functionality to Human Adenoviruses Facilitates Gene Delivery to Cancer Cells. *Journal of the American Chemical Society* **132**, 13615-13617 (2010).
65. Banerjee, P.S., Ostapchuk, P., Hearing, P. & Carrico, I.S. Unnatural Amino Acid Incorporation onto Adenoviral (Ad) Coat Proteins Facilitates Chemoselective Modification and Retargeting of Ad Type 5 Vectors. *Journal of Virology* **85**, 7546-7554 (2011).
66. Coleman, J.R. et al. Virus attenuation by genome-scale changes in codon pair bias. *Science* **320**, 1784-1787 (2008).
67. Mueller, S., Papamichail, D., Coleman, J.R., Skiena, S. & Wimmer, E. Reduction of the rate of poliovirus protein synthesis through large-scale codon deoptimization causes attenuation of viral virulence by lowering specific infectivity. *Journal of Virology* **80**, 9687-9696 (2006).
68. Agard, N.J., Baskin, J.M., Prescher, J.A., Lo, A. & Bertozzi, C.R. A Comparative Study of Bioorthogonal Reactions with Azides. *ACS Chemical Biology* **1**, 644-648 (2006).
69. Hogle, J.M. & Filman, D.J. The antigenic structure of poliovirus. *Philosophical Transactions of the Royal Society of London Series B-Biological Sciences* **323**, 467-& (1989).
70. Emini, E.A., Jameson, B.A. & Wimmer, E. Priming for and induction of anti-poliovirus neutralizing antibodies by synthetic peptides. *Nature* **304**, 699-703 (1983).
71. Wimmer, E., Emini, E.A. & Jameson, B.A. Peptide priming of a poliovirus neutralizing antibody-response. *Reviews of Infectious Diseases* **6**, S505-S509 (1984).
72. Crompton, J., Toogood, C.I.A., Wallis, N. & Hay, R.T. Expression of a foreign epitope on the surface of the adenovirus hexon. *Journal of General Virology* **75**, 133-139 (1994).
73. Ferguson, M. et al. Induction of synthetic peptides of broadly reactive, type-specific neutralizing antibody to poliovirus type-3. *Virology* **143**, 505-515 (1985).
74. Dommerholt, J. et al. Readily Accessible Bicyclononynes for Bioorthogonal Labeling and Three-Dimensional Imaging of Living Cells. *Angewandte Chemie International Edition* **49**, 9422-9425 (2010).

75. Chang, P.V. et al. Copper-free click chemistry in living animals. *Proceedings of the National Academy of Sciences of the United States of America* **107**, 1821-1826 (2010).
76. Marek, P., Woys, A.M., Sutton, K., Zanni, M.T. & Raleigh, D.P. Efficient Microwave-Assisted Synthesis of Human Islet Amyloid Polypeptide Designed to Facilitate the Specific Incorporation of Labeled Amino Acids. *Organic Letters* **12**, 4848-4851 (2010).
77. Stasny, J.T., Neurath, A.R. & Rubin, B.A. Effect of Formamide on the Capsid Morphology of Adenovirus Types 4 and 7. *Journal of Virology* **2**, 1429-1442 (1968).